Université Catholique de Louvain
Ecole Polytechnique de Louvain

Center for Operations Research and Econometrics

Nonlinear Pricing Schemes for Mobilizing Residential Flexibility in Power Systems

Yuting Mou

Doctoral Thesis

Supervisors:
Anthony Papavasiliou
(UCLouvain, Belgium)
Philippe Chevalier
(UCLouvain, Belgium)

Jury:
Per Agrell (UCLouvain, Belgium)
Hervé Jeanmart (UCLouvain, Belgium)
Bertrand Cornélusse (ULiège, Belgium)
Dimitrios Papadaskalopoulos (Imperial, UK)
Andreas Ehrenmann (Engie, Belgium)
Hanspeter Höschle (VITO, Belgium)

President:
Hervé Jeanmart (UCLouvain, Belgium)

PhD Organization

Yuting Mou
Université catholique de Louvain
École Politechnique de Louvain
Center of Operations Research and Econometrics

Thesis Supervisors

Anthony Papavasiliou
Associate Professor, Université catholique de Louvain
École Polytechnique de Louvain
Center of Operations Research and Econometrics

Philippe Chevalier
Professor, Université catholique de Louvain
Louvain School of Management
Center of Operations Research and Econometrics

Supervisory Committee

Per Agrell
Professor, Université catholique de Louvain
Louvain School of Management
Center of Operations Research and Econometrics

Bertrand Cornélusse
Assistant Professor, Université de Liège
Institut Montefiore

子曰: 朝闻道，夕死可矣。

《论语·里仁》

The Master said, "If a man in the morning hears the right WAY, he may die in the evening without regret."

the Analects of Confucius, translated by James Legge

Abstract

The increasing penetration of intermittent renewable production requires more flexibility in the power system. We propose priority service and multilevel demand subscription as two alternative methods for the mobilization of residential demand response. Whereas priority service relies on the differentiation and nonlinear pricing of electricity according to reliability, multilevel demand subscription further differentiates electricity service according to duration. The contributions of the dissertation are organized in two chapters.

In Chapter 2, we design a priority service menu as the equilibrium solution to a Stackelberg game, which is modeled as a bilevel optimization problem involving a vertically integrated utility and consumers. We reformulate the equilibrium as a mixed-integer problem. As a consequence of this approach, we can integrate the menu design problem within a day-ahead unit commitment model. In order to tackle the computational challenge brought about by introducing scenarios of renewable production, the model is decomposed by the alternating direction method of multipliers (ADMM) and solved on a high-performance computing infrastructure.We find that priority service pricing can reap 77.1% of the welfare gains of real-time pricing using a menu of 5 options in the large-scale simulation of the Belgian power system.

In Chapter 3, we extend the modeling approach to multilevel demand subscription and priority service is treated as a special case. We propose a framework for quantifying the trade-off between a complex but efficient multilevel demand subscription pricing menu and a simpler but less efficient priority service pricing menu. We evaluate the performance of the two contracting schemes in a system with system-level renewable supply, residential renewable supply, and residential storage. Based on a stylized case study of the Belgian power system, we conclude that the ability of multilevel demand subscription to better discriminate consumers can be beneficial for both the utilities and households. The utility is able to supply more energy to households at lower cost, while the service inconvenience of households is also reduced. We further analyze the conditions under which the cost of investing in home energy storage can be recovered under priority service and multilevel demand subscription.

Acknowledgments

This has been a short and long journey. Without the help of so many people, this thesis would have been impossible. I would like to express my gratitude to some of them.

Let me start with my supervisors. From my first meeting with Anthony and Philippe at seminar room B-101, to the final preparation for the public defense, my supervisors have been at my side, advising me, encouraging me and helping me from all aspects. I can never forget all the after-six-pm meetings and the ups and downs we have been through together. What is worth mentioning is our trips to Engie for the ColorPower project meeting. We had really productive brainstorming discussions in Anthony's car. These precious moments are memorable treasures in my life.

I would like to express my gratitude to my jury members, Prof. Per Agrell, Prof. Hervé Jeanmart, Prof. Bertrand Cornélusse, Dr. Andreas Ehrenmann Dr. Dimitrios Papadaskalopoulos and Dr. Hanspeter Höschle. They helped improve the thesis significantly, which is demonstrated by the thirty extra pages of analyses in the final thesis. I'd like to give a special thanks to Dr. Andreas Ehrenmann. He closely followed the development of this work in the framework of the ColorPower project. The valuable comments in the steering committee meetings were very helpful.

The great administrative support at CORE, LIDAM and SST made all the paperwork easy to handle. Catherine and other staff members were always ready to help. From the weekly check-in emails when I was waiting for my visa, to the last housing contract with Logement, Catherine showed great kindness and patience.

The friends at CORE made up another important aspect of my life. My amazing officemate Ignacio introduced me to the Siberian community on my first day in Belgium. I had great times together with András, Sabina & Claudio, Mery & Guzmán, Erika, Sonia, Bartosz, Valeria, Valerio, Robert, Sinem, Dagmara, Nicolas, Jonas, Manuela, Manuel, Risa, Cyrille, Avinash, Vladimir and Akylai at parties, at le Sablon, at le Piano, and in interesting conversions at CORE lounge. All these small moments made my PhD life more colorful. I would also like to express a special thank you to Huan and Sefane who were the last survivors with me in Louvain-la-Neuve.

I am also grateful to the support of the energy group, including Gilles, Céline, Ilyes, Jacques, Quentin, Loïc, Daniel, Jehum and Prof. Yves Smeers. The lively interaction at the energy seminar and valuable comments that helped me prepare for my conferences, private defense and job interview were greatly appreciated. I also need to mention the countless trips I took together with Gilles, where we learned how to be flexible and discussed democracy. I was lucky to have Céline as my second officemate. It has been a pleasure to discuss ColorPower with her.

I would like to express my gratitude to my VITO colleagues. Ann and Ana offered me the greatest flexibility and support during the last phase of my PhD. Hanspeter has always been an amazing mentor. I also enjoyed the team activities and collaborations with Janka, Kris, Gwen, Hélène, Anibal, Annelies, Helena, Lina, Enrique, Niels, Michiel, Ilia and Anubhav. Maurits and Inne helped me a lot with all the administrative work at VITO. Christy is a wonderful English language trainer and offered to help me with my thesis and presentation.

The Chinese community in Belgium has been helping me in one way or another. The precious time I spent with Linqi, Ying, Chenghong, Zijiang, Tengfei, Qian & Lei and Yazhou are memorable. Prof. Yue Zhang, Prof. Zhengyuan Gao and Yixiao Ma offered me great advice. I also had a great time with the alumni of Zhejiang University, including Yang, Xinyi and Junfeng.

My family and friends in China have been a great support. Whenever I went back home, to Shanghai or Hangzhou or Suzhou, I was always welcomed with great warmth and delicious food. My previous teachers and professors convinced me that I could achieve more. I would like to express a special thank you to Jessie, who has been supplying me with spiritual energy. Thank you for your encouragement, belief and confidence in me. Thank you for joining me on the road less traveled.

Last but not least, the financial and technical support from various institutions has been essential. This research has been supported by the ENGIE Chair in Energy Economics and Energy Risk Management and by the ENGIE-Electrabel ColorPower grant. The work is also supported via the energy transition funds project 'EPOC 2030-2050' organised by the FPS economy, S.M.E.s, Self-employed and Energy. Computational resources have been provided by the supercomputing facilities of the Université Catholique de Louvain (CISM/UCL) and the Consortium des Équipements de Calcul Intensif en Fédération Wallonie Bruxelles (CÉCI) funded by the Fond de la Recherche Scientifique de Belgique (F.R.S.-FNRS) under convention 2.5020.11. Academic licenses of mathematical programming solvers have been provided by Gurobi and FICO® Xpress.

Contents

1 Introduction **1**
1.1 Motivation 1
1.2 Residential Demand Response 2
1.2.1 Demand Response Potential 2
1.2.2 Approaches for Residential Demand Response 3
1.3 Nonlinear Pricing Theory 5
1.3.1 Quality-Differentiated Products 8
1.3.2 Priority Service Pricing and Multilevel Demand Subscription Pricing 9
1.4 Contributions 12

2 A Bilevel Optimization Formulation of Priority Service Pricing **17**
2.1 Introduction 17
2.1.1 Previous Work on Priority Differentiated Products . . . 18
2.1.2 Contribution and Chapter Organization 18
2.2 Preliminaries 19
2.2.1 Priority Service Pricing 19
2.2.2 Dual Decomposition 22
2.2.3 Alternating Direction Method of Multipliers 23
2.3 Modeling the Menu Design Problem as a Stackelberg Equilibrium 25
2.3.1 Overview of the Bilevel Model 25
2.3.2 The Consumer Model 27
2.3.3 The Producer Model 30
2.3.4 The Bilevel Model 32
2.4 Decomposition by ADMM 36
2.4.1 ADMM Formulation 36
2.4.2 Convergence 38
2.4.3 Runtime Complexity of the Algorithm 40
2.5 Case Studies 40
2.5.1 A Toy Example 40

2.5.2 The Belgian Power System Model 41
2.A Nomenclature 50
2.B A Toy Example to Illustrate ADMM 51
2.C Detailed Report on Run-time 53
2.D Sensitivity Analysis on the Number of Options 55
2.E Review of Assumptions 56
2.E.1 Constant Valuation over Time 56
2.E.2 Identical Consumption Profiles 58
2.E.3 Exogenous Valuation Breakpoints 60

3 Comparison of Priority Service and Multilevel Demand Subscription 63
3.1 Introduction 63
3.1.1 Previous Work on Tariff Design with Consideration of Prosumers 64
3.1.2 Contribution and Chapter Organization 64
3.2 Traditional Theory of Multilevel Demand Subscription Pricing 65
3.2.1 The Consumer Model 66
3.2.2 The Cost Model 67
3.2.3 Determining the Optimal Price Function 67
3.2.4 Our Contribution to the Literature 67
3.3 Multilevel Demand Subscription Pricing Menu Design 69
3.3.1 Modeling the Multilevel Demand Subscription Menu Design Problem as a Stackelberg Equilibrium 69
3.3.2 Menu Choice by Household 72
3.4 Performance Evaluation 73
3.4.1 Rolling Optimization for the Producer 74
3.4.2 Rolling Optimization for the Household 75
3.5 Case Study 79
3.5.1 System Settings 79
3.5.2 Optimal Menus 82
3.5.3 Policy Analysis 83
3.A Nomenclature 93
3.B Modeling the Multilevel Demand Subscription Menu Design Problem as a Stackelberg Equilibrium (Cont.) 94
3.B.1 Optimality Conditions of the Consumer Model 94
3.B.2 The Producer Model 96
3.B.3 The Bilevel Model 97
3.C Estimation of Demand Functions 98
3.D Household Menu Selection Problem 101
3.E Impact of VOLL on Menu Design 102

4 Conclusions and Perspectives **105**
4.1 A Summary of Conclusions 106
4.1.1 Case Study Comparing Flat Tariff, Priority Service and Real-Time Pricing 106
4.1.2 Case Study Comparing Priority Service and Multilevel Demand Subscription 106
4.2 Future Areas of Research 107

List of Figures

1.1 Illustration of linear pricing and several types of nonlinear tariffs. 7
1.2 Illustration of priority service pricing. 10
1.3 Illustration of the practical implementation of priority service pricing. 11
1.4 Envisioned implementation of multilevel demand subscription. . 11

2.1 Illustration of $R(v)$ in the traditional priority service pricing theory. 21
2.2 Interaction between the producer and consumers in the bilevel model. 26
2.3 A consumer of type l follows a load profile $D_{l,t}$ 28
2.4 Illustration of valid cuts derived from Proposition 2. 34
2.5 The application of ADMM as a heuristic for decomposing the reformulated MILP. 38
2.6 Installed capacity of different technologies in 2015 and 2050 in Belgium. 43
2.7 Total import and demand in 2015 and 2050 in Belgium. 43
2.8 Convergence of the cutting plane method in the case study of section 2.5.2. 44
2.9 Comparison of price duration curves in the case study of section 2.5.2. 46
2.10 Profitability of CCGT units in the case study of section 2.5.2. . 47
2.11 Interruption patterns of options in the case study in section 2.5.2. 47
2.12 Comparison of residential demand profiles in the case study of section 2.5.2. 48
2.13 Wind production profile of a sample day in the case study of section 2.5.2. 49
2.14 Comparison of residential demand profiles of a sample day in the case study of section 2.5.2. 49
2.15 Demand functions of three time periods of the toy example. . . 58
2.16 Profiles of different consumers (lower-indexed consumers have lower valuation). 60

3.1 Illustration of consumer types in multilevel demand subscription pricing theory. 66
3.2 The menu design and performance evaluation framework to compare priority service and multilevel demand subscription. 68
3.3 Interaction between the producer and consumers in the multilevel demand subscription bilevel model. 70
3.4 Illustration of the optimal choice problem of consumer type l. . 71
3.5 The mapping between the time period t of actual operations to its time index in the load duration curve. 75
3.6 Scenario tree for the household model ($H_{h,t}$) of section 3.4.2. . 76
3.7 Comparison of the variation of wind production in different seasons of 2015 in Belgium. 80
3.8 Comparison of the variation of solar production in different seasons of 2015 in Belgium. 80
3.9 Scenario tree for wind production Ω^W. 81
3.10 Comparison of consumption profiles for households that belong to SLP categories S21 and S22. 82
3.11 Comparison of subscribed energy of different types of households in the case study of section 3.5. 86
3.12 Cost breakdown for different types of households under priority service. 87
3.13 Cost breakdown for different types of households under multilevel demand subscription in the case study of section 3.5. . . . 88
3.14 Comparison of the total cost for the different types of households under priority service and multilevel demand subscription in the case study of section 3.5. 88
3.15 Comparison of the cost of service for the different types of households in the case study of section 3.5. 89
3.16 Comparison of demand functions for the eight types of households that are simulated in section 3.5. 100
3.17 The system-level demand function (left), and its concave approximation (right). 100

List of Tables

1.1 Residential electricity tariff structures in European countries. . 6

2.1 Price menu for the example of section 2.5.2 based on Chao's theory. 44
2.2 The price menu obtained by ADMM in the case study of section 2.5.2. 45
2.3 Economic performance of priority service pricing, flat tariff and real-time pricing in the case study of section 2.5.2. 45
2.4 Solution comparison of using different parameters in ADMM. . 55
2.5 Sensitivity Analysis on the Number of Options in the Priority Service Pricing Menu 56
2.6 Production of each generator in each time period in the toy example (Unit: MWh) 59
2.7 Price Menu in the toy example 59
2.8 Comparison of social welfare (unit: million €) 61

3.1 Technical specifications of household batteries in the case study of section 3.5. 82
3.2 Characteristics of different types of households in the case study of section 3.5. 82
3.3 Priority service menu in the case study of section 3.5. 83
3.4 Multilevel demand subscription menu in the case study of section 3.5. 83
3.5 Comparison of priority service (PSP) and multilevel demand subscription (MDSP) in the case study of section 3.5 [unit: M €/month]. 84
3.6 Priority service subscription for each type of household in the case study of section 3.5. 85
3.7 Multilevel demand subscription for each type of household in the case study of section 3.5. 85
3.8 Detailed results for each type of household under priority service in the case study of section 3.5. 90

3.9 Detailed results for each type of household under multilevel demand subscription in the case study of section 3.5. 92
3.10 Priority service menus under different VOLL assumptions. . . . 102

Chapter 1

Introduction

1.1 Motivation

The large-scale integration of renewable energy is progressing at an unprecedented pace. Europe is leading this endeavor at a global scale through the Clean Energy Package of the European Commission [EC20]. During the past five years, the installed capacity of solar power in Belgium has increased from 2.9 GW in 2014 to 3.9 GW at present and the installed wind capacity has increased from 1.8 GW in 2014 to 3.7 GW at present [Eli19b]. A similar trend has been observed in Germany, the Netherlands, and other countries of Central Western Europe [AP17].

The mobilization of demand-side resources is an essential requirement for enabling the large-scale integration of renewable resources. These resources can be instrumental in mitigating numerous system and market operation challenges resulting from the integration of renewable resources. On a short-term operational basis, demand-side flexibility can serve towards balancing the system on an instantaneous basis [PM14], and can contribute towards resolving numerous operational challenges related to the integration of renewable resources (e.g. ramping, the negative correlation of renewable supply with demand, and the wear and tear of thermal units due to startups). In the long term, the electrification of transportation and heating systems would increase peak demand, which necessitates upgrading current systems, including investment in backup capacity and T&D lines. Price-responsive consumers can contribute towards signaling scarcity in capacity [PBF13]. This is an essential step towards tackling the missing money problem [Sto02] by properly remunerating conventional resources that offer valuable services to the system.

Meanwhile, most residential consumers are still facing simple electricity tariffs, which do not reflect the time-varying cost of the system, so they do not have incentives to offer their flexibility to the system when the system

is stressed. In addition, an increasing number of households are becoming equipped with PV panels and batteries. Recent net-metering policies in 41 states of the USA enable these consumers to reduce their bill because of self-consumption [BHBW19, Ore17], which raises issues related to the recovery of grid costs and capital costs of generators from PV owners [PAK16]. The reliance of homeowners with storage and rooftop solar on the grid for energy decreases, while the reliance on the grid for capacity remains or even increases. This calls for a careful design of electricity tariffs moving forward.

This dissertation seeks to explore more advanced electricity tariff structures by casting traditional nonlinear pricing theory in a flexible modeling framework that exploits the power of modern optimization solvers while capturing the detail of advanced production simulation models. The overarching goal of this work is to mobilize the flexibility of residential consumers in order to enhance short-term power system operations and generate more robust long-term investment signals.

1.2 Residential Demand Response

1.2.1 Demand Response Potential

There exist numerous economic studies in the literature which demonstrate the value of mobilizing demand-side flexibility. Studies by Faruqui et al. [FG02, FS10a] quantify the benefits of dynamic pricing in terms of preventing peak capacity investments. Recent studies by Strbac and coauthors [SAP+15] support these observations by quantifying the economic value of flexibility (including the flexibility of distributed loads) at up to 8.1 billion British pounds per year for the UK alone, depending on scenario assumptions. These savings result from reduced short-term fuel costs, lower long-term investment costs in power generation capacity, and the deferral of avoidable reinforcements of the transmission and distribution grid.

A recent study by Gils [Gil14] has demonstrated that the *residential* sector is a significant source of demand-side flexibility. Serendipitously, some of the most energy-intensive appliances in households are also among the most flexible, in the sense that deferring or interrupting them may have minor impacts on the perceived quality of service. Such appliances include dish washers, laundry machines, dryers, heaters, and in the future possibly electric vehicles. Based on the LINEAR pilot project [WC14], D'Hulst et al. [DLB+15] analyze the flexibility potential of residential smart appliances. The consumption of all wet appliances (washing machine, tumble dryer, dish washer) in Belgium can be increased maximally by 2 GW at midnight on the weekend. Another recent pilot in Germany is described by Stamminger and Anstett [SA13]. The behavior of 41 consumers and their motivation to use and accept flexible tariffs and smart

appliances are investigated and analysed during this two-year pilot project. Considering wet appliances as the main appliances the operation of which can be shifted, this would allow a maximum shift of 10% of the residential electricity consumption from expensive hours to periods when cheap (and renewable) energy is available.

1.2.2 Approaches for Residential Demand Response

Although residential demand response presents very promising opportunities, it has failed to deliver its promise in electricity markets [PBF13]. The development of adequate business models for engaging flexible consumers [CO16] is an essential step in successfully enlisting demand-side flexibility in system operations. In the two extremes of the wide spectrum of options for mobilizing demand response [BJR02], one identifies price-based methods and quantity-based methods. In the following, we provide an overview of the two methods.

Quantity-based methods, such as direct load control, have been applied in the literature to certain types of appliances. For example, Callaway [Cal09] proposes to use thermostatically controlled loads in order to perform load following and regulation by adjusting the temperature set-point of large aggregations of residential consumers. Han et al. [HHS10] considers vehicle-to-grid service. An aggregator applies the dynamic programming algorithm to the control of the charging/discharging rate of a group of electric vehicles, in order to provide frequency regulation service. Mou et al. [MXLF15] develop a decentralized algorithm for controlling the charging of electrical vehicles, in order to reduce peak load. In addition, some researchers propose direct load control approaches for the whole residential sector, without being restricted to a certain type of appliance. Chen et al. [CWK14] build a two-layer communication-based control architecture. The upper layer receives a desired aggregated demand profile signal from the aggregator and the lower layer schedules the operation of household appliances, so that the mismatch between the actual consumption profile and the desired profile is minimized. Li et al. [LH15] develop a demand response management scheme and test bed for a residential smart grid. Customers are divided into two types based on their acceptance of inconvenience and smart plugs can be switched off when needed by the aggregator. Celik et al. [CRS+17] provides a broad survey regarding various structures and control techniques in order to coordinate multiple smart homes in residential areas. However, quantity-based methods are perceived as being excessively intrusive.

In terms of price-based methods, real-time pricing represents the benchmark of economic efficiency. Under real-time pricing, prices are adjusted in real-time balancing according to the instantaneous needs of the system. Real-time pricing suffers from the fact that an excessive information overhead is placed on residential consumers, who lack the attention span and economic incentives to voluntarily engage in the process of procuring electricity in real time.

Approaches that attempt to alleviate the complexity of real-time pricing have been proposed in practice, in order to make the active engagement of consumers less taxing in terms of information overhead and complexity. Time-of-use pricing is widely adopted in practice as a compromise, in which a day is typically divided into a peak period and an off-peak period. Some utilities also vary time-of-use tariffs seasonally. Time-of-use tariffs are intended to reflect the time-varying costs of supplying electricity to consumers, so that consumers are incentivized to reduce their peak consumption or shift the consumption to cheaper off-peak hours. However, the rates are only designed to reflect the expected long-run conditions of the system [FG02]. It is possible that the real peak does not coincide with the peak period defined in the time-of-use tariff. This is due to the fact that the real peak period becomes very hard to predict in advance with intermittent renewable production. Therefore, the inherent uncertainty of power supply cannot be captured. Consequently, utilities are still confronted with the risk of constructing peaking units. Furthermore, a simple time-of-use tariff does not adequately protect the system against significant (even if short-lived) spikes in consumer demand. Hence new mechanisms are needed to communicate the state of the system to consumers. Consequently, certain utility companies implement time-of-use pricing with a demand charge, which implies that consumers are also charged according to their peak demand, in addition to an energy charge based on the time-of-use tariff. An alternative approach that has been adopted widely in practice is critical peak pricing, which is based on time-of-use pricing, and includes additionally certain critical hours that can be announced to consumers by the utility with short notice. If consumers use electricity during these hours, they pay a significant markup. Both time-of-use tariffs with demand charges and critical peak pricing attempt to reduce peak demand. Critical peak pricing can better align demand response with the peak demand of the system, instead of focusing on the individual peak of consumers. Borenstein et al. [BJR02] provide a detailed discussion on these tariffs, and the underlying economic theory that guides their design.

Faruqui [FS10b] surveys experimental observations from 15 demand response pilots, experiments and full-scale implementations of dynamic pricing, including critical-peak pricing and time-of-use pricing. The study finds conclusive evidence that households respond to higher prices by lowering usage. More specifically, time-of-use tariffs are found to reduce the peak demand by 3-6%. By contrast, the decrease in peak demand induced by critical-peak pricing is more significant, ranging from 13% to 20%. The percentage can be further increased to 27% to 44% by enabling technologies. Faruqui et al. [FHH10] analyze the costs and benefits of installing smart meters in the EU and draw the conclusion that the adoption of smart meters enables dynamic pricing, which reduces peak demand and lowers the investment into peaking infrastructures. The analysis finds that the costs of deploying smart meters can be recovered from these benefits. A meta-analysis based on the Arcturus database, which

contains 63 pilots, has been conducted by Faruqui et al. [FSW17] recently. Their findings demonstrate that the discrepancy in peak demand reduction across different pilots is mainly caused by the peak to off-peak price ratio.

The LINEAR pilot project in Belgium was conducted from September 2013 until July 2014 and it demonstrates a significant shift of the flexible share of electricity consumption in households to lower price periods in a day-ahead dynamic pricing scheme [VDF+15]. The effectiveness of demand response was investigated in a Swedish field study covering 136 households in 2017. The results show that the effectiveness of demand response varies widely according to household types and households prefer price incentives to environmental incentives [NLBK18]. There are also field tests that cater for specific appliances, such as a demand response program for heat pumps under time-of-use pricing and critical peak pricing in the UK [SFOO19]. Kohlhepp et al. [KHW+19] review 16 international field studies that mobilize the flexibility of residential thermal energy storage.

Table 1.1 presents a classification of the implemented residential electricity tariffs in most European countries at the time of writing of this thesis. It can be observed that, in addition to flat tariffs, most countries adopt a simple time-of-use pricing system in order to differentiate consumers according to when they use electricity. However, time-of-use tariffs may not be effective in future power systems, because the peak or off-peak periods are difficult to specify, due to the unpredictable availability of renewable production. Other differentiated electricity service offerings, which were originally proposed in the early power system economics literature, have recently attracted the attention of researchers. These are essentially based on nonlinear pricing theory, which is introduced in the following section.

1.3 Nonlinear Pricing Theory

One challenge faced by the price menu designer is information asymmetry. In a typical setting, each consumer has a specific *type*, but due to information asymmetry, the type is private information known to the consumer only. Instead the menu designer is assumed to be able to estimate the distribution of consumer types. In other words, the menu designer has no information regarding which consumer is of which type, but he knows the existence of each type and its proportion in the whole population. By offering a nonlinear pricing menu, the designer tries to achieve some objective while discovering the type of the consumer in the process. And consumers will reveal their types to the menu designer by self-selection.

The generic term *nonlinear pricing* refers to any case in which the tariff is not strictly proportional to the quantity purchased [Rob93]. As shown in figure 1.1, the simplest example of a nonlinear tariff is a two-part tariff. In such a

Table 1.1: Residential electricity tariff structures in European countries. FT: flat tariff; TOU: time-of-use tariff; FT-D: flat tariff with demand charge; RTP: real-time pricing. The demand charge in Belgium applies to prosumers.

Countries \ Tariffs	FT	TOU	FT-D	TOU-D	RTP
Austria [Ver20]	✓	✓			
Belgium [Ele20a]	✓	✓	✓	✓	
Czech Republic [PRE20]			✓	✓	
Denmark [Ors20]	✓				✓
Finland [Hel20, Ene20b]	✓	✓			✓
France [EDF20]			✓	✓	
Germany [MVV20]	✓	✓			
Greece [SH20]			✓	✓	
Hungary [ELM20]	✓	✓			
Ireland [Ene20a]	✓	✓			
Italy [Naz20]			✓	✓	
Luxembourg [Eno20]	✓	✓			
Netherlands [Vat20]	✓	✓			
Norway [Gud20]	✓				✓
Poland [TAU20]	✓	✓			
Portugal [ELE20b]			✓	✓	
Slovakia [Ele20c]	✓	✓			
Slovenia [Ene20c]	✓	✓			
Spain [End20]			✓	✓	
Sweden [Mal20]	✓				✓
Switzerland [Vit20]	✓	✓			
UK [SEE20]	✓	✓			

tariff, the consumer pays an initial fixed fee for the first unit (often justified as a subscription charge), as well as an additional constant price for each unit after the first.

Nonlinear pricing is prevalent in many industries. For example, in the tariffs presented in table 1.1, consumers in most countries are required to pay an annual subscription. Therefore, in the case of a flat tariff for electricity with subscription charges, we exactly recover a two-part tariff. As we will explain later in this section, time-of-use pricing is also a form of nonlinear pricing.

The motivation of nonlinear pricing is that there exists heterogeneity among consumers[1]. Due to information asymmetry, utilities are not aware of which

[1]Note that in the nonlinear pricing theory, a consumer is an economic concept that refers to a consumer type rather than a consumer in the real word. For example, a slice of power in the household can be regarded as a consumer and the first 1 kW power carries higher

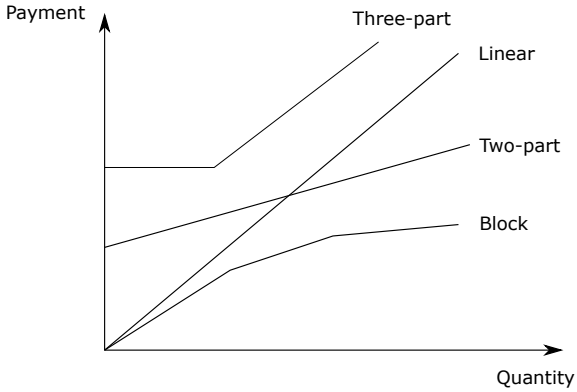

Figure 1.1: Illustration of linear pricing and several types of nonlinear tariffs.

consumers are characterized by higher valuation. However, by facing different prices for successive increments, consumers will reveal their valuation by self-selection. This can result in higher efficiency during normal operations but especially during scarcity conditions (the latter being especially relevant in a regime of large-scale renewable energy integration). In nonlinear pricing theory, increments are not necessarily restricted to quantity, but may also refer to the quality of service, such as the priority by which a consumer is served, or the time at which electricity becomes available. Concretely, in the case of time of use pricing, electricity that is delivered in peak periods is characterized by a higher quality than electricity delivered in off-peak periods. The differences in quality are charged differently, following the principles of nonlinear pricing. Examples exist in other industries as well. For example, telecommunication companies offer different plans for data with different monthly subscription fees.

The approach which is considered in this thesis is the quality differentiation of electricity service. This can be viewed as a compromise between price and quantity-based methods that attempts to combine the best of both worlds. As we explain above, quality-differentiated service traces its theoretical origins in nonlinear pricing , and is inspired by success stories in the telecommunications and information technology sectors. The promise of this approach as a viable paradigm for massively scalable demand response is exemplified by the notable amount of research that has been conducted recently in variations of the basic concept [MO16, NPNP$^+$16, CQV15, NNPPV16, BX17, BL12]. In the following, we discuss the products that have emerged from these papers. We will then introduce priority service pricing (PSP) and its generalization, multilevel demand subscription pricing (MDSP), which are the focus of this dissertation.

valuation than the second slice. In this sense, a household consists of different types of consumers.

1.3.1 Quality-Differentiated Products

Following the principles of nonlinear pricing, a deadline differentiated pricing policy for deferrable electric loads is proposed in Bitar et al. [BL12]. According to this approach, electricity is offered within a given deadline of service, with shorter service deadlines demanding a higher price. The authors apply the resulting product to electric vehicle charging parks equipped with variable renewable supply [BX17].

Another differentiation scheme based on the duration of the service and the power level is presented in Nayyar et al. [NNPPV16]. The authors refer to this approach as duration differentiated energy service. This service considers loads that require a fixed power level for a certain duration out of the total horizon, but are indifferent to when the power is delivered. At each power level, the supplier offers services of different duration levels at different prices. The service of a shorter duration at the same power level enjoys a lower per-unit energy price since more flexibility is offered by the load. This scheme is similar to multilevel demand subscription pricing, which is treated in detail in Chapter 3 of the thesis. The offerings are similar in the sense that both services are differentiated by duration. Nevertheless, multilevel demand subscription pricing additionally includes the reliability component.

Inspired by this work, an energy service differentiated by both the duration and the deadline is put forward in Chen et al. [CQV15]. The authors consider a group of flexible loads with each load requiring a constant power level for a specified duration before a specified deadline. The service at each power level is priced differently according to the service duration and the promised deadline that the total requested energy is delivered. The energy price per unit varies with the deadline and duration.

In addition, rate-constrained energy services [NPNP$^+$16] are also a recent approach for mobilizing flexible demand. Under this approach, service is characterized by a delivery window, the total amount of energy that must be supplied, and the maximum rate at which this energy may be delivered.

We point out that these approaches mainly cater for storage-like appliances and are not perfectly suitable for mobilizing demand response in a household. This is due to the fact that consumers in a household would prefer to retain their authority over electricity consumption. We therefore conduct our analysis under the assumption that control should only be imposed behind the meter. Consequently, in this thesis we investigate two types of differentiated products based on nonlinear pricing theory, which we argue better fit the institutional constraints of residential demand response.

1.3.2 Priority Service Pricing and Multilevel Demand Subscription Pricing

As mentioned previously, time-of-use pricing only reflects the expected long-run conditions of the system. The intermittent supply of renewable energy renders the static definition of peak periods and off-peak periods obsolete. By contrast, priority service and multilevel demand subscription offer products differentiated by reliability, which is directly linked to the uncertainty of renewable supply. We investigate the two pricing schemes in scenarios of large-scale renewable energy integration.

Priority service pricing [CW87] has been applied in different industries. As pointed out in Rao and Petersen [RP98]. "*For example, in transportation systems, railways offer express and regular freight services. The postal system offers priority and regular mail services. Most service industries provide some form of priority service in order to reduce waiting times for customers with high waiting costs. Other examples include computer service bureaus, job shops, and express toll roads.*" In power service, an early example of priority service pricing was the Pacific Gas and Electric tariff for large industrial customers that included explicit options for curtailable and interruptible power service [Rob93].

In this thesis, we focus on the application of interruptible power service to residential consumers, since the residential sector arguably places the greatest premium on *simple* service offerings that do not require excessive attention overhead.

We analyze a variant of priority service pricing which relies exclusively on capacity charges, and the capacity is differentiated by reliability levels. This is in contrast to the approach that splits priority service pricing to a priority charge and a service charge [CW87]. We will explain the exact implementation of our approach in the sequel, and we will then explain how duration can be introduced into our approach based on multilevel demand subscription.

The idea of the implementation of priority service pricing which we analyze is to offer residential consumers a menu of price–reliability pairs for *strips* of *power*, which can be illustrated via the concept of *ColorPower* [PBF13] as shown in figure 1.2. In the figure, the household subscribes for 0.6 kW to the red color[2], which has a reliability level of 100%, therefore this slice of power is guaranteed to be served. The 0.7 kW of yellow color may have a reliability of 90%, and this slice of electricity could be interrupted when the system is stressed. In contrast. the green color could be highly unreliable, for example, maybe it is only available when there is abundant renewable production. This slice of power can be used for flexible appliances, such as electric vehicles, water heaters and wet goods. These three levels of fuse limits are only imposed behind the smart meter and the household has full authority over which appliance is

[2]Since the household procures a consumption profile, the 0.6 kW refers to the average of the profile.

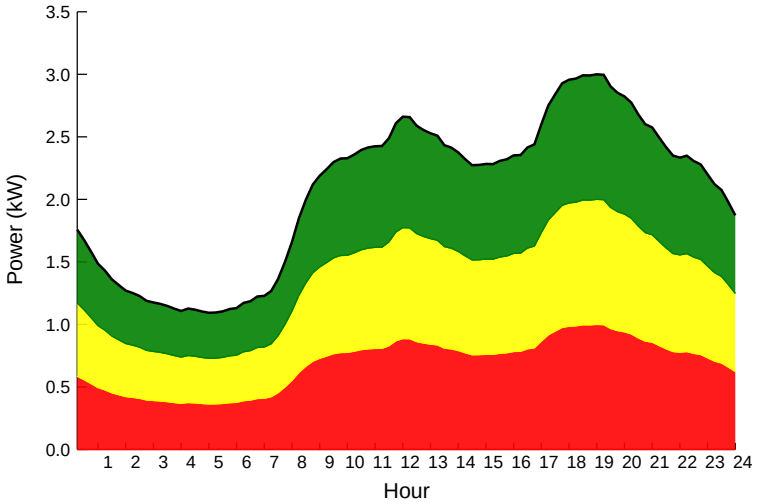

Figure 1.2: Illustration of priority service pricing. The black curve shows the intended consumption profile of a household in one day and strips of different colors indicate the subscription quantity of the household to power slices of different quality (reliability levels). The total power supplied to a household is stratified into three different levels (indicated in this figure by colors). Consumers can decide how to allocate their total power consumption among different levels of reliability, subject to the constraint that the total rating of devices switched into a given reliability level does not exceed the procured amount of power for that reliability level.

allocated to which color, as long as the limit of each color is not exceeded.

One way to implement this allocation is by tagging plugs with colors that correspond to reliability levels in the home [PBF13], either manually or automatically through a home energy router, as shown in figure 1.3. Thus, households enroll to an electricity service with an intuitive interpretation, while preserving control on their household consumption. This is the main appeal of priority service pricing, which strives to maintain the control of equipment under residential loads while engaging them in a service that is simple and intuitive. The necessary control and communication technology for implementing priority service pricing requires a means of tagging plugs according to reliability levels, an ability to monitor slices of different reliability in real time (e.g. 5-to-15 minute intervals), and an energy router that can receive control signals from a utility and relay them to plugs with the appropriate reliability tags, or undertake the color tagging on its own.

By selecting plans, consumers reveal their valuation for power. These valuations can be aggregated and bid into the wholesale electricity market. This promotes price discovery and an efficient allocation of resources under tight system conditions, which are expected to occur increasingly frequently in the

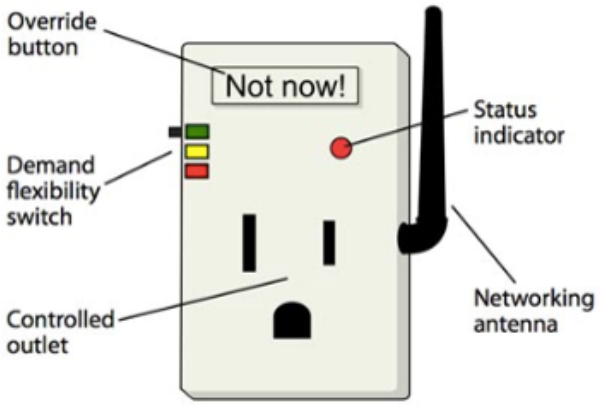

Figure 1.3: Illustration of the practical implementation of priority service pricing. In the proposal of [PBF13], major appliances or their outlets are equipped with switches that enable owners to select colors indicating their willingness to have the appliance shut on or off. Source: `http://energy.mit.edu/news/tomorrows-power-grid/`.

Figure 1.4: Envisioned implementation of multilevel demand subscription. Consumers can subscribe to different reliability levels and specify the desired duration by the scroll bar. The total subscription quantity and the corresponding payment are calculated according to a nonlinear pricing menu, which we are interested in designing.

future due to the integration of renewable resources.

Multilevel demand subscription is an extension of priority service pricing in

the sense that an extra component, i.e. duration, is an additional dimension according to which we differentiate pricing. This concept is further illustrated in figure 1.4. In an MDSP menu, each reliability level is associated with different duration levels and the price is a function of the duration. The duration can be interpreted as energy 'credits' that are topped up.

To further illustrate the concept, we consider a simple example with a horizon of 24 hours, and suppose that the red color is characterized by a reliability of 100%, while the green color is characterized by a reliability of 50%. The first household subscribes to 1 kW for the red color with a duration of 12 hours, whereas the second household subscribes for 1 kW of the green color for 24 hours. In this case, both households are entitled to consume 12 kWh over the entire horizon. However, the first household has a priority to be served first, in case of shortage in supply. Alternatively, suppose that the second household subscribes for 2 kW of the red color with a duration of 6 hours. In this case both households are entitled to consume 12 kWh over the entire horizon and they have the same priority. However, the peak demand of the first household is limited by 1 kW, whereas the peak demand of the second one is limited by 2 kW.

There are two merits brought about by the extra energy component, relative to priority service pricing limited to capacity charges. Firstly, consumers are afforded the freedom to specify the duration of their consumption, rather than subscribing for the whole horizon of service. This is especially relevant for households with rooftop PV panels, since it is likely that these households are self-sufficient during the daytime. Secondly, the hours when consumers utilize the credits indicate higher valuation, and the utility can take advantage of the revealed information in order to achieve higher efficiency. In contrast, in the implementation of priority service pricing that we consider in this work which is purely capacity based, a slice of power is assumed to carry the same valuation over the entire horizon. This results in the loss of important information regarding the valuation of consumers.

In multilevel demand subscription pricing, the requirement of differentiating the pricing of energy in addition to capacity makes the price menu more complicated relative to priority service pricing. This may present implementation complexity both for consumers as well as the utility. The trade-off between complexity and efficiency is to be investigated in this thesis.

1.4 Contributions

The main contributions of this dissertation are organized into two chapters, which are summarized in the following. We also summarize, in this section, a set of major assumptions in the present work under which our stated contributions are relevant.

In Chapter 2, we first revisit the textbook theory of priority service pricing and point out numerous stringent assumptions (such as non-convex production costs), which may not be respected in practice. We then design a priority service menu as the equilibrium solution to a Stackelberg game, which is modeled as a bilevel optimization problem involving a vertically integrated utility and consumers. We reformulate the equilibrium as a mixed-integer problem. As a consequence of this approach, we can integrate the menu design problem within a day-ahead unit commitment model. This allows us to design a menu which exactly meets the profit requirements of a firm. In order to tackle the computational challenge brought about by introducing scenarios of renewable production, the model is decomposed by ADMM and solved on a high-performance computing cluster. The quality of the solution is demonstrated by comparing the resulting solution with the bound obtained from dual decomposition. The approach is illustrated on a toy numerical example, as well as a large-scale model of the Belgian power market. This chapter is based on the following publications:

- Mou, Y., Papavasiliou, A., & Chevalier, P. (2017, June). Application of priority service pricing for mobilizing residential demand response in Belgium. In 2017 14th International Conference on the European Energy Market (EEM) (pp. 1-5). IEEE.
- Mou, Y., Papavasiliou, A., & Chevalier, P. (2019). A Bi-Level Optimization Formulation of Priority Service Pricing. IEEE Transactions on Power Systems, forthcoming. DOI: 10.1109/TPWRS.2019.2961173

The following assumptions have been adopted in this chapter. These assumptions will be further elaborated with the exposition of the models.

- Consumers are assumed to be risk-neutral. This is a standard assumption in the priority service pricing literature, and simplifies the formulation and resolution of the pricing model, since risk aversion introduces non-convexities which pose significant computational barriers to our analysis.
- The valuation of a consumer for power remains constant over time. Nonlinear pricing differentiates consumers according to their types, and each consumer type is represented by their valuation for power in our model. The dynamics of consumer preferences are captured by a time-varying consumption profile.
- All consumers follow the same consumption profile, which is therefore identical to the system-level profile. This assumption can be relaxed, however in this case the producer would need to know the profile of each type of consumer in order to design the price menu. Our presumption is that this is not practical, because this requires too detailed information on the side of the producer.

- The valuation breakpoints that separate consumers into different priority classes are determined exogenously in our model. Moreover, all consumers with non-negative valuations are served, i.e. the first valuation breakpoint is at 0 €/MWh.
- We examine a vertical setting in which the utility is assumed to be responsible for aggregating demand response and also for operating the production assets of the system. The assumption of a vertical monopoly is typical in nonlinear pricing theory. The price menu is designed from the perspective of a social planner, in order to maximize social welfare. One interesting extension of our work is to design the price menu with consideration of investment decisions [JT07].

In Chapter 3, we first introduce the traditional theory of multilevel demand subscription pricing and then improve it using a bilevel modeling approach similar to the one proposed in the previous chapter. The increased complexity of multilevel demand subscription for residential consumers promises increased operational efficiency, as it permits a finer differentiation of consumer classes by the producer. We propose an evaluation framework to compare the performance of priority service and multilevel demand subscription in a system with utility-scale renewable supply, residential renewable supplies, and residential storage. A case study is conducted on the Belgian power system in order to compare the performance in a quantitative way, in terms of social welfare and consumer costs. This chapter is based on the following publications:

- Mou, Y., Papavasiliou, A., & Chevalier, P. (2018, June). Application of multilevel demand subscription pricing for mobilizing residential demand response in Belgium. In 2018 IEEE International Energy Conference (ENERGYCON) (pp. 1-6). IEEE.
- Papavasiliou, A., Mou, Y., Cambier, L., & Scieur, D. (2017). Application of stochastic dual dynamic programming to the real-time dispatch of storage under renewable supply uncertainty. IEEE Transactions on Sustainable Energy, 9(2), 547-558.
- Working paper: Comparison of Priority Service and Multilevel Demand Subscription

This chapter is based on the following assumptions.

- We continue to assume that consumers are risk-neutral, and that the producer is a monopoly that maximizes social welfare when the price menu is designed.
- The production from roof-top PV panels is assumed to be perfectly correlated with the utility-level solar production and independent of the utility-level wind production.

- The surplus of roof-top PV production is injected to the grid without compensation for households.
- The roof-top PV production in different households is assumed to follow an identical profile.

In the last chapter, we draw conclusions and point out directions for future research.

Chapter 2

A Bilevel Optimization Formulation of Priority Service Pricing

2.1 Introduction

An important challenge of priority service is the pricing of different menu options. In order to appreciate the challenge, consider two extremes. In one extreme, an aggregator prices all levels of reliability at a very low price. In this case, all consumers enroll to the option with the highest level of reliability. This is undesirable, since the aggregator would neither be able to deliver the promised level of reliability, nor to discriminate consumers according to their valuation. On the other extreme, if the aggregator prices all levels of reliability at an excessively high price, then no consumers enroll voluntarily. In the middle ground there is an optimal menu which induces consumers to self-select options such that the utility can deliver power from an inherently uncertain supply side, while satisfying the quality of service that it commits to through the menu that it offers.

The theory for optimally designing such a menu has been developed by [CW87] and relies on strong assumptions. The appeal of the theory is that it only requires *aggregate* statistical information about the population, which is becoming increasingly available through real-world demand response pilots [FS10a, SA13, CB14, DLB+15].

2.1.1 Previous Work on Priority Differentiated Products

There has been further development of priority service pricing based on the seminal paper of Chao and Wilson [CW87], including menus differentiated by duration and reliability, and menus that account for capacity expansion [JT07]. Chao [Cha12] extends the consumer model to include the decision of actual consumption profile besides the subscription decision, and the difference between the subscribed profile and actual consumption profile is settled based on the spot price. Campaign [CO16] considers a profit-maximizing aggregator in a competitive setting. However, the aforementioned models involve stringent assumptions, are more difficult to implement in practice than what we propose in the present chapter, and rely on closed-form solutions that do not exploit the capabilities of powerful commercial optimization solvers.

The numerical appeal of our approach relies on the interpretation of the priority service pricing problem as a Stackelberg equilibrium, which is subsequently cast as a bilevel optimization problem. Game-theoretical approaches, especially Stackelberg games, have been widely adopted for solving practical tariff design problems. Askeland et al. [ABG19] formulate a bilevel model for describing the interaction between the end-users and a distribution system operator, in order to design the optimal grid tariff. Govaerts et al. [GBD18] study how the distribution tariff design influences the behavior of a strategic aggregator of residential consumers with PV panels and energy storage systems, on a wholesale market. The aggregator-wholesale market interaction is formulated as a Stackelberg game. Grimm et al. [GOS$^+$19] propose bilevel models for determining the optimal interplay between a retailer designing a tariff and prosumers who decide on using storage, consumption, electricity purchases, as well as electricity sales to the grid. Momber et al. [MWSR15] consider a specific application of bilevel programming for plug-in electric vehicle aggregators. Cervilla et al. [CVC15] propose new electricity tariffs for regulating distributed generation resources, as opposed to net metering. The authors put forward a bilevel model to obtain the evolution of the access tariffs. Then the optimal distributed generation investment of the consumers under net metering policy and access tariffs is investigated. Bilevel modes are also applied in other areas of the energy networks [KDPV$^+$15], such as optimal control of a virtual power plant, deregulated spot electricity markets, etc. In this chapter, we adopt the bilevel optimization method for the priority service menu design problem.

2.1.2 Contribution and Chapter Organization

In this chapter we revisit Chao's theory [CW87] and extend it to a more realistic set of assumptions. In doing so, we couple the menu design problem with production simulation models based on unit commitment. Embedding the menu design problem with unit commitment allows us to override a number of

weaknesses in the traditional theory, and creates numerous advantages from an analytical standpoint.

1. We are able to clarify exactly what the service of a certain reliability level means[1].

2. We are able to introduce profit targets that the menu should seamlessly achieve in our model, which are essential for cost-benefit analyses of smart meter deployment [FS10a].

3. Coupling realistic models of demand response with unit commitment, which has been attempted in past literature under less realistic settings such as real-time pricing or fixed retail pricing [SS09, Sio12, PO14], is essential for capturing the operational benefits of demand response (mitigation of ramping constraints, reduction of non-convex costs related to startup and min load, etc.).

4. The temporal coupling in the production model (due to min up/down time constraints, and ramp rates) is captured.

The rest of the chapter is organized as follows. Section 2.2 introduces the traditional theory of priority service pricing. The section additionally introduces some background on dual decomposition and the alternating direction method of multipliers (ADMM), which are used in the numerical case study of the Belgian system. Section 2.3 casts the menu design problem as a Stackelberg game, which is reformulated as an MILP. Section 2.4 presents the decomposition techniques that are adopted in order to solve the model. Section 2.5 conducts two case studies that include a toy example and a large-scale simulation of the Belgian power system.

2.2 Preliminaries

2.2.1 Priority Service Pricing

In this section, we introduce the traditional theory of priority service pricing based on [CW87] and [Ore13], and we point out several stringent assumptions that are typically not respected in practice.

On the consumer side, the aggregate demand function is represented by $D(\cdot, \omega)$ and the willingness-to-pay function is represented by $P(\cdot, \omega)$, both contingent on the 'state of the world' ω. The producer offers a menu of capacity strips with reliability r and price π. The objective of each consumer is to choose

[1] Five minutes of interruption every hour and one month of *straight* interruption every year imply large differences in consumer comfort, even if both are characterized by a reliability of 11/12.

from the menu $M = \{r, \pi\}$ an option that maximizes expected surplus. This is a restricted variant of priority service pricing since we do not split it into a priority charge and a service charge [CW87]. Assuming risk-neutral consumers, the consumer problem for type v is to solve

$$S(v) = \max \{r \cdot v - \pi | (r, \pi) \in M\}. \tag{2.1}$$

Regarding the cost model, the supply is assumed to be uncertain due to random outages of generators and renewable energy fluctuations. The short-run cost function in scenario ω at quantity z is denoted as $C(z, \omega)$.

In order to design the optimal price menu which induces consumers to choose the reliability level that the system can offer on aggregate under efficient dispatch, we need to compute the function $R(v)$ that describes the reliability level that a consumer with valuation v would obtain under efficient dispatch. Denote by $\hat{p}(\omega)$ the spot price, associated with a given random outcome ω, which is given by

$$\hat{p}(\omega) = \min\{\max[P(z, \omega), C(z, \omega)] | z \geq 0\}. \tag{2.2}$$

This is the intersection of the marginal willingness-to-pay function and the marginal cost function. Then the service reliability of a type v consumer is given by

$$R(v) = \Pr\{\hat{p}(\omega) \leq v\}. \tag{2.3}$$

Figure 2.1 illustrates the concept of reliability $R(v)$. The horizontal axis shows the equilibrium market clearing quantity under efficient dispatch, while the vertical axis presents the marginal cost of the system and the consumer valuation. On the production side, we consider two scenarios. In scenario ω_1, the cost function is $C(z, \omega_1)$ with a probability of 0.7; in scenario ω_2, the cost function is $C(z, \omega_2)$ with a probability of 0.3. Then the spot price will be $\hat{p}(\omega_1)$ with a probability of 0.7 and $\hat{p}(\omega_2)$ with a probability of 0.3. Consumers whose valuations are higher than the spot price will be served, so we can conclude

$$R(v) = \begin{cases} 0, & v < p(\omega_2) \\ 0.3, & p(\omega_2) \leq v < p(\omega_1). \\ 1, & v \geq p(\omega_1) \end{cases} \tag{2.4}$$

As shown in Chao et al. [CW87], the price menu which maximizes social welfare is as follows:

$$M^\star = \{p^\star(v), r^\star(v) | 0 \leq v \leq V\}, \tag{2.5}$$

$$r^\star(v) = R(v), \tag{2.6}$$

$$p^\star(v) = \int_0^v [r^\star(v) - r^\star(u)] du. \tag{2.7}$$

When implementing a priority service menu in practice, a finite number of priority classes is expected. We first divide consumers into n priority classes

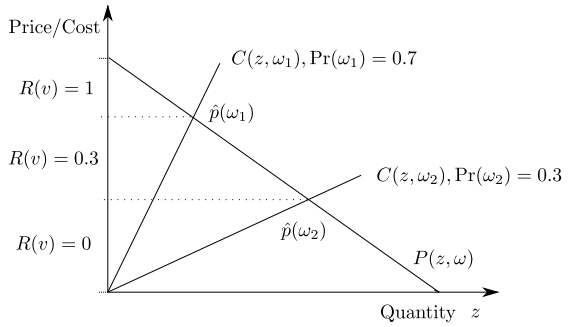

Figure 2.1: Illustration of $R(v)$ in the traditional priority service pricing theory. $C(z,\omega_1)$ and $C(z,\omega_2)$ describe the cost function in different scenarios. Whereas $P(z,\omega)$ shows the valuation function, which is assumed to be the same in both scenarios. The intersection between a cost function and the demand function indicates the spot price, which is $\hat{p}(\omega_1)$ with a probability of 0.7 and $\hat{p}(\omega_2)$ with a probability of 0.3. When the valuation of a consumer is lower than $\hat{p}(\omega_2)$, he can never get served, so $R(v) = 0$; similarly, if the valuation is even higher than $\hat{p}(\omega_1)$, this consumer can always be served and $R(v) = 1$; if the valuation falls between $\hat{p}(\omega_1)$ and $\hat{p}(\omega_2)$, the consumer is served in scenario ω_2 with a probability of 0.3, so $R(v) = 0.3$.

based on their valuation, say $[0, v_1], [v_1, v_2], \ldots, [v_{n-1}, v_n]$, where $0 = v_0 < v_1 < \ldots < v_{n-1} < v_n = V$. Suppose that the service is provided to consumers in such a manner that consumers in a higher value class are given a higher priority and pay more, but within each class, all consumers are treated equally and therefore are served in a random order. Then the probability that a consumer with a valuation v between v_i and v_{i+1} will be served is

$$r(v) = r_i = \int_{v_i}^{v_{i+1}} \left[\frac{D(v) - D(v_{i+1})}{D(v_i) - D(v_{i+1})} \right] dR(v) + R(v_i). \tag{2.8}$$

Using integration by parts, we rewrite the above expression as

$$r(v) = r_i = \frac{\int_{v_i}^{v_{i+1}} R(v) dD(v)}{D(v_{i+1}) - D(v_i)}. \tag{2.9}$$

The interpretation of Eq. (2.9) is as follows. The denominator is the demand between valuation v_i and v_{i+1}, while the numerator is the realized supply. Since within this priority class consumers are treated equally and served in a random order, r_i is the average reliability in this priority class. The corresponding price is given by

$$p(v) = p_i = v_0 \cdot r_0 + \sum_{j=1}^{i} v_j \cdot (r_j - r_{j-1}). \tag{2.10}$$

Nevertheless, from the description of the traditional theory we can see that

it requires certain limiting assumptions which are not necessarily satisfied in practice:

- The cost function is assumed be to convex, so non-convex production costs, such as start-up and min-load costs, cannot be handled.
- The presented model is static, in the sense that there is no coupling over time periods (e.g. due to minimum up and down times, ramp constraints, and so on).
- The reliability level r_i of each option does not reveal more specific information about how consumers could be interrupted.

To deal with these shortcomings, we incorporate unit commitment into the menu design problem and model it as a Stackelberg game, which is reformulated as a bilevel optimization problem. In this model, the non-convex costs are captured directly. The time-couping constraints of generators and the pumped hydra storage are modeled explicitly. Moreover, the output of the model allows us to investigate into the interruption pattern of each option. The model is presented in section 2.3.

2.2.2 Dual Decomposition

With the increasing integration of renewable production, the modeling of modern power systems is relying increasingly on scenario-based methods [Sag12, CCMGB06]. Due to their increased size, scenario-based models pose significant computational challenges. Decomposition methods, such as Benders decomposition, dual decomposition, and the alternating direction method of multipliers (ADMM) have been exploited ubiquitously in order to decompose the resulting large-scale models into subproblems, which can be solved in parallel. High-performance computing has increased the appeal of such methods by allowing an acceleration in the resolution of these problems. In this chapter, dual decomposition and ADMM are employed. We provide a brief introduction to dual decomposition in this section, and to ADMM in the next section.

This section is adapted from [BPC+11, KZ18]. Consider an optimization problem, where the objective function is separable:

$$\min_x \quad f(x) = \sum_{i=1}^{N} f_i(x_i) \tag{2.11}$$

$$(y) : \sum_{i=1}^{N} A_i x_i = b, \tag{2.12}$$

where $x = (x_1, \ldots, x_N)$, $x \in \mathcal{R}^n$ and $x_i \in \mathcal{R}_i^n$. The Lagrangian can be written

as

$$L(x,y) = \sum_{i=1}^{N} L_i(x_i,y) = \sum_{i=1}^{N} \big(f_i(x_i) + y^T A_i x_i - (1/N) y^T b\big), \tag{2.13}$$

where y are the dual variables of the equality constraints. For a fixed y, the Lagrangian dual function can be decomposed as

$$\phi(y) = \sum_{i=1}^{N} \phi_i(y), \tag{2.14}$$

where

$$\phi_i(y) := \min_{x_i} L_i(x_i,y) = f_i(x_i) + y^T A_i x_i - (1/N) y^T b. \tag{2.15}$$

We seek to find the best lower bound for the primal problem by solving the maximization of the Lagrangian dual problem:

$$z_{LB} := \max_{y} \sum_{i=1}^{N} \phi_i(y). \tag{2.16}$$

In a dual decomposition method, we iteratively search for dual values y that maximize the Lagrangian dual function. Many algorithms are available for tackling this problem, such as the subgradient method [POO11, PO13], the cutting plane method [KZ18], and bundle methods [Sag12]. In the model presented later, the dual variables are in a low-dimensional space, which is suitable for a standard cutting plane method. The cutting plane method approximates (2.16) by iteratively adding linear inequalities. We define the master problem:

$$m_k := \max_{\theta_i, y} \quad \sum_{i=1}^{N} \theta_i \tag{2.17}$$

$$\text{s.t.} \quad \theta_i \le \phi_i(y^l) + (A_i x_i^l - b/N)^T (y - y^l), \tag{2.18}$$

$$i = 1, \dots, N, l = 0, 1, \dots, k. \tag{2.19}$$

The dual variable y^{k+1} is obtained by solving the master problem at iteration k. The procedure is summarized in algorithm 1.

2.2.3 Alternating Direction Method of Multipliers

This section is adapted from [BPC+11] and we present two different formats of the ADMM algorithm. A typical format adds a regulation term to the dual decomposition formulation whereas the second format deals with a general constrained convex optimization problem by introducing a projection operator. The two formats are described as follows:

Algorithm 1 Dual Decomposition Based on Cutting-Plane Method

1: Initialize $k := 0$ and $y^0 := 0$.
2: **while** $m_k - z_{LB} > \varepsilon$ **do**
3: Solve (2.15) to obtain $\phi_i(y^k)$ and x_i^k for a given y^k and $\forall i = 1, \ldots, N$.
4: Set $z_{LB} \longleftarrow \max\{z_{LB}, \phi(y^k)\}$.
5: For a given $\phi_i(y^k)$ and x_i^k, add new cuts to the master problem and solve for m_k and y^{k+1}.
6: Set $k \longleftarrow k + 1$.
7: **end while**

The typical ADMM algorithm solves problems in the form

$$\min_{x,z} \quad f(x) + g(z) \tag{2.20}$$

$$(y) : Ax + Bz = c \tag{2.21}$$

with variables $x \in \mathcal{R}^n$ and $z \in \mathcal{R}^m$, where $A \in \mathcal{R}^{p\times n}$, $B \in \mathcal{R}^{p\times m}$ and $c \in \mathcal{R}^p$. The functions f and g are assumed to be convex.

The augmented Lagrangian is expressed as

$$L_\rho(x, y, z) = f(x) + g(z) + y^T(Ax + Bz - c) + (\rho/2)\|Ax + Bz - c\|_2^2. \tag{2.22}$$

ADMM consists of the iterations

$$x^{k+1} := \arg\min_x L_\rho(x, y^k, z^k) \tag{2.23}$$

$$z^{k+1} := \arg\min_z L_\rho(x^{k+1}, y^k, z) \tag{2.24}$$

$$y^{k+1} := y^k + \rho(Ax^{k+1} + Bz^{k+1} - c), \tag{2.25}$$

where $\rho > 0$. Define $u = (1/\rho) \cdot y$ as the scaled dual variable. One widely adopted version of ADMM can be expressed as

$$x^{k+1} := \arg\min_x \left(f(x) + (\rho/2)\|Ax + Bz^k - c + u^k\|_2^2\right) \tag{2.26}$$

$$z^{k+1} := \arg\min_z \left(g(z) + (\rho/2)\|Ax^{k+1} + Bz - c + u^k\|_2^2\right) \tag{2.27}$$

$$u^{k+1} := u^k + Ax^{k+1} + Bz^{k+1} - c. \tag{2.28}$$

The typical ADMM algorithm can be adapted to solve a generic constrained convex optimization problem

$$\min_x \quad f(x) \tag{2.29}$$

$$\text{s.t.} \quad x \in \mathcal{C}, \tag{2.30}$$

with $x \in \mathcal{R}^n$, where f and $\mathcal{C}$ are convex. We introduce an auxiliary variable z

and rewrite the problem as follows:

$$\min_{x,z} \quad f(x) + g(z) \tag{2.31}$$

$$\text{s.t.} \quad x - z = 0 \tag{2.32}$$

where g is the indicator function of $\mathcal{C}$. The augmented Lagrangian (using the scaled dual variable) is

$$L_\rho(x, z, u) = f(x) + g(z) + (\rho/2)\|x - z + u\|_2^2, \tag{2.33}$$

so the scaled form of ADMM for this problem is

$$x^{k+1} := \arg\min_x \left(f(x) + (\rho/2)\|x - z^k + u^k\|_2^2 \right) \tag{2.34}$$

$$z^{k+1} := \Pi_{\mathcal{C}}(x^{k+1} + u^k) \tag{2.35}$$

$$u^{k+1} := u^k + x^{k+1} - z^{k+1}, \tag{2.36}$$

where Π is the Euclidean projection. This is the ADMM formulation that is adopted in this chapter.

2.3 Modeling the Menu Design Problem as a Stackelberg Equilibrium

2.3.1 Overview of the Bilevel Model

In the following, we will cast the menu design problem as a Stackelberg game. The leader in the Stackelberg game is the producer who designs the menu. The followers are the consumers, who react to the menu offered by the leader. The information asymmetry arises from the fact that the followers have private knowledge of their *type*, whereas the leader is limited to statistical information about the distribution of types in the population (e.g. demand functions obtained from market surveys). The interesting aspect of the model is that the leader integrates the optimal reaction of the followers into the menu design problem. This gives rise to a mathematical program with equilibrium constraints. Although such problems are generally challenging, we exploit the specific structure of the game in order to cast the problem as a mixed integer linear program. This allows us to incorporate realistic production constraints to the problem, which are absent from the traditional literature on priority service pricing. We thus arrive at a model that integrates menu design with unit commitment.

A high-level description of the bilevel model is provided in Eqs. (2.37)-(2.41). The model is further illustrated in figure 2.2.

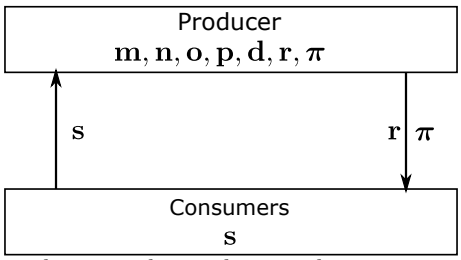

Figure 2.2: Interaction between the producer and consumers in the bilevel model.

$$\max_{\mathbf{m},\mathbf{n},\mathbf{o},\mathbf{p},\mathbf{d},\mathbf{r},\boldsymbol{\pi}} \; SW(\mathbf{m},\mathbf{n},\mathbf{o},\mathbf{p},\mathbf{d}) \tag{2.37}$$

$$\text{s.t.} \quad (\mathbf{m},\mathbf{n},\mathbf{o},\mathbf{p},\mathbf{d}) \in \mathcal{X} \tag{2.38}$$

$$\mathbf{r} = \phi(\mathbf{d},\mathbf{s}^\star) \tag{2.39}$$

$$\Pi_\star = \psi(\mathbf{m},\mathbf{o},\mathbf{p},\mathbf{s}^\star,\boldsymbol{\pi}) \tag{2.40}$$

$$\mathbf{s}^\star \in \arg\max_{\mathbf{s}} \{CS(\mathbf{r},\boldsymbol{\pi}) : \mathbf{s} \in \mathcal{Y}\} \tag{2.41}$$

The variables $\mathbf{m}$, $\mathbf{n}$, $\mathbf{o}$, $\mathbf{p}$ correspond to startup and shutdown decisions, unit commitment, and power generation. The subscription quantity of each consumer to each option is indicated by $\mathbf{s}$, while the supply to each option is indicated by $\mathbf{d}$. The reliability and price of the menu options is denoted by $\mathbf{r}$ and $\boldsymbol{\pi}$, respectively. The profit target of the producer[2] is denoted by $\Pi_\star$. All the notations are summarized in section 2.A.

The function SW in Eq. (2.37) is the objective of the producer, which is to maximize social welfare. Eq. (2.38) defines the technical constraints of the producer. Constraint (2.39) expresses the fact that the price menu which is designed by the producer needs to deliver a promised level of reliability $\mathbf{r}$, which is affected by how consumers react to the offered menu through their subscription decision $\mathbf{s}^\star$. Condition (2.40) further requires that the menu be designed in such a way that the profit target $\Pi_\star$ is reached. Consumers decide on their subscription by maximizing their surplus CS, as indicated by Eq. (2.41).

The model could be infeasible if the profit target $\Pi_\star$ is assigned an extremely large value. A reasonable one could be the profit from a flat tariff. The equality in (2.40) can be expressed as an inequality if the goal is to specify a minimum profit level for the aggregator. Alternatively, Wilson [Rob93] dualizes the profit target by using a Lagrange multiplier penalty in the objective function of the relaxed problem. This non-negative penalty can be adjusted in order to meet

[2]Nonlinear pricing theory typically considers the setting of a regulated monopoly that needs to recover certain amount of costs, such as investment costs, by imposing a target on the profit, see chapter 5 of [Rob93] for details.

different profit targets. When the penalty is equal to zero, the model maximizes social welfare whereas increasing the penalty arbitrarily results in a model that maximizes the profit of the aggregator.

In the following, we introduce the lower-level consumer model and the upper-level producer model in detail. We then present the bilevel model and its reformulation as an MILP.

2.3.2 The Consumer Model

The starting point of nonlinear pricing is to capture information asymmetry by assigning a type to consumers [Rob93]. This is private information, in the sense that the producer cannot know a priori the type of a given consumer (although this information is revealed to the producer after the consumers self-select their preferred menu option). In priority service pricing, types correspond to *valuation* for power. A household could be composed of many different consumer types.

Before presenting the consumer model, we point out two strong assumptions that are typically employed in the priority service pricing literature [COSW86] regarding the demand side of the model. The first assumption is that the priority ranking of consumers for power remains constant over time. The second assumption is that loads are synchronized.

Given the above assumptions, we arrive at the following consumer model. Given a set of consumer types, $\mathcal{L}$, a consumer of type $l \in \mathcal{L}$ is characterized by a valuation V_l, which represents the priority ranking of a consumer, and remains constant over the whole horizon according to the first assumption. This allows us to arrive at a single menu. Without loss of generality, we order consumers as $V_l < V_{l+1}$. In period t, the consumer of type l requires $D_{l,t}$ units of power, where $D_{l,t} = \bar{D}_l \cdot \Theta_t$. Here, $\bar{D}_l$ corresponds to the average load of type l and Θ_t corresponds to the dynamic profile of consumption. This dynamic profile is identical for all consumers and the same as the load profile of the residential sector, due to our second assumption that loads are synchronized. The synchronization of loads can be relaxed; however, that would place significant additional information requirements on the producer for knowing the dynamic profile of each different type. The load profile of the residential sector is a time series indicating the hourly electricity consumption of the residential sector. The concept is depicted in figure 2.3. By definition, $\sum_{t \in \mathcal{T}} \Theta_t = T$, where T is the number of time periods over which we are designing the menu.

As a follower, the consumer selects service options from a menu with a set of options $\mathcal{I}$. Each of the options corresponds to a unit of electricity consumption with reliability r_i and price π_i. Reliability r_i is defined as the fraction of energy offered to option i, divided by the energy requested under option i. More specifically, denote the subscription quantity to option i as s_i and the supply to this option at period t and scenario ω as $d_{i,t,\omega}$. In choosing option i, consumer

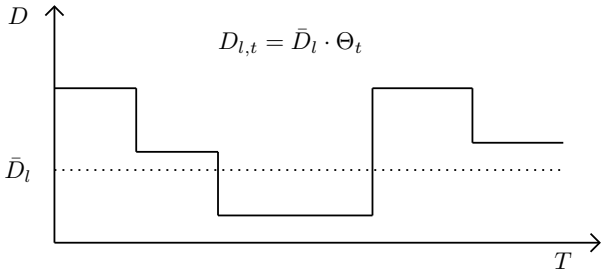

Figure 2.3: A consumer of type l follows a load profile $D_{l,t}$. Since loads are assumed to be synchronized, this profile can be expressed as $D_{l,t} = \bar{D}_l \cdot \Theta_t$, where Θ_t is the dynamic profile of the system and $\bar{D}_l$ is the average electricity consumption of type l.

l essentially procures $s_{l,i} \cdot \Theta_t$ following a *profile* Θ_t, so that the energy that is requested under option i is given as $\sum_{t\in\mathcal{T}} s_i \cdot \Theta_t$. The energy that is actually offered to option i is calculated as $\sum_{\omega\in\Omega} P_\omega \sum_{t\in\mathcal{T}} d_{i,t,\omega}$, where P_ω is the probability of scenario ω. Thus, r_i is expressed as $\sum_{\omega\in\Omega} P_\omega \sum_{t\in\mathcal{T}} d_{i,t,\omega} / \sum_{t\in\mathcal{T}} s_i \cdot \Theta_t$. This is the origin of constraint (2.59), which we present later.

Since π_i is the hourly price of option i, the total payment of subscribing for a unit of power under option i for the entire horizon T of the contract amounts to $\pi_i \cdot T$. Concretely, given r_i and π_i from the upper level producer model, the optimization problem of the consumer of type l can be described as follows:

$$\max_{s_{l,i}} \quad V_l \cdot \sum_{t\in\mathcal{T}} \sum_{i\in\mathcal{I}} r_i \cdot s_{l,i} \cdot \Theta_t - \sum_{i\in\mathcal{I}} s_{l,i} \cdot \pi_i \cdot T \tag{2.42}$$

$$\text{s.t.} \quad \sum_{i\in\mathcal{I}} s_{l,i} \cdot \Theta_t \leq D_{l,t}, t \in \mathcal{T} \tag{2.43}$$

$$s_{l,i} \geq 0, i \in \mathcal{I} \tag{2.44}$$

The variable $s_{l,i}$ indicates the amount of power that consumer l allocates to option i. The first term in the objective function indicates the benefit of a risk-neutral consumer for this profile. The second term in the objective function corresponds to the payment that needs to be submitted to the producer in order to secure this service. Constraint (2.43) requires that the total subscription of the consumer should not exceed the load of the consumer. Since $\sum_{t\in\mathcal{T}} \Theta_t = T$ and $D_{l,t} = \bar{D}_l \cdot \Theta_t$, we can rewrite the model equivalently as

$$(CP_l) : \max_{s_{l,i}} \quad \sum_{i\in\mathcal{I}} (V_l \cdot r_i \cdot s_{l,i} - s_{l,i} \cdot \pi_i) \tag{2.45}$$

$$(\gamma_l) : \sum_{i\in\mathcal{I}} s_{l,i} \leq \bar{D}_l \tag{2.46}$$

$$s_{l,i} \geq 0, i \in \mathcal{I} \tag{2.47}$$

We wish to use the optimality conditions of this problem as constraints of the producer problem. We do this in order to capture the fact that, when designing a menu, the producer accounts for the optimal reaction of the consumers. In complementarity form, these conditions will be problematic. Since CP_l is an LP, we wish to express the optimality conditions of the consumer problem as a collection of primal feasibility, dual feasibility, and strong duality conditions [MAG05, GCGBR09], and we further exploit the special structure of the consumer problem so as to describe the optimal subscription of the consumer as a binary variable. As we illustrate later in the thesis, this is essential for our MILP formulation of the bilevel problem.

The dual of (CP_l) can be expressed as:

$$(CD_l): \min_{\gamma_l} \quad \gamma_l \cdot \bar{D}_l \tag{2.48}$$

$$\text{s.t.} \quad \gamma_l \geq r_i \cdot V_l - \pi_i, i \in \mathcal{I} \tag{2.49}$$

$$\gamma_l \geq 0 \tag{2.50}$$

The interpretation of γ_l is that it captures the surplus that the consumer achieves by selecting the best option. Strong duality requires that

$$\gamma_l \cdot \bar{D}_l = \sum_{i \in \mathcal{I}} r_i \cdot s_{l,i} \cdot V_l - \sum_{i \in \mathcal{I}} \pi_i \cdot s_{l,i}. \tag{2.51}$$

Eq. (2.51) involves bilinear terms when it is treated as a constraint of the reformulated single-level problem, which cannot be dealt with by MILP solvers. We override this problem by showing that the optimal decision of the consumer is binary.

Proposition 1. *There exists* $\tilde{\mathbf{s}}_l = (\tilde{s}_{l,i}, i \in \mathcal{I})$ *with* $\tilde{s}_{l,i} \in \{0, \bar{D}_l\}$ *which attains the optimal objective function value.*

Proof. The KKT conditions of (CP_l) are given by

$$0 \leq s_{l,i} \perp -r_i \cdot V_l + \pi_i + \gamma_l \geq 0 \tag{2.52}$$

$$0 \leq \gamma_l \perp \bar{D}_l - \sum_i s_{l,i} \geq 0 \tag{2.53}$$

There are two cases to be considered:

Case 1: If $\bar{D}_l - \sum_i s^\star_{l,i} > 0$, then $\gamma_l = 0$, which implies that consumer l derives zero benefits at the optimal solution, so $\tilde{s}_{l,i} = 0$ for all $i \in \mathcal{I}$ is optimal.

Case 2: If $\bar{D}_l - \sum_{i \in \mathcal{I}} s^\star_{l,i} = 0$, then it suffices to show that if two options are 'active' (in the sense that $s > 0$) then they have an equal payoff, and can therefore be equivalently replaced by a single option. Applying this argument for all options that are active gives the desired conclusion: consider any two options i and j for which $s^\star_{l,i} > 0$ and $s^\star_{l,j} > 0$. Then $-r_i \cdot V_l + \pi_i + \gamma_l = 0$ and $-r_j \cdot V_l + \pi_j + \gamma_l = 0$, and substituting out γ_l, we have $r_i \cdot V_l - \pi_i = r_j \cdot V_l - \pi_j$. $\square$

The above proposition implies that $s_{l,i}$ can be expressed as $s_{l,i} = \bar{D}_l \cdot \mu_{l,i}$, where $\mu_{l,i} \in \{0, 1\}$ are binary variables. Thus, Eq. (2.51) is rewritten as

$$\gamma_l = \sum_{i \in \mathcal{I}} r_i \cdot \mu_{l,i} \cdot V_l - \sum_{i \in \mathcal{I}} \pi_i \cdot \mu_{l,i}. \tag{2.54}$$

Combined with McCormick envelopes[3], this reformulation will allow us to cast the lower-level optimality conditions of the Stackelberg game as a set of mixed integer linear constraints. This will be detailed in section 2.3.4.

2.3.3 The Producer Model

We follow the standard literature on priority service pricing [Rob93, CW87, COSW86] in assuming a vertical setup where the utility which is responsible for aggregating demand response also owns the production assets of the system.

An interesting extension of the present work is to extend our mathematical programming reformulation in order to analyze aggregator competition. This model may be cast as an equilibrium problem with equilibrium constraints, where aggregators maximize profit by offering different price menus and consumers aim at extracting the greater possible surplus.

As a leader of the Stackelberg game, the producer seeks to price reliability so that residential consumers self-select reliability levels which are consistent with the generation mix of the system. Information asymmetry implies that the producer does not know, at the menu design stage, the type (i.e. the valuation) of an individual consumer. Instead, the producer has access to the *distribution* of types in the population. This is exactly the demand function of the system. For the derivation of constraint (2.61), we will specifically assume an affine demand function of the form $D(v) = -K \cdot v + b$. Note, however, that the priority service model is not limited to affine demand functions. We use a discrete approximation of the demand function, with the valuation breakpoints[4] V_i^B $(i = 0 \dots I)$, with the valuation of the first breakpoint corresponding to $V_0^B = 0$ €/MWh. These breakpoints separate consumers into I groups and $(V_{i-1}^B + V_i^B)/2$ corresponds to the average valuation of consumer group $i \in \mathcal{I}$, while $K \cdot (V_i^B - V_{i-1}^B)$ corresponds to the load (in MW) of group $i \in \mathcal{I}$. *Given* a choice of options by individual consumers, $s_{l,i}^\star$, the producer problem then is written as follows.

[3] We use McCormick envelopes in order to represent the product of a binary variable and a continuous variable. This is therefore an exact linearization, rather than a relaxation.

[4] In determining these breakpoints, we follow the standard priority service literature by assuming that these values are determined exogenously.

$$\max_{\substack{\mathbf{m},\mathbf{n},\mathbf{o},\mathbf{p} \\ r_i,\pi_i,d_{i,t,\omega}}} \quad \sum_{\omega\in\Omega} P_\omega \sum_{t\in\mathcal{T}} \Big(\sum_{i\in\mathcal{I}} 0.5\cdot(V^B_{i-1}+V^B_i)\cdot d_{i,t,\omega} - h_{t,\omega}(\mathbf{m},\mathbf{n},\mathbf{o},\mathbf{p}) \Big) \tag{2.55}$$

$$\text{s.t.} \quad f_{g,\omega}(\mathbf{m},\mathbf{n},\mathbf{o},\mathbf{p}) \le 0, g\in\mathcal{G}, \omega\in\Omega \tag{2.56}$$

$$\sum_{i\in\mathcal{I}} d_{i,t,\omega} = \sum_{g\in\mathcal{G}} p_{g,t,\omega} + S_{t,\omega} + W_{t,\omega}, t\in\mathcal{T}, \omega\in\Omega \tag{2.57}$$

$$d_{i,t,\omega} \le s_i\cdot\Theta_t, i\in\mathcal{I}, t\in\mathcal{T}, \omega\in\Omega \tag{2.58}$$

$$T\cdot r_i\cdot s_i = \sum_{\omega\in\Omega} P_\omega \sum_{t\in\mathcal{T}} d_{i,t,\omega}, i\in\mathcal{I} \tag{2.59}$$

$$T\cdot\sum_{i\in\mathcal{I}} s_i\cdot\pi_i - \sum_{\omega\in\Omega} P_\omega \sum_{t\in\mathcal{T}} h_{t,\omega}(\mathbf{m},\mathbf{n},\mathbf{o},\mathbf{p}) = \Pi_\star \tag{2.60}$$

$$s_i = K\cdot(V^B_i - V^B_{i-1}), i\in\mathcal{I} \tag{2.61}$$

$$\sum_{l\in\mathcal{L}} s^\star_{l,i} = s_i, i\in\mathcal{I} \tag{2.62}$$

$$d_{i,t,\omega}, p_{g,t,\omega} \ge 0, i\in\mathcal{I}, g\in\mathcal{G}, t\in\mathcal{T}, \omega\in\Omega \tag{2.63}$$

$$m_{g,t,\omega}, n_{g,t,\omega}, o_{g,t,\omega} \in \{0,1\}, g\in\mathcal{G}, t\in\mathcal{T}, \omega\in\Omega \tag{2.64}$$

The goal of the producer is to maximize welfare by using the available production assets of the system. The cost is expressed by the function $h_{t,\omega}$, and can include production costs as well as non-convex costs related to startup and minimum load. The variables $\mathbf{m}$, $\mathbf{n}$, $\mathbf{o}$, $\mathbf{p}$ correspond to startup and shutdown decisions, unit commitment and power generation. The set of generators is denoted as $\mathcal{G}$. The generator constraints are expressed by the function $f_{g,\omega}$, and can include standard constraints of unit commitment problems, such as minimum up and down times, ramp rates, startup profiles, production limits, and so on [PBF13]. The quantity of consumers signed up under option i is indicated by s_i. Their hourly supply is $d_{i,t,\omega}$. Constraint (2.57) describes demand and supply balance. Note that uncertainty in the model corresponds to a set of solar and wind production scenarios, with the corresponding output of these resources denoted by $S_{t,\omega}$ and $W_{t,\omega}$. Constraint (2.58) requires that the supply to consumers be limited by their subscription decisions. Constraint (2.59) determines the reliability of option i as the fraction of energy offered to option i, divided by the energy requested under option i. In the case study, this constraint considers the reliability over the entire horizon of the menu design problem (which we assume to be one year). The constraint can be adapted straightforwardly in order to guarantee that the reliability is delivered on a daily/weekly/monthly basis. But the extra computational challenge brought about by the adaptation is to be investigated. The producer seeks to achieve a profit target $\Pi_\star$, as indicated in constraint (2.60). Constraint (2.61) implies

that the subscription quantity of each option is equal to the estimated demand of the corresponding demand group. This constraint makes sure the average valuation of consumers in option i is $0.5 \cdot (V_{i-1}^B + V_i^B)$, which is consistent with (2.55). Note that we implicitly require that the designed menu induces *all* consumers to select a specific option in the menu. However, by setting the first valuation breakpoint V_0^B to a cut-off level, the present model can be easily extended to the case where certain consumers are intentionally induced not to select *any* option from the menu. The subscription quantity of each option is equal to the sum of the subscription quantity of consumers in this option, as indicated by (2.62). One single menu is designed for the whole horizon, but the model can be easily adapted to offer monthly/seasonal menus.

2.3.4 The Bilevel Model

Given a choice $s_{l,i}^\star$ of menu options by consumer types, the producer model is a welfare maximizing commitment and dispatch of the system, of the sort encountered in the standard unit commitment literature. The delicate task of the producer is to offer a price menu (r_i, π_i) so that consumers' reaction $s_{l,i}^\star$ is compatible with the estimated grouping of consumers indicated by V_i^B, while achieving its profit target. We thus revisit the mathematical programs of section 2.3.2 and section 2.3.3 in order to develop the full bilevel formulation. Concretely, we are interested in expressing the following bilevel problem in MILP form:

$$\min_{\substack{\mathbf{m},\mathbf{n},\mathbf{o},\mathbf{p} \\ r_i,\pi_i,d_{i,t,\omega}}} \quad \sum_{\omega\in\Omega} P_\omega \sum_{t\in\mathcal{T}} \Big(h_{t,\omega}(\mathbf{m},\mathbf{n},\mathbf{o},\mathbf{p}) - \sum_{i\in\mathcal{I}} 0.5 \cdot (V_{i-1}^B + V_i^B) \cdot d_{i,t,\omega} \Big) \tag{2.65}$$

$$\text{s.t.} \quad (2.56) - (2.64) \tag{2.66}$$

$$s_{l,i}^\star \in \arg\max_{s_{l,i}} \{ \sum_{t\in\mathcal{T}} \sum_{i\in\mathcal{I}} (V_l \cdot r_i \cdot s_{l,i} \cdot \Theta_t - s_{l,i} \cdot \pi_i) : \sum_{i\in\mathcal{I}} s_{l,i} \le \bar{D}_l, s_{l,i} \ge 0, i \in \mathcal{I} \} \tag{2.67}$$

We reduce the bilevel problem to a single level by appending the equilibrium constraints of the Stackelberg followers to the leader problem. We do so by treating $s_{l,i}$, r_i and π_i as *variables*, and describing the behavior of $s_{l,i}$ as a *function* of (π_i, r_i) through the primal feasibility, dual feasibility, and strong duality conditions of section 2.3.2.

The primal feasibility constraints (2.46) and (2.47) and the dual feasibility constraints (2.49) and (2.50) can be inserted directly to the bilevel formulation. Instead, the strong duality constraint (2.54) becomes a bilinear non-convex constraint when r_i and π_i are treated as decision variables.

In order to overcome this challenge, we express constraint (2.54) equivalently by its McCormick envelope. We do so by noting that the reliability

variable is naturally bounded in the interval $0 \leq r_i \leq 1$, and by imposing a price limit on the menu offering, $0 \leq \pi_i \leq \Pi^+$. This allows us to express $\pi_i \cdot \mu_{l,i}$ by a new variable $y_{l,i}$, and $r_i \cdot \mu_{l,i}$ by a new variable $w_{l,i}$. The strong duality constraint (2.54) for every type $l \in \mathcal{L}$ can then be rewritten as follows:

$$\begin{aligned}
&\gamma_l = \sum_{i \in \mathcal{I}} w_{l,i} \cdot V_l - \sum_{i \in \mathcal{I}} y_{l,i} \\
&y_{l,i} \leq \Pi^+ \cdot \mu_{l,i},\ y_{l,i} \geq 0,\ y_{l,i} \leq \pi_i \\
&y_{l,i} \geq \Pi^+ \cdot \mu_{l,i} + \pi_i - \Pi^+ \\
&w_{l,i} \leq \mu_{l,i},\ w_{l,i} \geq 0,\ w_{l,i} \leq r_i, \\
&w_{l,i} \geq \mu_{l,i} + r_i - 1.
\end{aligned}$$

We thus arrive to a reformulation of the equilibrium conditions of the lower level as a mixed integer linear set. However, this reformulation results in a significant increase of binary variables and constraints, which results in prohibitive run times for realistic-scale problems. We overcome this challenge by *(i)* using the structure of the lower-level problem in order to propose a set of valid cuts, and *(ii)* noting that the variables $\mu_{l,i}$ are then implied by the constraints of the problem. We first recall theorem 1 of [CW87]:

Proposition 2. *Consider two consumers with valuation V_m and V_n respectively, and denote the optimal choice of reliability and the corresponding price as $r^\star(V_m) = \sum_{i \in \mathcal{I}} r_i \cdot \mu^\star_{m,i}, \pi^\star(V_m) = \sum_{i \in \mathcal{I}} \pi_i \cdot \mu^\star_{m,i}$. If $V_m > V_n$, then we have $r^\star(V_m) \geq r^\star(V_n)$ and $\pi^\star(V_m) \geq \pi^\star(V_n)$. In other words, consumers with higher valuation select more reliable plans and pay more.*

Proposition 2 yields the following set of valid cuts:

$$\sum_{i=k}^{I} \mu_{l,i} \leq \sum_{i=k}^{I} \mu_{l+1,i},\ l = 1..L-1,\ k \in \mathcal{I}$$

As shown in figure 2.4, these conditions can be understood as follows. Given a consumer of type l and a consumer of type $l+1$ (recall from section 2.3.2 that we order consumers by increasing valuation, i.e. $V_l < V_{l+1}$), type $l+1$ subscribes to an option which is at least of the same quality as that of l, because of the higher valuation of type $l+1$. This implies that the value of 1 appears in the sequence $\{\mu_{l+1,i}, i \in \mathcal{I}\}$ no later than it does for the sequence $\{\mu_{l,i}, i \in \mathcal{I}\}$, counting from I.

The second observation which allows us to arrive to a computationally tractable model is the observation that a unique solution of the variables $\mu_{l,i}$

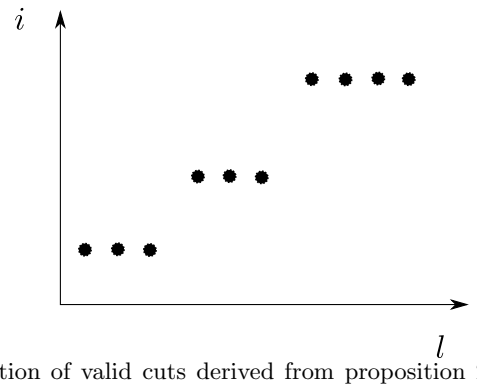

Figure 2.4: Illustration of valid cuts derived from proposition 2. The l-axis shows the indices of consumer types while the i-axis represents the indices of options. The black dots indicate the optimal choices of consumers.

is obtained from the following set of constraints:

$$\mu_{l,i} \in \{0,1\}, l \in \mathcal{L}, i \in \mathcal{I} \tag{2.68}$$

$$\sum_{i \in \mathcal{I}} \mu_{l,i} = 1, l \in \mathcal{L} \tag{2.69}$$

$$\sum_{l \in \mathcal{L}} \bar{D}_l \cdot \mu_{l,i} = K \cdot (V_i^B - V_{i-1}^B), i \in \mathcal{I} \tag{2.70}$$

$$\sum_{i=k}^{I} \mu_{l,i} \leq \sum_{i=k}^{I} \mu_{l+1,i}, \quad l = 1..L-1,\ k = 1..I-1 \tag{2.71}$$

Here, the first constraint has been established by proposition 1, the second constraint is implied by condition (2.61) and the fact that the lowest valuation breakpoint is $V_0^B = 0$ €/MWh, the third constraint is condition (2.61), and the fourth constraint is derived from proposition 2. We state this observation as a corollary.

Corollary 1. *A unique solution of the variables $\mu_{l,i}$ is inferred from the set of constraints (2.68) - (2.71).*

Proof. We create a feasible solution first, and then show that this feasible solution is unique by contradiction.

The constraints (2.68) - (2.71) are essentially placing consumers with a higher consumer index (corresponding to a higher valuation) to options with a higher option index (corresponding to a higher reliability and price).

A feasible solution to this set of constraints can be created in the following way. Staring from consumer L and in descending order, consumers are assigned to option I , until this option is full, as indicated by (2.70). Define l_I such that consumers from L to l_I are in this option. Then consumers staring from index

$l_I - 1$ will be in option $I - 1$, until the consumer indexed by l_{I-1} when this option is full. Similarly, consumers from index $l_{i+1} - 1$ to l_i will be in option i. We carry on in decreasing order of options. Since all consumers will subscribe to a certain option according to (2.69), in the end, consumers from $l_3 - 1$ to l_2 are in option 2, and consumers from $l_2 - 1$ to 1 are in option 1.

We proceed to show that this feasible solution is the unique solution. Suppose that there is another way to assign consumers, then we can only swap consumer m in option j with consumer n in option k, because the subscription quantity in each option is limited according to (2.70). Suppose that $m > n$, and that consumer types m and n are not assigned to the same option, then $j > k$. If consumer m is swapped with consumer n, it means that a higher-index consumer is placed in a lower-index option, which contradicts (2.71).

In conclusion, the feasible solution obtained through the procedure of the previous paragraph is the unique solution to (2.68) - (2.71). □

Note that this observation implies that the variables $\mu_{l,i}$ of the bilevel model can be replaced by fixed values $\bar{\mu}_{l,i}$. Effectively, the collection of these four conditions is an assignment of the consumers of highest type to the options of highest reliability. Even though $\mu_{l,i}$ is implied by these conditions, the challenge of designing a price menu that will induce consumers to self-select the corresponding options *remains*. Achieving this consistency is the goal of the reformulated single level problem, which can be written as follows:

$$
\begin{aligned}
&(\text{MILP}): \\
&\min_{\substack{\mathbf{m},\mathbf{n},\mathbf{o},\mathbf{p} \\ d_{i,t,\omega}, c_{t,\omega}, r_i \\ \pi_i, w_{l,i}, y_{l,i}, \gamma_l}} \quad \sum_{\omega\in\Omega} P_\omega \sum_{t\in\mathcal{T}} \Big(c_{t,\omega} - \sum_{i\in\mathcal{I}} 0.5 \cdot (V^B_{i-1} + V^B_i) \cdot d_{i,t,\omega} \Big) && (2.72) \\
&\text{s.t.} \quad f_{g,\omega}(\mathbf{m},\mathbf{n},\mathbf{o},\mathbf{p}) \le 0, g \in \mathcal{G}, \omega \in \Omega && (2.73) \\
&\qquad \sum_{i\in\mathcal{I}} d_{i,t,\omega} = \sum_{g\in\mathcal{G}} p_{g,t,\omega} + S_{t,\omega} + W_{t,\omega}, t \in \mathcal{T}, \omega \in \Omega && (2.74) \\
&\qquad d_{i,t,\omega} \le K \cdot (V^B_i - V^B_{i-1}) \cdot \Theta_t, i \in \mathcal{I}, t \in \mathcal{T}, \omega \in \Omega && (2.75) \\
&\qquad d_{i,t,\omega}, p_{g,t,\omega} \ge 0, i \in \mathcal{I}, g \in \mathcal{G}, t \in \mathcal{T}, \omega \in \Omega && (2.76) \\
&\qquad m_{g,t,\omega}, n_{g,t,\omega}, o_{g,t,\omega} \in \{0,1\}, g \in \mathcal{G}, t \in \mathcal{T}, \omega \in \Omega && (2.77) \\
&\qquad c_{t,\omega} = h_{t,\omega}(\mathbf{m},\mathbf{n},\mathbf{o},\mathbf{p}), t \in \mathcal{T}, \omega \in \Omega && (2.78) \\
&(\boldsymbol{\nu}): \quad T \cdot \sum_{l\in\mathcal{L}} w_{l,i} \cdot \bar{D}_l - \sum_{\omega\in\Omega} P_\omega \sum_{t\in\mathcal{T}} d_{i,t,\omega} = 0, i \in \mathcal{I} && (2.79) \\
&(\lambda): \quad T \cdot \sum_{i\in\mathcal{I}} \sum_{l\in\mathcal{L}} y_{l,i} \cdot \bar{D}_l - \sum_{\omega\in\Omega} P_\omega \sum_{t\in\mathcal{T}} c_{t,\omega} - \Pi_\star = 0 && (2.80)
\end{aligned}
$$

$$y_{l,i} \leq \Pi^+ \cdot \bar{\mu}_{l,i}, l \in \mathcal{L}, i \in \mathcal{I} \tag{2.81}$$
$$y_{l,i} \leq \pi_i, l \in \mathcal{L}, i \in \mathcal{I} \tag{2.82}$$
$$y_{l,i} \geq \Pi^+ \cdot \bar{\mu}_{l,i} + \pi_i - \Pi^+, l \in \mathcal{L}, i \in \mathcal{I} \tag{2.83}$$
$$w_{l,i} \leq \bar{\mu}_{l,i}, l \in \mathcal{L}, i \in \mathcal{I} \tag{2.84}$$
$$w_{l,i} \leq r_i, l \in \mathcal{L}, i \in \mathcal{I} \tag{2.85}$$
$$w_{l,i} \geq \bar{\mu}_{l,i} + r_i - 1, l \in \mathcal{L}, i \in \mathcal{I} \tag{2.86}$$
$$\gamma_l \geq r_i \cdot V_l - \pi_i, l \in \mathcal{L}, i \in \mathcal{I} \tag{2.87}$$
$$\gamma_l = \sum_{i \in \mathcal{I}} w_{l,i} \cdot V_l - \sum_{i \in \mathcal{I}} y_{l,i}, l \in \mathcal{L} \tag{2.88}$$
$$y_{l,i}, w_{l,i}, \gamma_l, r_i, \pi_i \geq 0, l \in \mathcal{L}, i \in \mathcal{I} \tag{2.89}$$

In this new formulation, s_i has been substituted out. Constraint (2.75) is the result of substituting constraint (2.61) in constraint (2.58). Note that, in constraint (2.78), we introduce a new set of free variables $c_{t,\omega}$ for representing the cost $h_{t,\omega}(\mathbf{m}, \mathbf{o}, \mathbf{p})$. Although redundant from a modeling standpoint, these variables will be useful for decomposing the problem, as described in the following section.

2.4 Decomposition by ADMM

The bilevel model is reformulated as a single-level MILP, which can potentially be solved by commercial solvers. However, the case study of the Belgian market in section 2.5.2 cannot be solved directly, due to the renewable production scenarios. Therefore, in this section we propose a heuristic based on ADMM [BPC+11] in order to decompose the problem. The idea of the decomposition is to relax the coupling constraints (2.79) and (2.80) so that the unit commitment problem of each scenario can be tackled independently.

2.4.1 ADMM Formulation

Concretely, we define $\mathcal{C}_1$ as the set of constraints (2.73) - (2.78) that relate to the unit commitment part of the problem and $\mathcal{C}_2$ as the set of constraints (2.79) - (2.89) that relate to the consumer problem. We define $\mathbf{x}_1 = (\mathbf{m}, \mathbf{n}, \mathbf{o}, \mathbf{p}, \mathbf{c}, \mathbf{d})$ and $\mathbf{x}_2 = (\mathbf{y}, \mathbf{w}, \boldsymbol{\gamma}, \mathbf{r}, \boldsymbol{\pi}, \boldsymbol{\mu})$. Our goal in using an ADMM algorithm is to decompose the overall problem to a part that relates to the unit commitment, and to a part that relates to the consumer. The general idea of the approach is to create copies of $d_{i,t,\omega}$, denoted as $\mathbf{d}^x$ and $\mathbf{d}^z$, that are shared between so-called x-updates (the x updates involve unit commitment problems that are decomposable by scenario) and z-updates (the z updates implicate the consumer

variables). In creating these clones of the original variables, we can move the complicating constraint (2.79) to the consumer sub-problem, and decouple the unit commitment sub-problem by scenario. In the same spirit, in order to relax constraint (2.80), we create copies of the variable $c_{t,\omega}$ that we denote by $\mathbf{c}^x$ and $\mathbf{c}^z$ respectively. These variables are handled by the unit commitment problems (x-updates) and the consumer problems (z-updates) respectively. An illustration of the algorithm on a toy example is presented in the appendix of this chapter.

In abstract form, we left-multiply $\mathbf{x}_1$ by a matrix A of appropriate dimension, which gives us $A\mathbf{x}_1 = (\mathbf{c}, \mathbf{d})$ and we create a copy $\mathbf{z}$ of $A\mathbf{x}_1$.

The MILP formulation of the model (2.72)-(2.89) can thus be rewritten in a stylized form as follows :

$$\min_{\mathbf{x}_1, \mathbf{x}_2, \mathbf{z}} \quad f(\mathbf{x}_1) \tag{2.90}$$

$$\text{s.t.} \quad \mathbf{x}_1 \in \mathcal{C}_1 \tag{2.91}$$

$$(\mathbf{x}_2, \mathbf{z}) \in \mathcal{C}_2 \tag{2.92}$$

$$A\mathbf{x}_1 - \mathbf{z} = 0 \tag{2.93}$$

We can define an indicator function g of $\mathcal{C}_2$, and the problem is rewritten as

$$\min_{\mathbf{x}_1 \in \mathcal{C}_1, \mathbf{x}_2, \mathbf{z}} \quad f(\mathbf{x}_1) + g(\mathbf{x}_2, \mathbf{z}) \tag{2.94}$$

$$\text{s.t.} \quad A\mathbf{x}_1 - \mathbf{z} = 0 \tag{2.95}$$

The ADMM iterations can then be expressed as follows:

$$\mathbf{x}_1^{k+1} := \arg\min_{\mathbf{x}_1 \in \mathcal{C}_1} \left(f(\mathbf{x}_1) + (\rho/2) \| A\mathbf{x}_1 - \mathbf{z}^k + \mathbf{u}^k \|_2^2 \right) \tag{2.96}$$

$$(\mathbf{x}_2^{k+1},\ \mathbf{z}^{k+1}) := \Pi_{\mathcal{C}_2}(A\mathbf{x}_1^{k+1} + \mathbf{u}^k) \tag{2.97}$$

$$\mathbf{u}^{k+1} := \mathbf{u}^k + A\mathbf{x}_1^{k+1} - \mathbf{z}^{k+1} \tag{2.98}$$

where $\Pi_{\mathcal{C}}$ is the projection operator on the set $\mathcal{C}$ and $\mathbf{u}$ are the scaled dual variables. For our specific problem, each element of $A\mathbf{x}_1 - \mathbf{z} = 0$ implicates only variables of a given month and scenario, therefore the regularization term in (2.96) can be decoupled by month and scenario, which is the original motivation for using a decomposition method.

The scheme is further illustrated in figure 2.5. The light gray blocks correspond to constraints $\mathcal{C}_1$ and the dark gray block corresponds to constraints $\mathcal{C}_2$. Note that the unit commitment problem in each scenario is decomposed into 12 independent monthly unit commitment problems[5], which are solved in parallel, so that there are $12 \cdot |\Omega|$ unit commitment subproblems in total. The light gray blocks updates the $\mathbf{x}_1$ variables. The dark gray block is used for updating $(\mathbf{x}_2, \mathbf{z})$. The variables $\mathbf{u}$ are then used for updating the light gray

[5]Boundary effects are handled by wrapping the monthly commitment problem around itself.

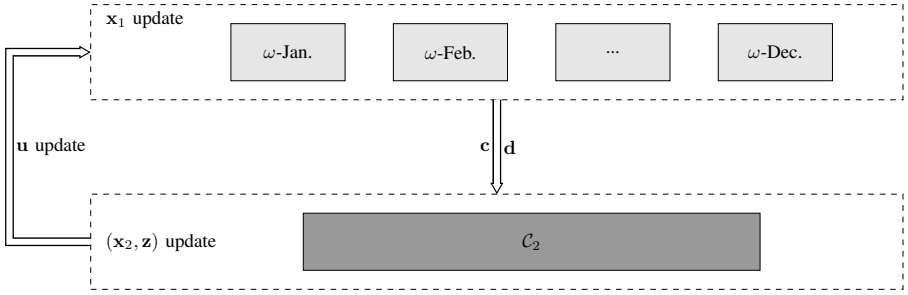

Figure 2.5: The application of ADMM as a heuristic for decomposing the reformulated MILP.

blocks in the next iteration.

2.4.2 Convergence

In practice, the *dual residual* and *primal residual* are used to check the convergence of ADMM for a convex problem. However, the model presented in this paper is non-convex. Therefore, residuals are not a proper indication of convergence in this case, since there is no reason to expect that they should eventually vanish. Instead, we determine the convergence by checking the gap between an upper bound and lower bound of the problem. We derive the upper and lower bound as part of our algorithmic implementation. More specifically, recovery of a feasible primary solution is carried out in order to calculate an upper bound and dual decomposition is adopted for computing the lower bound[6].

2.4.2.1 Upper Bounding by Recovery of Primal Feasible Solutions

The idea of the upper bounding method is to fix the unit commitment part of the problem, and seek a menu design and a set of consumer choices that are consistent with the fixed unit commitment decisions. In doing so, we fix the majority of variables of the original problem, and are left with a relatively light MILP that can potentially yield a feasible solution and an upper bound. Even though there is no convergence guarantee for ADMM when applied to this model, at the end of each ADMM iteration we can fix part of the solution, i.e., $\mathbf{x}_1$, and solve the following problem:

$$(\text{PR}): \quad (\mathbf{x}_2, \mathbf{z}) \in \mathcal{C}_2 \tag{2.99}$$

$$A\mathbf{x}_1^\star - \mathbf{z} = 0 \tag{2.100}$$

[6]Dual decomposition applies to our model, but the primal solution from dual decomposition is not of acceptable quality. Therefore, we only use it to obtain a lower bound.

If (PR) is feasible, we obtain an upper bound as $f(\mathbf{x}_1^\star)$, otherwise the upper bound returned from the iteration in question is $+\infty$. Note that there is no theoretical guarantee that we can find a feasible solution to (PR). Nevertheless, in the case study presented later, we can find a good upper bound after a certain number ADMM iterations. This is because, in later iterations, the solution from the unit commitment part of the problem evolves, so that the total cost and price region defined by the consumer choice constraints change, which enable the profit constraint to be satisfied.

2.4.2.2 Lower Bounding by Dual Decomposition

The following computation is performed once at the outset of the problem, in order to yield a lower bound, before launching the ADMM algorithm. We relax constraints (2.79) and (2.80) in problem (MILP) by using the corresponding dual variables $\boldsymbol{\nu}$ and λ, so that the whole problem is decomposed into the following dual subproblems.

Dual subproblem - producer in scenario ω:

$$\min_{d_{i,t,\omega},\mathbf{m},\mathbf{n},\mathbf{o},\mathbf{p}} \quad P_\omega \sum_{t\in\mathcal{T}} \Big(h_{t,\omega}(\mathbf{m},\mathbf{n},\mathbf{o},\mathbf{p}) - \tag{2.101}$$

$$\sum_{i\in\mathcal{I}} 0.5\cdot(V_{i-1}^B + V_i^B)\cdot d_{i,t,\omega}\Big) \tag{2.102}$$

$$-\sum_{i\in\mathcal{I}} \nu_i \cdot P_\omega \cdot \sum_{t\in\mathcal{T}} d_{i,t,\omega} \tag{2.103}$$

$$-\lambda\cdot P_\omega \cdot \sum_{t\in\mathcal{T}} h_{t,\omega}(\mathbf{m},\mathbf{n},\mathbf{o},\mathbf{p}) \tag{2.104}$$

$$\text{s.t.} \quad (2.73)-(2.77) \tag{2.105}$$

Dual subproblem - consumer:

$$\min_{r_i,\pi_i,w_{l,i},y_{l,i},\gamma_l} \quad \sum_{i\in\mathcal{I}} \nu_i \cdot T \cdot \sum_{l\in\mathcal{L}} w_{l,i}\cdot \bar{D}_l \tag{2.106}$$

$$+\lambda\cdot T\cdot \sum_{i\in\mathcal{I}}\sum_{l\in\mathcal{L}} y_{l,i}\cdot\bar{D}_l - \lambda\cdot\Pi_\star \tag{2.107}$$

$$\text{s.t.} \quad (2.81)-(2.89) \tag{2.108}$$

This is a standard scenario decomposition of the problem. Many algorithms are available for solving the dual decomposition, such as the subgradient method [POO11, PO13], the cutting plane method [KZ18], and bundle methods [Sag12]. In our study, we adopt a standard cutting plane method which is suitable for low-dimensional spaces. Note that, in the implementation of the dual decomposition, the unit commitment problem of each scenario is also decomposed by month. The maximum of the dual function which is obtained

from the cutting plane method (which is the sum of the objective values of the dual sub-problems) is a lower bound of (MILP). We can compare this lower bound to the upper bound obtained from the primal feasible solution recovery in order to decide when to terminate the algorithm.

2.4.3 Runtime Complexity of the Algorithm

The total run time of the proposed decomposition algorithm depends on the run time of each iteration and the number of iterations needed to converge to an acceptable optimality gap. Note that the run time of the x-update of the ADMM algorithm dominates that of the other steps because it involves unit commitment problems. Regarding the number of iterations needed to converge, it is related to the choice of ρ. If ρ is larger, it is likely that feasible solutions are found in earlier iterations of the ADMM algorithm, however the larger choice of ρ also has an adverse effect on the quality of the solution. A more detailed discussion on the run-time of the algorithm is available in section 2.C

2.5 Case Studies

In this section, we present two illustrations of the model. The first one is a toy example used for validation, which compares the closed-form solution provided by priority service pricing theory [CW87] to the solution of the bilevel model. The second case study is a realistic model of the Belgian power system. For this realistic case study, we compare priority service pricing to real-time pricing and an optimal flat tariff in terms of social welfare, and we analyze the interruption patterns of priority service pricing.

2.5.1 A Toy Example

Consider a system with the demand function $D(v) = 1620 - 4 \cdot v$. The system consists of two generators. The first generator is reliable and has a marginal cost of 65.1 €/MWh, and a capacity of 295 MW. The other generator is unreliable. It is operational with a probability $P_1 = 83.3\%$ and is out of service with a probability $P_2 = 16.7\%$. The second generator has a capacity of 1880 MW and a marginal cost of 0 €/MWh.

Consider the breakpoints $V_0^B = 0$, $V_1^B = 331.25$, $V_2^B = 405$ €/MWh. In this case, 1325 MW subscribe to the first option, and 295 MW subscribe to the second option. The closed-form solution [CW87] prescribes the following service menu:

$$\pi(r) = \begin{cases} 0 \text{ €/MWh}, & r = 83.3\% \\ 55.3 \text{ €/MWh}, & r = 100\% \end{cases}$$

The profit of the producer amounts to 13106.3 €.

In order to implement the bilevel model in this toy example, we discretize the demand function into 1620 consumer *types*. Given a profit target of 13106.3 €, the model yields a price menu which is identical to that of [CW87] within one significant digit. If we increase the profit requirement of the firm to 15000 €, we obtain the following price menu from the bilevel model:

$$\pi(r) = \begin{cases} 0.1 \text{ €/MWh}, & r = 81.5\% \\ 61.3 \text{ €/MWh}, & r = 100\% \end{cases}$$

Note that the increased profit target of the producer is largely covered by increasing the price of the second option.

2.5.2 The Belgian Power System Model

This section presents a case study of the Belgian system in a forward-looking scenario of the year 2050. We consider this forward-looking scenario because priority service pricing is more relevant in the situation where there could be shortages due to highly variable supply. The expected large scale of renewable energy integration targeted by 2050 renders it suitable for the case study. A full-year horizon and one-hour resolution is considered.

The conventional generator fleet of the model consists of 55 units. The installed capacity of each technology follows the projected capacity of the year 2050 according to the EU 2050 reference scenario [EC17]. The technical specifications of the units are available from the website of the Belgian TSO Elia [Eli19b]. The installed capacity of conventional generators, which totals 15784 MW, can be broken down as follows: gas (14965 MW), oil (10 MW), biomass (542 MW), and waste (267 MW). The long-term maintenance schedule of units is accounted for by derating the maximum capacity of the units by a certain availability ratio. The availability ratio follows the hourly profiles of 2015 [Eli19b].

Wind and solar production profiles corresponding to the years 2013 to 2017 and import profiles for the year 2015 with hourly resolution are collected from [Eli19b]. These profiles are scaled up according to the projected value of the year 2050, according to the EU 2050 reference scenario [EC17]. Ten scenarios of wind and solar production are created, in order to better characterize uncertainty in renewable production. In order to preserve seasonal effects, the scenarios of wind and solar power production are created as follows. In the case of solar, we shuffle the days within the same week. For example, the days in the first week of 2013-2017 are regarded as samples of the same day (35 in total), and then we randomly draw one day from this set. The hourly load factor (production divided by installed capacity) of this day is used in order to derive the production profile of the first day in 2050. For wind, we shuffle the months in the same season. The projected ratio of renewable energy production to total energy production for 2050 is 27.4%, with the peak production amount-

ing to 11690 MW. The projected peak load in 2050 amounts to 18700 MW. It is worth noting that, during some hours, curtailment of renewable production could occur.

The pumped hydro storage in Belgium has a pumping capacity amounting to 1200 MW, while the energy storage capacity of pumped hydro amounts to 5700 MWh. Pumped hydro resources are assumed to have a roundtrip efficiency of 76.5% [PS17].

The total load profile of year 2015 is also available from [Eli19b]. We split this profile into a residential, industrial and commercial load, according to *Synthetic Load Profiles (SLP)* [Syn17], which are normalized electricity consumption time series with 15-minute resolution that are publicly available for the residential and non-residential sectors. The load profiles are scaled up to the year 2050 according to the EU 2050 reference scenario [EC17]. The dynamic profile of consumption Θ_t is estimated using SLP.

We focus on residential demand. Thus, industrial and commercial demand is assumed to follow a fixed profile[7]. Hourly demand functions for residential consumers are assumed to be linear, and are calibrated by assuming a price elasticity of -0.5 at the historically observed consumption and price for each hour of the data[8].

Figures 2.6 and 2.7 highlight the differences between the Belgian system in 2015 and the projected system in 2050 according to [EC17]. It is observed from figure 2.6 that the power plants fueled by nuclear and solid fuels phase out in 2050. On the other hand, the total installed capacity of conventional generators increases, due to the significant growth in gas plants. The capacity of renewable resources increases as well, especially insofar as wind power is concerned. The electricity imported from other countries decreases slightly, as presented in figure 2.7. In contrast, the total demand increases by around 36.7%.

2.5.2.1 Price Menu Designed According to Chao's Theory

The original theory of priority service pricing relies on a convex cost function, i.e. an economic dispatch model which does not account for startup costs, minimum load costs and minimum capacity constraints of generators. Ignoring

[7]Industrial and commercial consumers are already active in demand response and they are willing to engage in more sophisticated demand response programs due to the substantial cost saving potential. For instance, some utilities offer real-time pricing to the industrial and commercial sectors [HBPV18]. We consider priority service as being out of scope for these classes of demand-side flexibility, since the major motivation for priority service is simplicity. This simplicity is a necessary condition for residential consumers, but has not been proven not to be a prerequisite for the proliferation of demand response in the commercial and residential sectors. Therefore, in this work we focus on the application of priority service to the residential sector.

[8]According to the Tempo program of EDF, the estimated elasticity is between -0.18 to -0.79 [FS10a].

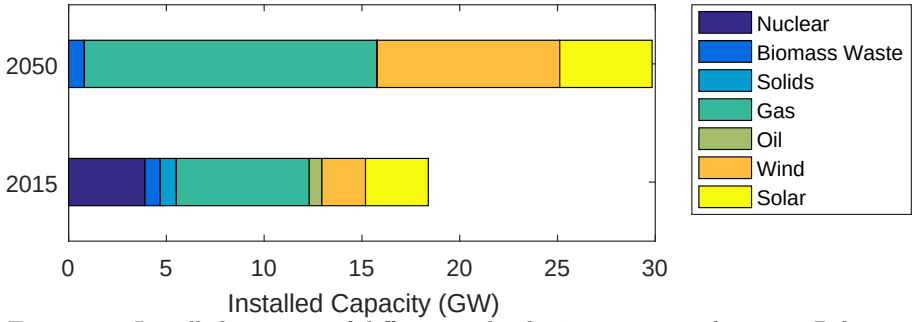

Figure 2.6: Installed capacity of different technologies in 2015 and 2050 in Belgium.

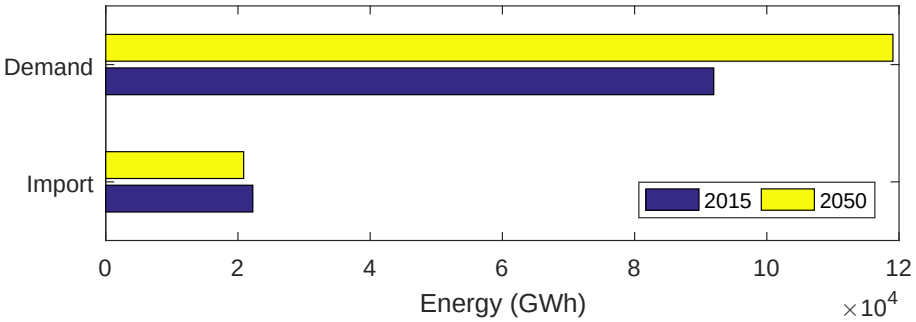

Figure 2.7: Total import and demand in 2015 and 2050 in Belgium.

these conditions may result in a mismatch between promised and delivered reliability.

In table 2.1 we present the results of the menu designed according to the theory of Chao [CW87]. We have discretized the menu into 5 options. The price and reliability of each option are presented in the first two columns of table 2.1. The fourth and fifth column indicate the average valuation and total demand of each group of types within a given option. Based on this information, a piecewise constant demand function is used as an input to the *true* unit commitment model of the Belgian system. The *realized* reliability of each option is indicated in the third column of the table. We observe a significant deviation between promised and delivered reliability, especially for the first two options.

2.5.2.2 Performance of the ADMM Algorithm

Figure 2.8 presents the convergence of dual decomposition based on the cutting plane method. The lower bound that is obtained by dual decomposition amounts to - 5767.5 million.

ADMM is implemented in Julia [BEKS17] and we utilize 120 CPUs on the CÉCI cluster [CEC19] in order to solve the model, with one CPU being

Table 2.1: Price menu for the example of section 2.5.2 based on Chao's theory.

Price (€/MWh)	Reliability (%)	Realized Reliability (%)	V_i (€/MWh)	D_i (MW)
0.0	21.6	0.6	31.7	436.8
46.0	94.2	93.2	116.9	739.1
52.8	98.2	97.8	231.3	839.9
57.3	99.7	99.7	353.1	839.9
58.3	100.0	100.0	450.5	504.0

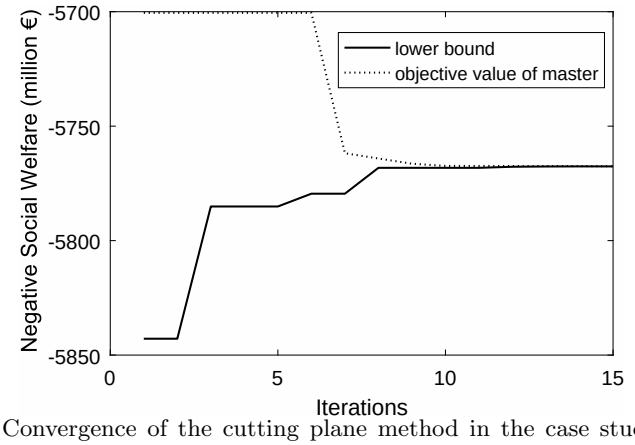

Figure 2.8: Convergence of the cutting plane method in the case study in section 2.5.2. The solid curve presents the evolution of the lower bound of the dual function. The dotted curve presents the evolution of the objective value of the master problem in the cutting plane method. A valid cut that limits the objective value of the master problem under -5700.5 million (which is the performance of a flat tariff) is added to the master problem in order to stabilize the first few iterations.

dedicated to each subproblem in the x-update of ADMM. Gurobi is chosen as the solver and the MIP gap is set to be 0.1%. The run time for 30 iterations of the algorithm amounts to 2.7 hours. The first feasible solution is obtained at the 16th iteration and the corresponding objective value amounts to -5763.4 million. The absolute gap of the algorithm, compared with the lower bound, is 4.1 million, which accounts for 0.34% of the operating costs of serving residential consumers[9]. The required run time for 16 iterations amounts to 1.3 hours. The best solution is achieved at the 27th iteration, with an objective of -5763.5 million. Note that this is very close to the objective function value of the 16th iteration.

[9]We consider this gap as being acceptable, based on typical optimality gaps that are used in the stochastic unit commitment literature [POO11, PO13, PS15] that are in the order of 1%.

Table 2.2: The price menu obtained by ADMM in the case study of section 2.5.2.

Reliability (%)	Realized Reliability (%)	Price (€/MWh)
5.3	5.3	0.0
92.9	92.9	55.6
97.8	97.8	64.0
99.7	99.7	69.6
100.0	100.0	70.6

Table 2.3: Economic performance of priority service pricing, flat tariff and real-time pricing in the case study of section 2.5.2.

Policy	Social Welfare (M €)	Consumer Benefits (M €)	Consumer Net Benefits (M €)	Producer Profits (M €)	Producer Costs (M €)
FT	5700.5	6876.8	5234.5	466.1	1176.2
PSP	5763.4	6952.0	5297.4	466.1	1188.6
RTP	5782.3	6992.4	5515.1	267.2	1210.2

2.5.2.3 Welfare Comparison

This section compares the results of priority service pricing with those of the optimal flat tariff and of real-time pricing.

Table 2.2 presents the promised reliability, realized reliability and price that are obtained from solving the model using our proposed algorithm. It is observed that there is no deviation between the promised reliability and realized reliability, which is in stark contrast to the results of table 2.1 that are obtained from traditional priority service pricing theory. This is a powerful aspect of integrating menu design with unit commitment. We further test our model *out of sample* by running it against 1000 scenarios that are drawn from the same distribution, but do not correspond to the scenarios used in the bilevel model. We find that the realized reliability levels amount to 5.9%, 93.4%, 97.8%, 99.7% and 100.0%, and are therefore very close to the *in-sample* reliability levels.

Table 2.3 compares the economic performance of priority service pricing, flat tariffs and real-time pricing. It is observed that priority service pricing increases social welfare by 1.1% compared to the welfare achieved by a flat tariff. This corresponds to 77.1% of the welfare gains that can be achieved from moving from a flat tariff to real-time pricing. The producer profit under the flat tariff is set as the profit target of the bilevel model. We can achieve this profit target exactly when solving the bilevel model. The welfare gains are all allocated to consumers in this case study, but the allocation can be adjusted by setting a different profit target for the producer.

Figure 2.9 compares the price duration curves under different pricing po-

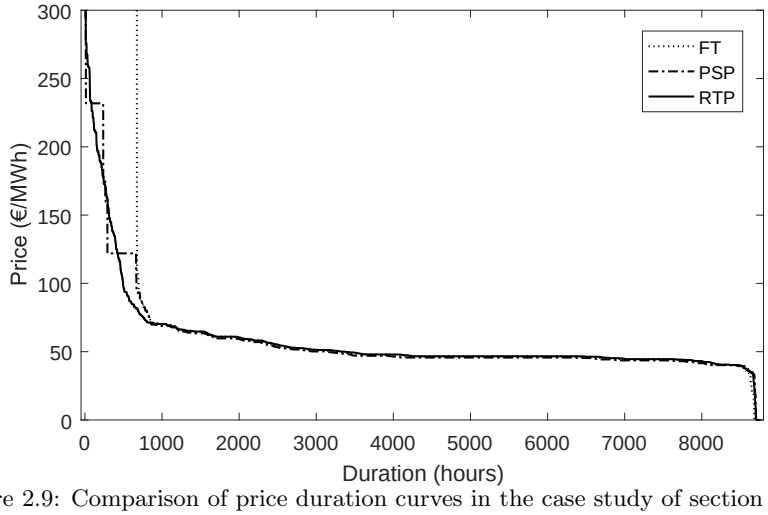

Figure 2.9: Comparison of price duration curves in the case study of section 2.5.2.

lices. The models involve binary unit commitment decision variables, so we solve the linear relaxation and the dual variables associated with the supply demand balance constraint are regarded as the market prices [GHP07]. Under priority service pricing and real-time pricing the market price is determined by the valuation of consumers during scarcity. The price plateaus that are observed in the figure under priority service pricing are due to the fact that consumers are categorized into several priority classes. The market prices under real-time pricing and priority service pricing prove to be beneficial for allowing peaking generators to recover investment costs, as we comment below.

We comment specifically on the financial viability of CCGT units, due to recent concerns related to the adequate presence of flexible capacity in the Belgian electricity market [PSdMd19]. The running investment cost of CCGT ranges from 6.03 to 8.66 €/MW per hour, assuming an overnight cost of 595 €/kW, an annual discounting rate of 8 to 12% and an investment lifetime of 25 to 30 years [PSdMd19]. As observed from figure 2.10, the profit of CCGT units under real-time pricing ranges from 15.81 to 23.78 €/MW per hour, while under priority service it ranges from 15.54 to 22.29 €/MW per hour. The results indicate that priority service can contribute towards keeping peaking generators in the market and avoiding further scarcity. The relatively high profit of CCGT units mainly stems from the 1000 hours when the system is stressed, and at which time price-responsive consumers are setting the clearing price. One attribute which is not captured in the model of the present chapter is the fact that, during these hours, households are expected to use their local storage for part of the electricity consumption. This feature is investigated in the next chapter. The result indicates that priority service pricing is able

to signal scarcity in capacity. This motivates the extension of the model by considering investment decisions [JT07].

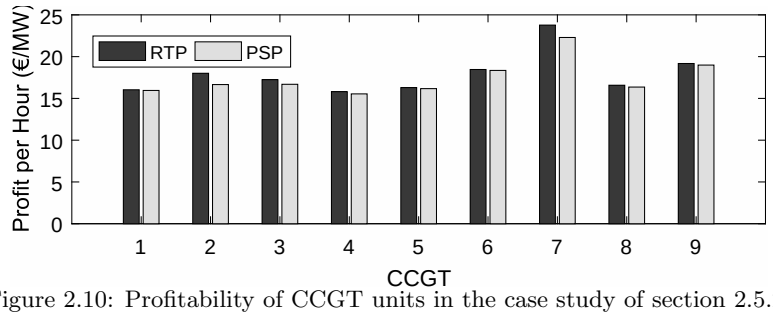

Figure 2.10: Profitability of CCGT units in the case study of section 2.5.2.

2.5.2.4 Interruption Patterns

A powerful feature of our proposed model is that it reveals the interruption patterns associated with a given level of reliability. These interruption patterns are the *direct* output of our model, in particular they correspond to the $d_{i,t,\omega}$ variables. This illuminates the impact of different options on the discomfort that is experienced by households.

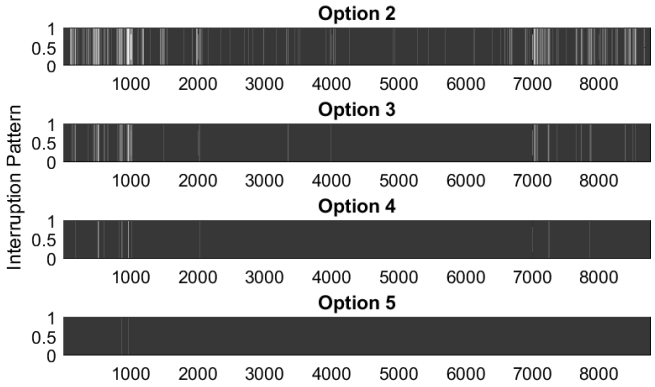

Figure 2.11: Interruption patterns of 1 kW power in the most reliable four options for the case study of section 2.5.2. In this figure, white parts show that 1 kW power in the corresponding hours is interrupted.

In figure 2.11 we present the interruption pattern for 1 kW of supply into the four most reliable options of table 2.2. To illustrate the usefulness of this model, note that although option 2 corresponds to a reliability level of 92.9% (which, if evenly distributed, implies an interruption frequency of 4.4 minutes per hour), around hour 1000 of the simulation, loads under this option expe-

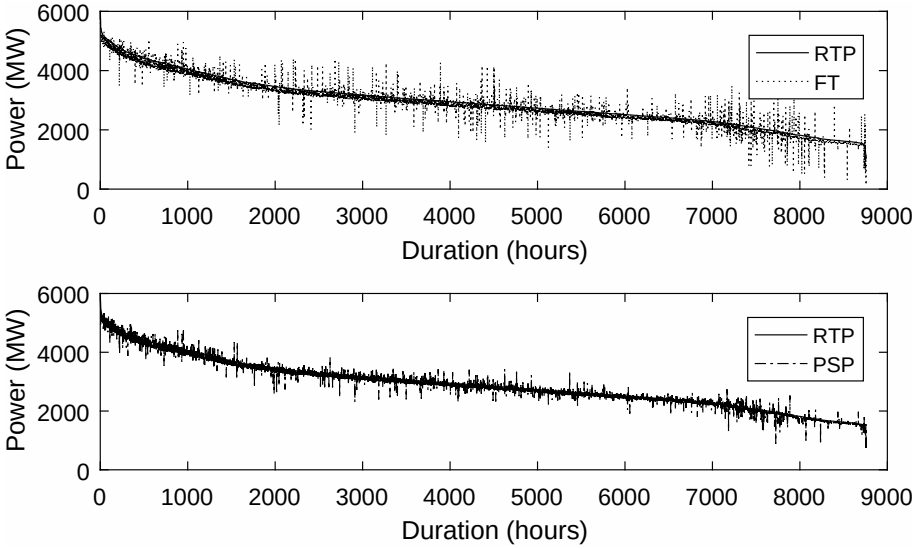

Figure 2.12: Comparison of residential demand profiles in the case study of section 2.5.2.

rience a *continuous* interruption of 20 hours. The severity of such continuous interruptions needs to be carefully accounted for by utilities, and cannot be furnished by the classical theory of priority service pricing [CW87]. We note that the excessive stress that the system experiences around hours 500, 1000 and 7000 is driven by three factors: high industrial and commercial demand, low renewable production and low availability of conventional generators due to maintenance.

2.5.2.5 Impacts on Demand Profiles

Figure 2.12 compares the residential demand profiles under different policies. The solid curve shows the load duration curve under real-time pricing and the profiles under the flat tariff and priority service pricing are sorted according to the same order, presented as the dotted curve in the upper panel and the dash-dot curve in the lower panel, respectively. It can be seen that the residential demand profile of priority service pricing deviates less from the profile of real-time pricing than the flat tariff. This indicates that priority service pricing is able to distinguish the valuation of consumers and serve them when the valuation justifies the cost, resulting in higher efficiency.

In order to further illustrate the effect of demand response on consumers, we present a sample day with abundant wind production during the winter. In figure 2.13 we observe that the production of wind power is significant over

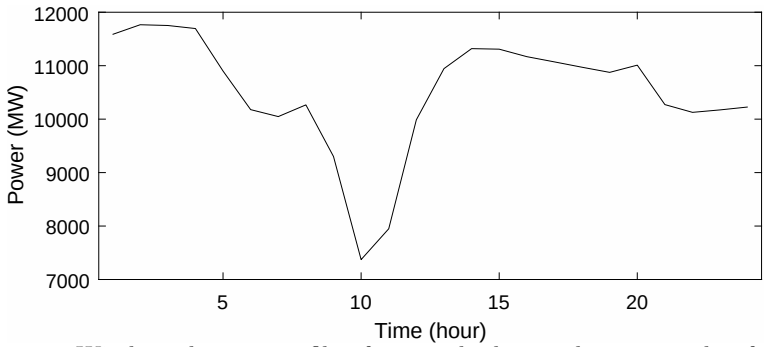

Figure 2.13: Wind production profile of a sample day in the case study of section 2.5.2.

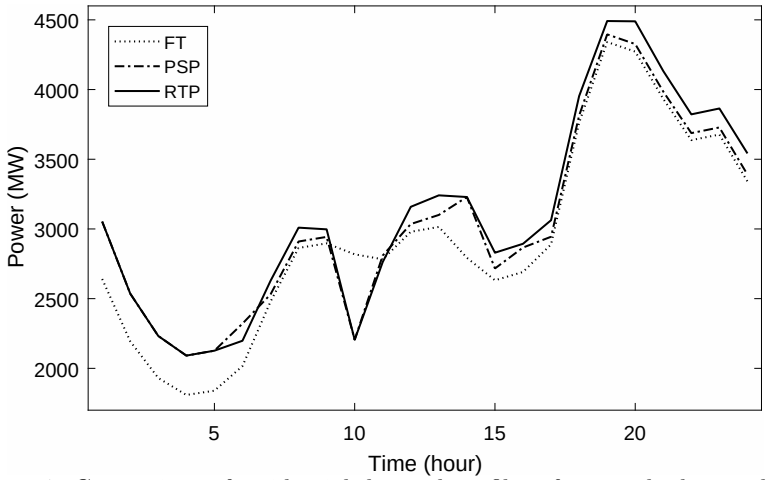

Figure 2.14: Comparison of residential demand profiles of a sample day in the case study of section 2.5.2.

the day except for a drop at hour ten. Figure 2.14 compares the residential profiles of this day under different demand response policies. It is evident that, under real-time pricing and priority service, consumers are able to react to the fluctuation of wind production by consuming more during the periods with more wind production, and reducing consumption at hour ten. In stark contrast, consumers under the flat tariff do not align their consumption with the availability of renewable energy.

2.A Nomenclature

This section gives the nomenclature used in section 2.3.

Sets

$\mathcal{L}, L$	Set of consumers and its cardinality
$\mathcal{T}, T$	Set of time periods and its cardinality
$\mathcal{I}, I$	Set of options and its cardinality
Ω	Set of scenarios
$\mathcal{G}$	Set of generators
$\mathcal{X}$	Domain of the unit commitment variables
$\mathcal{Y}$	Domain of subscription quantity of consumers

Parameters

Θ_t	Dynamic profile of consumption
V_l	Valuation of consumer l [€/MWh]
$\bar{D}_l$	Average demand of consumer l [MW]
V_i^B	Valuation breakpoint, $i = 0 \dots I$ [€/MWh]
V_i	Average valuation of group i [€/MWh]
D_i	Demand of group i [MW]
K	Slope of demand function
$\Pi_\star$	Profit target [€]
Π^+	Upper bound on prices in the menu [€/MWh]
P_ω	Probability of scenario ω
$S_{t,\omega}$	Solar production at hour t in scenario ω [MW]
$W_{t,\omega}$	Wind production at hour t in scenario ω [MW]
$\bar{\mu}_{l,i}$	Inferred consumer subscription decision

Variables

π_i	Price of option i [€/MWh]
r_i	Reliability of option i [%]
$\mu_{l,i}$	Binary decision of consumer l for option i
$y_{l,i}$	Auxiliary variable to represent $\pi_i \cdot \mu_{l,i}$
$w_{l,i}$	Auxiliary variable to represent $r_i \cdot \mu_{l,i}$
$s_{l,i}$	The subscription quantity of consumer l under option i [MW]
s_i	The total subscription quantity under option i [MW]
$d_{i,t,\omega}$	Supply to option i at hour t in scenario ω [MW]
$c_{t,\omega}$	Total costs at hour t in scenario ω [€]
$p_{g,t,\omega}$	Production of generator g at hour t in scenario ω [MW]
$m_{g,t,\omega}$	Start up decision of generator g at hour t in scenario ω, binary
$n_{g,t,\omega}$	Shut down decision of generator g at hour t in scenario ω, binary
$o_{g,t,\omega}$	Unit commitment decision of generator g at hour t in scenario ω, binary
$\mathbf{m}$	Compact form of $m_{g,t,\omega}$, similarly for $\mathbf{n}$, $\mathbf{o}$, $\mathbf{p}$, $\mathbf{c}$, $\mathbf{d}$, $\mathbf{y}$, $\boldsymbol{\gamma}$, $\mathbf{r}$, $\boldsymbol{\pi}$, $\boldsymbol{\mu}$ and $\boldsymbol{\nu}$
$\mathbf{s}$	Compact form of $s_{l,i}$

Functions

$h_{t,\omega}$	Cost function including production costs, startup and minimum load costs

$f_{g,\omega}$	Constraints of unit commitment problems, including minimum up and down times, ramp rates and production limits	CS	Consumer surplus function
		ϕ	Abstract function to calculate reliability
SW	Social welfare function	ψ	Abstract function to calculate the profit

2.B A Toy Example to Illustrate ADMM

In section 2.4, we decompose the full model by making copies of some variables and adopting ADMM algorithm. The presentation could be involved due to the scale of the model, so we illustrate the methodology on a toy example in this section to get the idea better conveyed.

Consider a system with $\mathcal{L}$ consumers, whose valuation is indicated by $V_l, l \in \mathcal{L}$, and whose power demand is uniformly equal to D. We design a menu with a single option, assuming that the total target subscription is $D = K \cdot (V_1^B - V_0^B)$ with valuation breakpoints V_0^B and V_1^B. Suppose that the system consists of one generator, which is operational with a probability of P_1 and is out of service with a probability P_2. The generator is assumed to have a capacity of $P_{\max}$ and a marginal cost of MC. The profit target is $\Pi_\star$. The overall model can be formulated as follows:

$$\min_{d_1,d_2,c_1,c_2,r,\pi} \quad P_1 \cdot c_1 + P_2 \cdot c_2 \\ -0.5 \cdot (V_0^B + V_1^B) \cdot (P_1 \cdot d_1 + P_2 \cdot d_2) \tag{2.109}$$

$$\text{s.t.} \quad 0 \le d_1 \le P_{\max} \tag{2.110}$$
$$d_2 = 0 \tag{2.111}$$
$$d_1 \le D \tag{2.112}$$
$$c_1 = MC \cdot d_1 \tag{2.113}$$
$$c_2 = 0 \tag{2.114}$$
$$r \cdot D - (P_1 \cdot d_1 + P_2 \cdot d_2) = 0 \tag{2.115}$$
$$\pi \cdot D - (P_1 \cdot c_1 + P_2 \cdot c_2) = \Pi_\star \tag{2.116}$$
$$r \cdot V_l - \pi \ge 0, l \in \mathcal{L} \tag{2.117}$$
$$0 \le r \le 1 \tag{2.118}$$
$$0 \le \pi \le \Pi^+ \tag{2.119}$$

where d_1 denotes the supply in scenario ω_1 and d_2 in scenario ω_2. The objective (2.109) minimizes the negative of social welfare. Constraints (2.110) and (2.111) require that supply be limited by the available capacity in each scenario. Constraint (2.112) requires that the supply be limited by the subscription quantity. Constraints (2.115) and (2.116) are the reliability and profit

constraints, respectively. Constraint (2.117) guarantees that consumers obtain a non-negative surplus.

We drop d_2 and c_2 since they are equal to 0 and create a copy of d_1 and c_1 (we denote the variable and its copy as d_x and d_z, c_x and c_z, respectively), yielding

$$\min_{d_x,d_z,c_x,c_z,r,\pi} \; P_1 \cdot c_x - P_1 \cdot 0.5 \cdot (V_0^B + V_1^B) \cdot d_x \tag{2.120}$$

$$\text{s.t.} \;\; 0 \leq d_x \leq P_{\max} \tag{2.121}$$

$$d_x \leq D \tag{2.122}$$

$$c_x = MC \cdot d_x \tag{2.123}$$

$$r \cdot D - P_1 \cdot d_z = 0 \tag{2.124}$$

$$\pi \cdot D - P_1 \cdot c_z = \Pi_\star \tag{2.125}$$

$$r \cdot V_l - \pi \geq 0, l \in \mathcal{L} \tag{2.126}$$

$$0 \leq r \leq 1 \tag{2.127}$$

$$0 \leq \pi \leq \Pi^+ \tag{2.128}$$

$$d_x - d_z = 0 \tag{2.129}$$

$$c_x - c_z = 0 \tag{2.130}$$

The correspondence between the variables of the model and the stylized formulation in section 2.4 is as follows: $\mathbf{x}_1 = (d_x, c_x)$, $\mathbf{x}_2 = (r, \pi)$ and $\mathbf{z} = (d_z, c_z)$. The function $f(\mathbf{x}_1)$ refers to objective (2.120). The set $\mathcal{C}_1$ corresponds to constraints (2.121) - (2.123) while the set $\mathcal{C}_2$ corresponds to constraints (2.124) - (2.128). The equalities $A\mathbf{x}_1 - \mathbf{z} = 0$ correspond to constraints (2.129) and (2.130).

The augmented Lagrangian using scaled dual variables is written as:

$$L_\rho(d_x, d_z, c_x, c_z, r, \pi, u_1, u_2)$$

$$= P_1 \cdot c_x - P_1 \cdot 0.5 \cdot (V_0^B + V_1^B) \cdot d_x \tag{2.131}$$

$$+ \; \rho/2 \cdot \big((d_x - d_z + u_1)^2 + (c_x - c_z + u_2)^2\big) \tag{2.132}$$

The x-update of the update (2.96) corresponds to solving:

$$(PX): \min_{d_x,c_x} \; P_1 \cdot c_x - P_1 \cdot 0.5 \cdot (V_0^B + V_1^B) \cdot d_x \tag{2.133}$$

$$+ \rho/2 \cdot \big((d_x - d_z^k + u_1^k)^2 + (c_x - c_z^k + u_2^k)^2\big) \tag{2.134}$$

$$\text{s.t.} \;\; (2.121) - (2.123) \tag{2.135}$$

The z-update which corresponds to (2.97) is:

$$(PZ): \min_{d_z,c_z,r,\pi} \; \rho/2\big((d_x^{k+1} - d_z + u_1^k)^2 + (c_x^{k+1} - c_z + u_2^k)^2\big) \tag{2.136}$$

$$\text{s.t.} \;\; (2.124) - (2.128) \tag{2.137}$$

The u-update which corresponds to (2.98) is:

$$u_1^{k+1} := u_1^k + d_x^{k+1} - d_z^{k+1} \tag{2.138}$$

$$u_2^{k+1} := u_2^k + c_x^{k+1} - c_z^{k+1} \tag{2.139}$$

2.C Detailed Report on Run-time

The total run time of the algorithm depends on the the run time of each iteration and the number of iterations required for convergence. We analyze the two factors in turn.

The run time of one iteration can be deduced as follows. Each iteration consists of four steps, the x-update, the z-update, the u-update, and the recovery of primal feasible solutions. The run times of these processes are denoted respectively as X, Z, U and R. Then, the run time of one iteration is $X + Z + U + R$ and the run time of the x-update dominates the run time of the other processes because it involves unit commitment problems. For example, in the case study reported in the Belgian case study, the 16th iteration requires 398.1 seconds in total and the x-update alone requires 380.3 seconds, which accounts for 95.5% of the total run time. The run-time of the x-update depends on the run time of each unit commitment subproblem (S), the number of CPUs (C) available to solve unit commitment subproblems and the number of subproblems ($C \cdot N$). So the run time of the x-update is approximately $O(S \cdot N)$, which corresponds to the run time of the iteration.

However, it is worth noticing that the run time of each subproblem could differ significantly. We still use the 16th iteration as an example. We use 120 CPUs and the number of subproblems is $12 \cdot |\Omega| = 120$ (12 months, 10 scenarios). The shortest run time amounts to 67.8 seconds, the longest run time amounts to 380.3 seconds, and the average run time is 125.3 seconds. One method to reduce the run time of one iteration is to implement ADMM in an asynchronous fashion [CHLW16]. Since the run time of the current implementation is reasonable and asynchronous ADMM is not guaranteed to outperform synchronous ADMM, we do not explore this approach further in this study. Another way to achieve further computational efficiency is to decompose the unit commitment problem of each scenario into 52 subproblems instead of 12, i.e., the horizon of each subproblem becomes one week instead of one month. Meanwhile, more computing resources are required since the number of subproblems in the x-update increases to $52 \cdot |\Omega| = 520$ and the weekly horizon should be justified[10].

[10]In particular, the time scale of the reserve market is a relevant factor, since it couples the operations across multiple days. The tertiary reserve market in Belgium is cleared monthly whereas primary and secondary reserve is clearly weekly is currently weekly and is gradually transitioning to day-ahead clearing [Eli19a]. The reserve market in some other countries is cleared weekly, such as Germany [HAE+14]. Therefore, a weekly time horizon for Central

The run time of the unit commitment subproblem is also likely to increase if the number of generators increase, because more binary decision variables will be involved. The number of consumers will not affect the run time of the x-update significantly, because the choices of consumers are inferred from their privately known types, as described by proposition 2. The number of options in the price menu tends to increase the complexity of the model, but too many options would anyways violate the principle of priority service pricing since they would exert an overwhelming information processing burden on households. We therefore consider three to five options as a reasonable compromise. Proposition 6 in [CW87] shows that the deadweight loss decrease is inversely proportional to the square of the number of options, so that a few options will anyways reap most of the benefits that one can hope to gain from priority service pricing.

Regarding the number of iterations needed to yield a solution of desired quality, this depends strongly on the choice of ρ. For a larger choice of ρ, it is likely that the first feasible solution is found earlier, but the larger ρ also has an adverse effect on the quality of the solution.

In table 2.4, we report on the impact that the choice of different algorithm parameters can have on run time.

In the table, ρ is the penalty imposed on the regularization term in ADMM; the second column presents the number of subproblems in the x-update, which depends on the horizon of the unit commitment problems (weekly or monthly); the third column shows the number of CPUs that are used in the computations; the fourth column indicates the index of the first iteration that returns a solution and the corresponding run time and social welfare. We say the first solution is yielded when the relative gap with respect to operating costs is less than 1%, as indicated in the table. In other words, the algorithm converges when the relative gap is less than 1%. Since the objective is to minimize negative social welfare, the relative gap is calculated as

$$\begin{aligned}\text{Relative Gap} &= \frac{\text{UpperBound} - \text{LowerBound}}{\text{OperatingCosts}} \\ &= \frac{|\text{LowerBound}| - \text{SocialWelfare}}{\text{OperatingCosts}}\end{aligned}$$

The absolute gap (|LowerBound| - SocialWelfare) is presented in the last column. By comparing the first two rows, we can observe that if we reduce the number of CPUs that are employed in order to run the algorithm, the run time will increase, but the efficiency is not linear. By comparing the second row with the third row, it is observed that with a larger ρ, we arrive to the first solution in fewer iterations, but the quality of the solution also decreases. By comparing the second and fourth row, we can see that when the horizon of

Western European systems with weekly or daily reserve clearing and where the only means of storage are pumped hydro reservoirs (as opposed to large hydro reservoirs) is also a reasonable assumption.

Table 2.4: Solution comparison of using different parameters in ADMM.

(a)

ρ	No. of Subproblems	No. of CPUs	Iterations to 1st solution	Run Time to 1st solution (hrs)
0.2	120	40	16	2.2
0.2	120	120	16	1.3
3	120	120	13	0.82
0.2	520	130	17	0.52
0.2	520	520	17	0.27

(b)

ρ	Social Welfare of 1st solution (M €)	Relative Gap	Absolute Gap (M €)
0.2	5763.4	0.34%	4.1
0.2	5763.4	0.34%	4.1
3	5757.8	0.81%	9.7
0.2	5763.9	0.27%	3.6
0.2	5763.9	0.27%	3.6

the unit commitment problem is reduced to one week, we can achieve further computational efficiency. As we demonstrate in the last row, the computing time can be further reduced to 0.27 hours with 520 CPUs. By comparing the gap of the second and fourth row, we can conclude that the performance of the algorithm is stable for different horizons of the unit commitment problem in the x-update.

There are other heuristics that can potentially speed up the convergence of the ADMM algorithm. For example, ρ could assume dynamic values that change over iterations [HYW00]. In addition, warm-start strategies can be adopted at each iteration by exploiting solutions from previous iterations. We have not explored these techniques in this work, since the run time is satisfactory.

2.D Sensitivity Analysis on the Number of Options

The efficiency gains of priority service depend on the number of options in the price menu. However, relying on too many options would violate the principle of simplicity in priority service, since a large number of options would exert an overwhelming information processing burden on households. We therefore

Table 2.5: Sensitivity Analysis on the Number of Options in the Priority Service Pricing Menu

Number of Options	Social Welfare (M €)	Efficiency Gain (%)
5	5763.4	77.1
4	5760.8	73.7
3	5750.7	61.4

consider three to five options as a reasonable compromise. Proposition 6 in [CW87] shows that the deadweight losses resulting from priority service are inversely proportional to the square of the number of options, so that a few options will anyways reap most of the benefits that one can hope to gain from priority service pricing.

In our model, numerous assumptions that are employed in the traditional priority service theory are dropped. Therefore, it is not guaranteed that Proposition 6 still applies to our model. For this reason, we analyze the sensitivity of the welfare gains of priority service on the number of options. Table 2.5 presents the social welfare that can be achieved under priority service, and the gains that can be derived, relative to real-time pricing. The menu with four options attains similar performance to the menu with five options. On the other hand, the gain drops by 12.3% when the fourth option is dropped.

2.E Review of Assumptions

In section 1.4, we summarize the assumptions that are used in this chapter. In the following, we further elaborate on these assumptions and how relaxing them might affect our conclusions.

2.E.1 Constant Valuation over Time

Mathematically, this assumption means that V_l, the valuation of consumer type l, remains constant during the whole horizon, i.e. it is not indexed by time step t. If the assumption of constant valuation is dropped, the valuation of consumer l becomes $V_{l,t}$, which means that the valuation of consumer l changes over time. We consider various ways in which we could re-write our model, and why these new ways of casting the model are either not implementable in practice, or equivalent to the model that we present in the main body of the chapter.

In order to exploit the richer information provided by $V_{l,t}$, the objective of (CP_l) needs to be reformulated. Recall that the objective of the consumer is written as (2.140):

$$\max_{s_{l,i}} V_l \cdot \sum_{t\in\mathcal{T}} \sum_{i\in\mathcal{I}} r_i \cdot s_{l,i} \cdot \Theta_t - \sum_{i\in\mathcal{I}} s_{l,i} \cdot \pi_i \cdot T. \tag{2.140}$$

For the sake of clear comparison with different reformulations when $V_{l,t}$ is considered, (2.140) is rewritten as:

$$\max_{s_{l,i}} \sum_{t\in\mathcal{T}} V_l \cdot \Theta_t \cdot \sum_{i\in\mathcal{I}} r_i \cdot s_{l,i} - \sum_{t\in\mathcal{T}}\sum_{i\in\mathcal{I}} s_{l,i}\cdot\pi_i \tag{2.141}$$

We proceed with analyzing the outcomes of different reformulations one by one.

2.E.1.1 Reformulation 1

$$\max_{s_{l,i}} \sum_{t\in\mathcal{T}} V_{l,t} \cdot \Theta_t \cdot \sum_{i\in\mathcal{I}} r_i \cdot s_{l,i} - \sum_{t\in\mathcal{T}}\sum_{i\in\mathcal{I}} s_{l,i}\cdot\pi_i \tag{2.142}$$

In (2.142), $s_{l,i}, r_i, \pi_i$ remain the same as in (2.141), so that one single menu is offered to consumers and consumers only subscribe once. The difference between (2.141) and (2.142) is that $\sum_{t\in\mathcal{T}} V_l \cdot \Theta_t$ is changed into $\sum_{t\in\mathcal{T}} V_{l,t} \cdot \Theta_t$. Recall that $\sum_{t\in\mathcal{T}} \Theta_t = T$, we can define $V_l^{'} = \frac{\sum_{t\in\mathcal{T}} V_{l,t}\cdot\Theta_t}{T}$ and then $\sum_{t\in\mathcal{T}} V_{l,t} \cdot \Theta_t = \sum_{t\in\mathcal{T}} V_l^{'} \cdot \Theta_t$. As a result, (2.142) can be written as

$$\max_{s_{l,i}} \sum_{t\in\mathcal{T}} V_l^{'} \cdot \Theta_t \cdot \sum_{i\in\mathcal{I}} r_i \cdot s_{l,i} - \sum_{t\in\mathcal{T}}\sum_{i\in\mathcal{I}} s_{l,i}\cdot\pi_i \tag{2.143}$$

Thus, replacing V_l in (2.141) with $V_l^{'}$, we obtain (2.143). In conclusion, the new formulation of (2.142) is equivalent to (2.141), and this formulation cannot take advantage of richer information from $V_{l,t}$, because $V_{l,t}$ is only used to calculate $V_l^{'}$.

2.E.1.2 Reformulation 2

$$\max_{s_{l,i,t}} \sum_{t\in\mathcal{T}} V_{l,t} \cdot \Theta_t \cdot \sum_{i\in\mathcal{I}} r_i \cdot s_{l,i,t} - \sum_{t\in\mathcal{T}}\sum_{i\in\mathcal{I}} s_{l,i,t}\cdot\pi_i \tag{2.144}$$

In (2.144), one single menu is offered to the consumer since r_i and π_i are not indexed by t. However, $s_{l,i,t}$ is indexed by t, which means that the consumer must change its subscription to different options in each hour according to its valuation $V_{l,t}$, which is not practical.

2.E.1.3 Reformulation 3

$$\max_{s_{l,i}} \sum_{t\in\mathcal{T}} V_{l,t} \cdot \Theta_t \cdot \sum_{i\in\mathcal{I}} r_{i,t} \cdot s_{l,i} - \sum_{t\in\mathcal{T}}\sum_{i\in\mathcal{I}} s_{l,i}\cdot\pi_{i,t} \tag{2.145}$$

In (2.145), $s_{l,i}$ is not indexed by t, which means that consumers only subscribe once during the whole horizon. However, since $r_{i,t}$ and $\pi_{i,t}$ are indexed by t, one price menu at each period will be offered to consumers, which is not practical as well.

Alternatively, multi-level demand subscription [COSW86] is able to exploit the time-varying valuation of consumers by offering an extra duration component in the price menu. We explore this scheme in the next chapter.

2.E.2 Identical Consumption Profiles

This assumption implies that every consumer follows the same profile Θ_t, as described by $D_{l,t} = \bar{D}_l \cdot \Theta_t$. When all the consumers are synchronized, and follow the system-level profile Θ_t, the aggregate profile of consumers in option i also follows Θ_t. Therefore, the subscription limit constraint can be formulated as $d_{i,t,\omega} \leq s_i \cdot \Theta_t$, and implies that the supply to option i at hour t in scenario ω cannot exceed the subscription quantity. If the assumption of identical profiles were dropped, the producer would then need to know the profile $\Theta_{l,t}$ of each different type of consumer in option i in order to express this constraint. Our presumption is that this is not practical, because this requires too detailed information on the side of the producer.

In the following, we use a toy example and a case study on the Belgian market to illustrate the impacts of non-identical profiles, in terms of efficiency losses.

2.E.2.1 A toy example

In the toy example, we consider three hours and two generators. The marginal cost of the first generator is 80 €/MWh and it has a capacity of 3.5 MW, which is available during all the periods. The second generator has a marginal cost of 30 €/MWh and a capacity of 3.5 MW, but the generator is only available during the first period. The demand functions of consumers in the three periods are shown in figure 2.15.

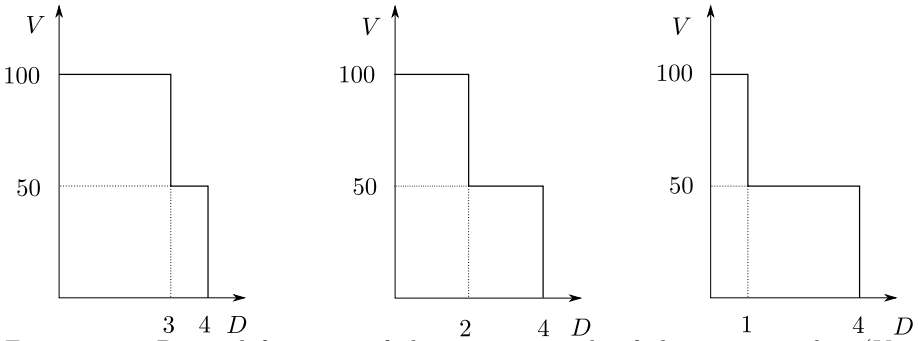

Figure 2.15: Demand functions of three time periods of the toy example. (V - €/MWh; D - MWh)

From figure 2.15 we can observe that there are two types of consumers on the demand side. The high-valuation consumer (100 €/MWh) follows a

profile of [1.5, 1, 0.5] with an average demand of 2 MW and the low-valuation consumer (50 €/MWh) follows a profile of [0.5, 1, 1.5] with an average demand of 2 MW. However, the producer is only aware of the system-level profile, which follows the profile [1 1 1]. The social welfare of priority service pricing is 250 €, which is 30 € lower than the optimal social welfare from real-time pricing. These efficiency losses are due to the fact that the assumption that consumption profiles are identical is not true in reality.

Table 2.6: Production of each generator in each time period in the toy example (Unit: MWh)

	t_1	t_2	t_3
G_1	0	2	**2**
G_2	3.5	0	0

The decrease in social welfare can be explained in table 2.6. Generator G_1, with a marginal cost of 80 €/MWh, should only produce 1 MWh at t_3, because the demand function is 1 MW with a valuation of 100 €/MWh and 3 MW with a valuation of only 50 €/MWh. However, it supplies 1 MWh to the consumer whose valuation is 50 €/MWh, at a cost of 80 €/MWh, which amounts to a loss of 30 €/MWh in terms of social welfare. This overproduction is due to the fact that the producer is only aware of the system profile, and assumes the profile of each consumer is synchronized with the system profile. Thus, the producer misinterprets the demand function at this period as 2 MW with a valuation of 100 €/MWh and 2 MW with a valuation of only 50 €/MWh.

Table 2.7: Price Menu in the toy example

r (%)	π (€/MWh)
25	12.5
100	68.75

Even though the assumption of identical profiles results in some loss of efficiency, we can still use the theory to design a price menu, as shown in table 2.7, to differentiate the two types of consumers. The efficiency losses that result from our simplifying assumption about synchronism are relatively small. Next, we conduct a more extensive case study on the Belgian market.

2.E.2.2 The Belgian Market

For the simulation of the Belgian market, we first calibrate piece-wise linear demand functions which generalize the affine demand functions that are used before. The change in the slope of the demand functions implies that loads are no longer synchronous. Figure 2.16 presents the profiles of different types of consumers in the first 120 hours of the year and the system-level profile.

For the sake of our discussion, let us suppose that the menu designer assumes that the consumers' profiles are the same as the system profile when designing

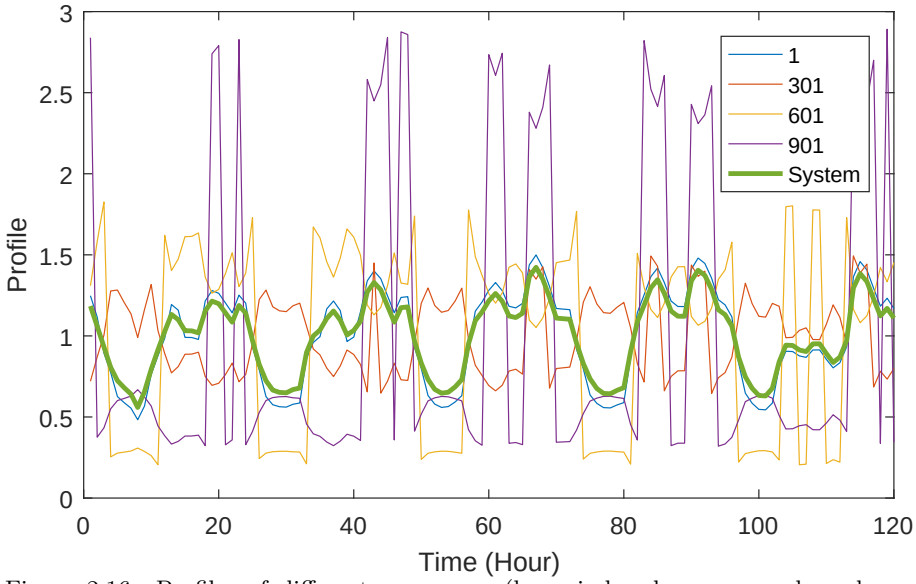

Figure 2.16: Profiles of different consumers (lower-indexed consumers have lower valuation).

the menu. Suppose, also, that the producer dispatches the system according to the priority of the consumers, i.e., according to the option that they choose.

The realized social welfare[11] amounts to 11452.6 million €. In contrast, the social welfare of real-time pricing is 11477.6 million €, and the flat tariff policy achieves a welfare of 11353.3 million €. When consumers do not follow the same profiles, priority service pricing still achieves 79.9% of the efficiency gains that can be achieved by real-time pricing, relative to a flat tariff. This case study illustrates that priority service pricing remains a workable solution when consumers' profiles are not identical, even if the assumptions under which the menu is designed depart from the true complexity of consumers' valuation.

2.E.3 Exogenous Valuation Breakpoints

In our case study, we follow the same approach as in [CW87] to choose the breakpoints that separate consumers into priority service classes exogenously. If the breakpoints were treated as decision variables, the model would involve bilinear terms, which is generally difficult to solve.

Alternatively, we use McCormick envelopes and the binary expansion technique to convert the bilinear optimization problem to a MILP. We conduct a

[11] Note that the demand functions are different from the ones used in the case study in the main body of this chapter before, so the values of social welfare will differ in general.

case study that only optimizes V_0^B, i.e. consumers whose valuation is lower than V_0^B are not included in the service.

In this case study, we only consider one scenario for simplicity, and the results are presented in table 2.8. The two left columns present the upper bound on social welfare from dual decomposition and social welfare from ADMM when V_0^B is treated as a parameter that is equal to 0. In the third column, V_0^B is regarded as a decision variable and we rely on dual decomposition for solving for the upper bound of the social welfare. The result is 5.3 million € higher than the welfare when V_0^B is not optimized. We then solve the model by enumerating different values of V_0^B as a heuristic and the resulting social welfare is 5770.2 million €, which is only 2.2 million € lower than the upper bound.

From this case study, we draw two conclusions: i) by optimizing the first valuation breakpoint, we are able to further increase social welfare, however, the increment is marginal; ii) It is a workable heuristic to enumerate different values of V_0^B, in order to solve the model.We leave it for future research to develop decomposition algorithms for solving the model that optimizes all breakpoints.

Table 2.8: Comparison of social welfare (unit: million €)

DD ($V_0^B = 0$)	ADMM ($V_0^B = 0$)	DD (Optimize V_0^B)	Enumerate V_0^B
5767.1	5764.2	5772.4	5770.2

Chapter 3

Comparison of Priority Service and Multilevel Demand Subscription

3.1 Introduction

In Chapter 2, we present a bilevel optimization formulation of priority service pricing, which is one of the simplest approaches for quality-differentiated pricing. In this chapter, we explore a more sophisticated structure, where the duration component is introduced. This implies that the offering of electricity is now differentiated by both reliability and duration. Our extension is motivated by the fact that an increasing number of households are equipped with rooftop PV panels and batteries, which we refer to as prosumers. Prosumers tend to be self-sufficient during the daytime and their energy surplus can be stored in the battery to be used in the peak hours. Thus, they may prefer a service that does not span the entire horizon, whereas priority service pricing does. Multilevel demand subscription extends priority service by adding a duration component, which can be financially advantageous for prosumers.

The menu design and performance evaluation framework that we develop in this chapter is aimed at comparing priority service with multilevel demand subscription, with an explicit consideration of the storage capability and local supply uncertainty of prosumers. The trade-off between a complex yet efficient multilevel demand subscription menu and a simple yet less efficient priority service pricing menu is investigated quantitatively.

3.1.1 Previous Work on Tariff Design with Consideration of Prosumers

Faced with the development of rooftop PV panels, a number of utility companies have recently adopted a simple net metering policy. Net metering allows prosumers to receive compensation at the retail electricity price or as credits that can offset their bill. Thus, prosumers only pay for their aggregate net consumption over the billing period, e.g. monthly.

Net metering has recently been criticized by academics and practitioners. Gautier et al. [GJP18] demonstrate that net metering results in a decrease in the bills of prosumers who adopt net metering. This decrease is achieved by increasing the bill of traditional consumers and results in too many adopters of net metering. Moreover, the decrease in the energy needs of prosumers may result in a failure to recover grid costs [Kub18]. In certain states in the US, the net metering policy has been withdrawn after its introduction. For example, *"the Hawaii Public Utility Commission concluded that simple retail rate net metering credit is driving uncontrolled, undirected growth, and raising questions about cost shifting to non-solar customers"* [Ore17]. This resulted in the discontinuation of net metering in 2015 in Hawaii. This demonstrates that the electricity tariff needs to be carefully designed as prosumers become an increasing segment of the retail base.

Recent work has focused on proposing electricity tariff structures that aim at efficiently integrating prosumers into the system. Darghouth et al. [DWBM16] develop a quantitative model for evaluating net metering and market feedback loops, and show that the adoption of distributed PV is highly sensitive to retail rate structures. Five different tariff scenarios are benchmarked by Bloch et al. [BHBW19], including real-time pricing, a capacity-based tariff and a block rate tariff. The case studies provide insights into the effects of the tariffs on the amount of installed PV capacity, the ratio of energy curtailment, and the investment into battery systems. Schittekatte et al. [SMM18] consider the grid cost recovery problem as a non-cooperative game between consumers with PV panels and batteries and the DSO. The modeling approach proposed by the authors is aimed at assessing volumetric energy charges with net-metering, volumetric energy charges for both injection and withdrawal, and capacity-based charges.

3.1.2 Contribution and Chapter Organization

The contributions of this chapter can be listed as follows:

1. We extend traditional multilevel demand subscription theory to a more realistic setting via a bilevel optimization formulation.

2. We propose a menu design and evaluation framework with considera-

tion of prosumers for both priority service pricing and multilevel demand subscription pricing. In this framework,

- we extend priority service by including duration choices in the price menu;
- the interruption of different reliability levels in the price menu, the uncertainty of rooftop PV production and the behavior of the battery are incorporated into a household model based on stochastic programming;
- a rolling horizon approach is adopted to simulate the gradual revelation of uncertainties;
- we are able to capture the interaction of the system-level renewable production uncertainty and the uncertainty from the roof-top PV panels in the household.

The remainder of the chapter is organized as follows. Section 3.2 revisits the traditional theory of multilevel demand subscription, and points out some strong assumptions that are generally not satisfied in practice. Section 3.3 first casts the multilevel demand subscription pricing menu design problem as a Stackelberg game, which is reformulated into an MILP. This formulation incorporates priority service as a special case without differentiation of durations. Then an evaluation framework is proposed in section 3.4 to compare priority service with multilevel demand subscription. The results of the comparison are presented in a quantitative way based on a case study of the Belgian power system in section 3.5.

3.2 Traditional Theory of Multilevel Demand Subscription Pricing

This section presents the theory of multilevel demand subscription pricing based on Chao et al. [COSW86]. The starting point of the theory is a set of consumer types who correspond to horizontal slices in a system load duration curve. The authors consider a price plan that offers the option of selecting a different duration and reliability level for each consumer type (equivalently, load slice). In other words, consumer types are represented by their indices on the load duration curve, as shown in figure 3.1. The general form of the price plan is $\pi(r, t)$, which is the total charge for a load slice of duration t at specified reliability level r. The reliability r is defined as the long-run average fraction of a load slice that will be served when reliability r is selected. Each load slice is priced independently. The producer is assumed to have a fixed capacity and the uncertainty is represented by scaling the load duration curve with a factor in each scenario. This section proceeds with the consumer choice model and

the cost model, and then describes how one designs such a price menu with the objective of maximizing social welfare.

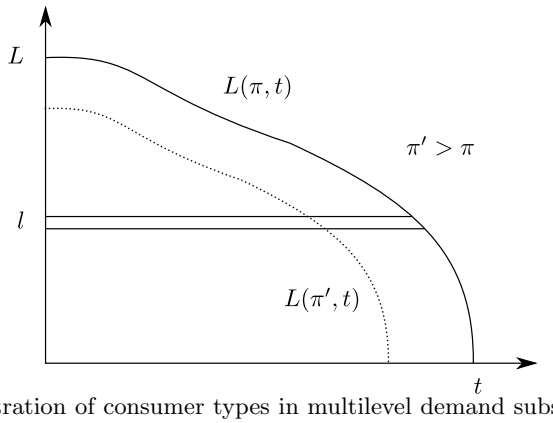

Figure 3.1: Illustration of consumer types in multilevel demand subscription pricing theory [COSW86]. $L(\pi, t)$ is the load duration curve, parametric on a price π; $t(l, \pi)$ is the duration demand function, parametric on a price π.

3.2.1 The Consumer Model

Since the model is focused on pricing reliability, uncertainty has a key role. Chao et al. [COSW86] introduce uncertainty in their model on the consumer side. Concretely, consider a reference π_0 and a random variable ω, which is assumed to be uniformly distributed between zero and one. Then the actual load duration curve under realization ω is denoted by $h(\omega) \cdot L(t)$, where $L(t)$ (π_0 is dropped for simplicity) is the average load duration curve given reference price π_0, and $h(\omega)$ is a scaling function which is assumed to be increasing with ω. We also define the willingness-to-pay for the load type l for duration t as $v(l, t)$ and $\partial v(l, t)/\partial t = \pi$. Then, the optimal pair $\{r(l), t(l)\}$ which maps a consumer type to its chosen level of reliability and duration is determined by solving the following consumer surplus maximization problem:

$$\max_{0 \le r \le 1, 0 \le t \le T} \{S(r, t, l) = H(r) \cdot [v(l, t) - \pi(r, t)]\}, \tag{3.1}$$

where

$$H(r) = \int_0^r h(\omega) d\omega, \text{with } H(0) = 0, H(1) = 1. \tag{3.2}$$

The objective function corresponds to the expected consumer surplus. The integral $H(r)$ corresponds to the probability of service under reliability choice r.

3.2.2 The Cost Model

Using l to denote the index of each load slice, the first term of the objective function gives the benefits of consumer type l. Assuming the generation system has a fixed capacity configuration, the operating cost attributed to an individual load slice is denoted by $c(r,t,l)$, which is the average cost for serving a load slice of level l with duration t and service reliability r. And the function $c(r,t,l)$ is linear in t. Aggregating all types of consumers, the social welfare maximization problem can be formulated as

$$\max_{r(l),t(l),l_0} \int_0^{l_0} \left[H(r(l)) \cdot v(l,t(l)) - c(r(l),t(l),l)\right] dl \tag{3.3}$$

$$\text{s.t.} \quad 0 \le r(l) \le R(l) \tag{3.4}$$

$$0 \le t(l) \le T \tag{3.5}$$

where l_0 is the cutoff level, beyond which no service is offered to consumers. The function $R(l)$ is the maximum reliability that the system can offer to a given load level l due to capacity limits, and T is the horizon of service (e.g. 8760 hours for a one-year contract).

3.2.3 Determining the Optimal Price Function

Given the optimal trajectory $\{r(l),t(l)\}$, the goal of the menu design problem is to derive an optimal menu that induces consumers to choose the optimal trajectory when they maximize their surplus. Denote the optimal price function as $\pi\big(r(l),t(l)\big)$, then as shown by Chao et al. [COSW86], this price function is calculated as

$$\pi\big(r(l),t(l)\big) = v\big(l,t(l)\big) + \{1/H\big(r(l)\big)\} \int_l^{l_0} H\big(r(l')\big) \cdot v_l\big(l',t(l')\big) dl', \tag{3.6}$$

where $v_l < 0$ is the partial derivative of $v(l,t)$ with respect to l.

3.2.4 Our Contribution to the Literature

The closed-form solution to the problem which is presented in the work of Chao et al. requires certain strong assumptions, which may not be obeyed in practice:

- The generation system is assumed to have a fixed capacity. Moreover, the cost function is convex and linear with respect to duration. This is not true in practice due to the start-up and min-load costs, outage and maintenance of generators, and intermittence of renewable production.
- The source of uncertainty in the model presented above is the demand side and this uncertainty is represented by scaling the load slices.

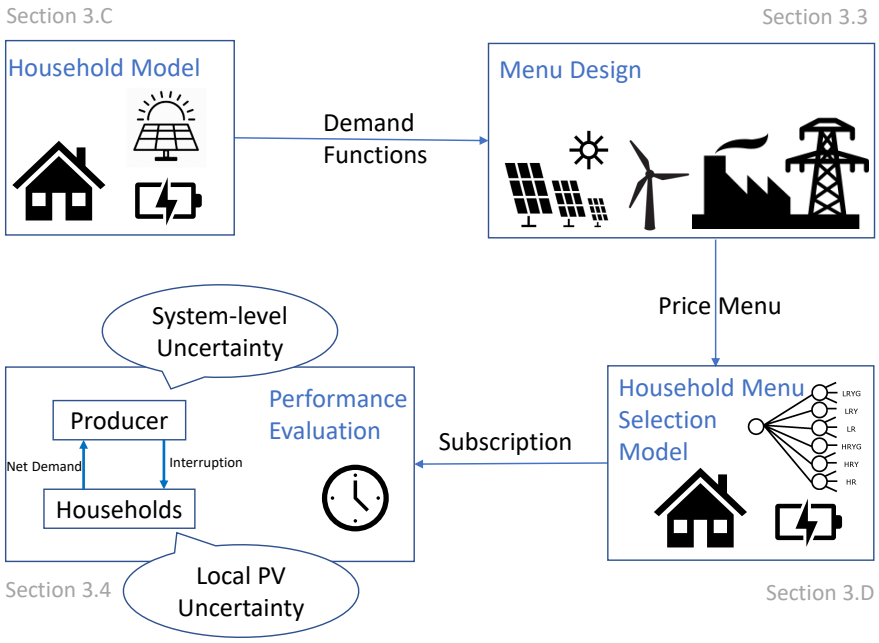

Figure 3.2: The menu design and performance evaluation framework to compare priority service and multilevel demand subscription.

- Neither the system-level nor the household-level uncertainty is modeled explicitly. The behavior of storage cannot be captured.

To deal with these shortcomings, we propose a four-step menu design and performance evaluation framework which is presented in figure 3.2. We briefly introduce each block as follows:

- We consider different types of households that are equipped with rooftop PV panels, but differ in the size of batteries and consumption profiles. The valuation of power increments is calculated and extrapolated for each *type* of household, in order to derive a system-level demand function. This demand function is used as an ingredient for the design of a reliability-duration menu. The corresponding model is presented in section 3.C.

- Subsequently, a multilevel demand subscription price menu is designed. The designed menu is based on the bilevel model that is presented in section 3.3. Unit commitment decisions of conventional generators are considered in the upper-level producer model, thus the non-convex costs of the production pool are captured. Moreover, scenarios of system-level

renewable production are modeled explicitly. In this step, we also design a priority service menu as a special case of the multilevel demand subscription menu, where the duration is the entire horizon.

- Given the price menu designed in the previous step, households decide on their subscription based on a stochastic scheduling model, which is presented in section 3.D. In this model, the interruption of different options and the rooftop PV production are modeled as a scenario tree. The behavior of the battery is optimized as well.

- In the last step, we evaluate and compare the performance of priority service and multilevel demand subscription via a rolling horizon approach. At each period, households optimize the behavior of the battery until the end of the horizon, against the realization of rooftop PV supply and the interruption of options. Generators are then dispatched in order to meet the net demand of all households, with consideration of the system-level renewable uncertainty. This process is described in section 3.4.

Note that this menu design and performance framework is fundamentally different from Chapter 2. In principle, the optimal pricing problem would need to be cast as a bilevel program with a multi-stage stochastic program in the lower level. This is computationally intractable, even if valuable for representing the uncertainty and storage capability of prosumers. Instead, we separate the performance evaluation step from the menu design step. In the menu design step of multilevel demand subscription, each duration option maps to specific time periods. This requirement is relaxed in the performance evaluation step by interpreting the duration as energy credits. By relying on this approach, households are allowed to consume electricity throughout the entire horizon, so long as their power consumption is within the capacity limit of the household, and so long as the energy credits of the household are not depleted.

3.3 Multilevel Demand Subscription Pricing Menu Design

3.3.1 Modeling the Multilevel Demand Subscription Menu Design Problem as a Stackelberg Equilibrium

In this section, we follow a similar approach as in section 2.3 to model the multilevel demand subscription (MDSP) menu design problem as a bilevel optimization problem, which is reformulated as an MILP. The exposition here focuses on multilevel demand subscription pricing, with priority service pricing being a special case.

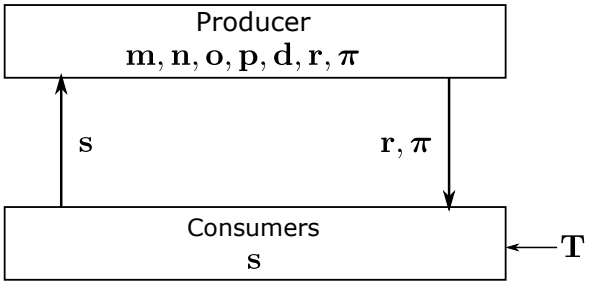

Figure 3.3: Interaction between the producer and consumers in the multilevel demand subscription bilevel model.

The major difference between MDSP and PSP is that, in MDSP, consumers decide not only about their reliability level $\boldsymbol{r}$, but also about the duration of their service $\boldsymbol{T}$. The corresponding prices $\boldsymbol{\pi}$ differ according to the duration and reliability levels. In the model, the producer restricts the offering of duration to several options based on the temporal resolution of the offered product. For example, considering a resolution of 6 hours and a horizon of 24 hours, the producer could offer four duration options, i.e., 6 hours, 12 hours, 18 hours and 24 hours. The producer designs the proposed menu such that it induces consumers to choose options that maximize social welfare, taking into account the cost and constraints of production. In this study, T is treated as a parameter that is predetermined by the producer. The model can be extended in order to regard T as a decision variable of the producer, however this poses computational challenges. In what follows, we introduce the lower-level consumer model. The upper-level producer model, the bilevel model and its reformulation as an MILP are presented in section 3.B of the appendix. We delegate the presentation of the bilevel model to the appendix due to its similarity to section 2.3 in terms of methodology.

In the traditional MDSP theory presented in section 3.2, uncertainty is represented by scaling load slices according to $h(\omega)$, which is the ratio of the load duration curve under the random condition ω to the average load duration curve. In the model that we propose in this chapter, we assume that the load duration curve remains the same and then the consumer model can be described as follows.

Consumer l represents the l-th slice of power on the load duration curve, and its valuation for t periods of consumption is denoted as $V_l(t)$. Suppose that the producer offers a price menu with I reliability levels, each of which is associated with J duration levels. Given a price menu $\{r_i, T_j, \pi_{i,j}\}$, $i \in \mathcal{I}, j \in \mathcal{J}$, the

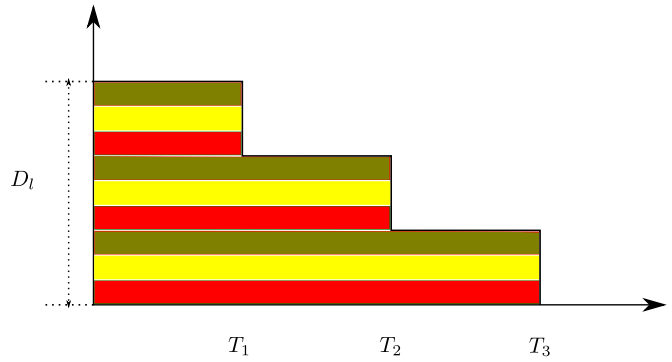

Figure 3.4: Illustration of the optimal choice problem of consumer type l. The consumer needs to choose the reliability level (indicated by colors) and the duration associated with this color. In a priority service pricing menu, only full duration is offered.

consumer problem is expressed as:

$$(CP_l) : \max_{s_{l,i,j}} \sum_{i\in\mathcal{I},j\in\mathcal{J}} s_{l,i,j} \cdot \Big(r_i \cdot V_l(T_j) - \pi_{i,j}\Big) \tag{3.7}$$

$$(\gamma_l) : \sum_{i\in\mathcal{I},j\in\mathcal{J}} s_{l,i,j} \leq D_l \tag{3.8}$$

$$s_{l,i,j} \geq 0,\ i \in \mathcal{I}, j \in \mathcal{J}. \tag{3.9}$$

The variable $s_{l,i,j}$ indicates the amount of power that consumer l allocates to option (i, j). The first term in the objective function indicates the benefit of the consumer, while the second term corresponds to the payment that needs to be submitted to the producer for this service. Constraint (3.8) expresses the fact that options are stacked up to the amount of kilowatts that the household wishes to procure. The decision problem faced by a consumer of type l is further illustrated in figure 3.4. The consumer chooses color options in the set $\mathcal{I}$ and duration options in the set $\mathcal{J}$, up to the level where it fully satisfies its total power demand D_l.

The function $V_l(t)$ is an increasing function of t, since more hours of consumption increase the benefit of the household. Note that the formulation of the problem above implicitly assumes that $V_l(t)$ is further a concave function of t. In section 3.C of the appendix, we describe how the producer can estimate this data based on information about residential households.

Given a duration option $j \in \mathcal{J}$ and a mapping from the time indexing of a load duration curve to the time indexing of actual operations, we can define indicator parameters $N_{j,t} \in \{0, 1\}$ which determine whether a certain duration option $j \in \mathcal{J}$ is being served in time period t of actual operations or not. This

parameter is used in the producer model presented in section 3.B. Note that, by definition, $\sum_{t\in\mathcal{T}} N_{j,t} = T_j$. In other words, service option j corresponds to T_j time periods of service. This formulation requires that all consumers have the same order of periods, since the delivery of the service is decided by $N_{j,t}$. This is generally not true in practice due to the uncertain production of photovoltaic power, and the inter-temporal constraints of the battery. This assumption is only adopted in the menu design step and is dropped in the performance evaluation step which is presented later.

An important insight that allows us to arrive to the bilevel formulation of the Stackelberg equilibrium is that any consumer type l may as well limit its choice to a unique option out of the menu offered by the producer.

Proposition 3. *There exists* $\tilde{\mathbf{s}}_l = (\tilde{s}_{l,i,j}, i \in \mathcal{I}, j \in \mathcal{J})$ *with* $\tilde{s}_{l,i,j} \in \{0, D_l\}$ *which attains the optimal objective function value.*

Proof. The KKT conditions of (CP_l) are given by (3.10) and (3.11).

$$0 \leq s_{l,i,j} \perp -r_i \cdot V_l(T_j) + \pi_{i,j} + \gamma_l \geq 0 \tag{3.10}$$

$$0 \leq \gamma_l \perp D_l - \sum_{i,j} s_{l,i,j} \geq 0 \tag{3.11}$$

There are two cases to be considered:

Case 1: If $D_l - \sum_{i,j} s^\star_{l,i,j} > 0$, then $\gamma_l = 0$. This implies that consumer l derives zero net benefit at the optimal solution. Thus, $\tilde{s}_{l,i,j} = 0$ for all $i \in \mathcal{I}, j \in \mathcal{J}$ is optimal.

Case 2: If $D_l - \sum_{i,j} s^\star_{l,i,j} = 0$, then it suffices to show that if two options are 'active' (in the sense that $s > 0$) then they have an equal payoff, and can therefore be equivalently replaced by a single option. Applying this argument for all options that are active gives the desired conclusion. Consider any two options (i, j) and (i', j') for which $s^\star_{l,i,j} > 0$ and $s^\star_{l,i',j'} > 0$. Then $-r_i \cdot V_l(T_j) + \pi_{i,j} + \gamma_l = 0$ and $-r_{i'} \cdot V_l(T_{j'}) + \pi_{i',j'} + \gamma_l = 0$, and substituting out γ_l, we have $r_i \cdot V_l(T_j) - \pi_{i,j} = r_{i'} \cdot V_l(T_{j'}) - \pi_{i',j'}$. □

The above proposition implies that $s_{l,i,j}$ can be expressed as $s_{l,i,j} = D_l \cdot \mu_{l,i,j}$, where $\mu_{l,i,j} \in \{0, 1\}$ are binary variables.

The producer model and the reformulation of the bilevel model as an MILP are presented in sections 3.B.2 and 3.B.3 of the appendix.

3.3.2 Menu Choice by Household

For the performance evaluation of section 3.4, we need to determine which specific option each household procures. Thus, each household solves a menu subscription problem, which is described in section 3.D of the appendix. This problem determines parameters $S_{h,i,j}$, i.e. the kilowatts procured by household type h for option $(i, j) \in \mathcal{I} \times \mathcal{J}$. Note that the household type h is different from

the consumer type l. Household types are categorized according to consumption profiles, the size of batteries, and the installation of PV panels. In contrast, a consumer type l is an index of the slice of power on the load duration curve. A household type h is composed of multiple consumer types.

3.4 Performance Evaluation

In order to simulate the performance of different residential pricing methods, we need to account for the interplay between system-level uncertainty and distributed rooftop solar uncertainty. Concretely, a realization of a sample path of uncertainty over the horizon that we are simulating is a realization of $(\omega^W, \omega^S) \in \Omega^W \times \Omega^S$. Here, Ω^W is the set of sample paths of renewable supply from system-level wind resources, and Ω^S is the set of sample paths of renewable supply from system-level solar resources.

The interface between the producer and the household is the service contract. The service contract allows the producer and the household to decentralize their decision-making according to locally observable information related to uncertainty. More specifically, from the point of view of the producer, the uncertainty in the system comprises of system-level renewable supply and *net residential demand*. The net residential demand is of course driven by rooftop solar supply at the households, however the producer meters and reacts to net demand. Similarly, from the point of view of the household, a realization of uncertainty comprises of rooftop solar power supply as well as the *interruption of different service options*. The interruption patterns are of course driven by system-level renewable supply, however the household does not observe or react to this information. Essentially, the residential service contracts can be viewed as a way of decentralizing a dynamic optimization problem under uncertainty (that of dispatching the *entire* system against *system-level* uncertainty) between the producer and the household.

In this section we describe our approach to simulating this decentralized decision-making process, in order to quantify the efficiency of different residential pricing options. The overall procedure can be described as follows. For each day type $s \in \mathcal{S}$:

1. Draw a sample path of uncertainty $(\omega^W, \omega^S) \in \Omega^W \times \Omega^S$ using the underlying statistical measure.

2. For every time step $t \in \mathcal{T}$ of actual operations in the simulation horizon:

   (a) Solve a household decision problem $(H_{h,t})$ for every type of household $h \in \mathcal{H}$ (where $\mathcal{H}$ represents the set of household types) and a producer decision problem (U_t) in order to determine the action of the households and the producer.

(b) Increment t, update the state of the system, and return to step 2a.

In the remainder of the section, we describe the problems (U_t) and $(H_{h,t})$ described in step 2a of the simulation procedure above. We describe the simpler producer model first in the sequel, as it amounts to a simple economic dispatch. We then describe the multi-stage optimization that drives household consumption.

3.4.1 Rolling Optimization for the Producer

We ignore inter-temporal unit commitment constraints (startup costs, and min up/down time constraints), ramp constraints, and pumped hydro constraints, so we are able to describe the decisions of the producer as a single-period optimization problem. Concretely, the producer solves the following problem[1]:

$$(U_t):$$

$$\max_{\mathbf{m},\mathbf{n},\mathbf{o},\mathbf{d},\mathbf{p}} \sum_{i\in\mathcal{I}} \bar{V}_i \cdot d_i - \sum_{g\in\mathcal{G}} h_g(\mathbf{m}_g,\mathbf{n}_g,\mathbf{o}_g,\mathbf{p}_g) \tag{3.12}$$

$$\text{s.t.} \quad f_g(\mathbf{m}_g,\mathbf{n}_g,\mathbf{o}_g,\mathbf{p}_g) \leq 0, g\in\mathcal{G} \tag{3.13}$$

$$d_i \leq ND_{i,t}, i\in\mathcal{I} \tag{3.14}$$

$$\sum_{i\in\mathcal{I}} d_i \leq \sum_{g\in\mathcal{G}} p_g + W_{t,\omega^W} + S_{t,\omega^S} \tag{3.15}$$

$$d_i \geq 0, p_g \geq 0, i\in\mathcal{I}, g\in\mathcal{G} \tag{3.16}$$

The objective function of the producer is expressed in Eq. (3.12). The valuation $\bar{V}_i$ corresponds to the estimate of the average valuation that the producer assigns to priority class i, based on how households decide to subscribe to the multilevel demand service. Concretely, the parameter in time step t is estimated as follows:

$$\bar{V}_i = \sum_{l\in\mathcal{L}:s^\star_{l,i,j(t)}=D_l} \frac{\partial_t V_l(T_{j(t)})\cdot D_l}{\sum_{l\in\mathcal{L}:s^\star_{l,i,j(t)}=D_l} D_l}, \tag{3.17}$$

where $s^\star_{l,i,j}$ corresponds to the solution of problem (CP_l) in section 3.3.1 and $\partial_t V_l(T)$ corresponds to the *marginal* benefit of consumer type l for consuming at the T-th time step of the load duration curve.

The definition in Eq. (3.17) relies on the mapping $j(t)$, which is the duration option corresponding to period t of actual operations. Note that, for a given time step t of actual operations, there exists a *unique* value $j(t)\in\mathcal{J}$.

This mapping $j(t)$ depends on the mapping $\tau(t)$, which maps a time period t of actual operations to its time index in the load duration curve, and on the

[1] We describe the problem for the case of multilevel demand subscription, of which priority service is a special instance.

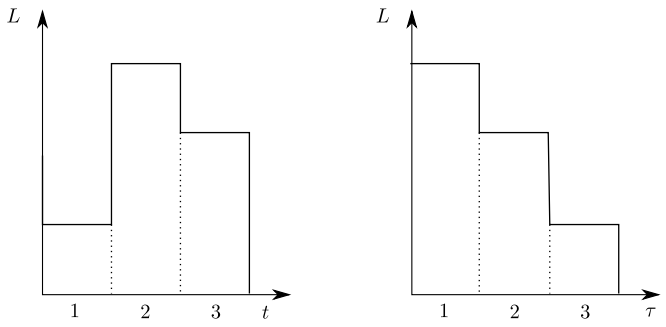

Figure 3.5: The mapping between the time period t of actual operations to its time index in the load duration curve. The figure on the left describes the load in each period of actual operations and the figure to the right depicts the corresponding load duration curve. In this three-period example, the first time period of actual operations corresponds to the third highest demand, the second time period of actual operations corresponds to the highest demand, and the third time period corresponds to the second highest demand. Then, $\tau(1) = 3$, $\tau(2) = 1$ and $\tau(3) = 2$. Moreover, suppose that the three periods have been split into two duration classes, with the first duration class covering the first two hours of the load duration curve, and the second duration class covering the full horizon. Then $j(1) = 2$, $j(2) = 1$ and $j(3) = 1$, i.e. the first period of the actual operations belongs to the second duration class, while both the second and third periods of actual operation belong to the first duration class.

definition of the duration classes $\mathcal{J}$. The mapping is illustrated in figure 3.5.

Constraint (3.13) expresses the production constraints of the producer. Constraint (3.14) implies that the producer may not offer more than the net demand that a certain priority class actually decides to consume at any given time period. Constraint (3.15) expresses the power balance constraint for the producer, where we use an inequality in order to allow for renewable production shedding at zero cost.

The wind supply W_{t,ω^W} and solar supply S_{t,ω^S} in constraint (3.15) are at the system level, and are drawn in step 1 of the performance evaluation procedure described above. The net demand $ND_{i,t}$ in constraint (3.14) is obtained as the solution of the household rolling optimization which is presented in the following section.

3.4.2 Rolling Optimization for the Household

In contrast to the producer model in the previous section which has been simplified in order to relax inter-temporal dependencies, the household rolling optimization is a dynamic optimization under uncertainty. The household faces

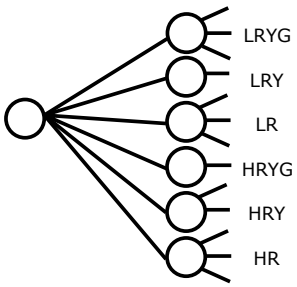

Figure 3.6: Scenario tree for the household model ($H_{h,t}$) of section 3.4.2.

uncertainty related to the supply of rooftop solar power at its premises and the interruption history of the service tiers in the home. This uncertainty is depicted in figure 3.6. The nodes of the scenario tree are named according to the realization of renewable supply (with 'L' indicating *low* solar supply, and 'H' indicating *high* solar supply) as well as the service interruption (with 'R' indicating that only the red color is served, 'RY' indicating that only the red and yellow color are served, and 'RYG' indicating that all colors are served).

The probability of each node can be calculated as follows. We denote P_{RYG} as the probability that all three colors are served, P_{RY} as the probability that only the red and yellow are served, P_R as the probability that only the red color is served. The reliability of green, yellow and red color options are denoted as r_1, r_2 and r_3, respectively. Since yellow color and red color are always served if green color is served, we have $P_{RYG} = r_1$. When yellow color is served, it is possible that all three colors are served or only yellow and red are served, yielding $P_{RYG} + P_{RY} = r_2$ and then $P_{RY} = r_2 - r_1$. There are three cases when the red color is served: all three colors are served or only the yellow and red are served or only the red is served, so we get $P_{RYG} + P_{RY} + P_R = r_3$ and then $P_R = r_3 - r_2$. The realization of PV panel production is assumed to be independent of the interruption of colors, so $P_{LRYG} = P_L \cdot P_{RYG}$. The conclusion is similar for other nodes.

In this rolling optimization, the household reacts to a history of realizations that have transpired up to stage t. We capture this information (which is a trajectory[2] in the scenario tree up to stage t) as $\mathcal{I}_t$. The scenario tree is modeled as a set of sample paths $\Omega^C = \Omega^I \times \Omega^S$, where Ω^I is the set of sample paths of interruptions, and Ω^S is the set of sample paths of renewable supply available at the household level. Each stage t of the scenario tree has an associated set of bundles, $\mathcal{B}_t$. Every bundle collects nodes in the given stage with the same history. The bundle to which a certain node n in the scenario tree belongs is

[2]For example, $\mathcal{I}_2 = \{(HR), (LRYG)\}$ corresponds to the history up to the second time stage whereby (i) there was high solar supply in the first period and only the red color was served, and (ii) there was low solar supply in the second period, and all colors were served.

denoted as $\mathcal{B}_t(n)$. Let us define as $\Omega(\mathcal{I}_t)$ the subset of sample paths with a history corresponding to $\mathcal{I}_t$:

$$\Omega(\mathcal{I}_t) = \{\omega^C \in \Omega^I \times \Omega^S : \mathcal{B}_t(\omega^C) = \mathcal{I}_t\}. \tag{3.18}$$

We can then describe the household model as follows.

$$(H_{h,\tau}):$$

$$\min_{\mathbf{x}=\mathbf{ls},\mathbf{nd},\mathbf{bd},\mathbf{bc},\mathbf{e}} \sum_{t=\tau}^{|\mathcal{T}|} \sum_{\omega^C \in \Omega(\mathcal{I}_\tau)} VOLL \cdot P_{\omega^C|\mathcal{I}_\tau} \cdot ls_{t,\omega^C} \tag{3.19}$$

$$\text{s.t. } bd_{t,\omega^C} \leq BD_h, t \in \{\tau, \dots, |\mathcal{T}|\}, \omega^C \in \Omega(\mathcal{I}_\tau) \tag{3.20}$$

$$bc_{t,\omega^C} \leq BC_h, t \in \{\tau, \dots, |\mathcal{T}|\}, \omega^C \in \Omega(\mathcal{I}_\tau) \tag{3.21}$$

$$e_{t,\omega^C} \leq E_h, t \in \{\tau, \dots, |\mathcal{T}|\}, \omega^C \in \Omega(\mathcal{I}_\tau) \tag{3.22}$$

$$e_{t,\omega^C} - e_{t-1} + bd_{t,\omega^C}/\eta_h^d - bc_{t,\omega^C} \cdot \eta_h^c = 0, \omega^C \in \Omega(\mathcal{I}_\tau) \tag{3.23}$$

$$e_{t,\omega^C} - e_{t-1,\omega^C} + bd_{t,\omega^C}/\eta_h^d - bc_{t,\omega^C} \cdot \eta_h^c = 0,$$
$$t \in \{\tau+1, \dots, |\mathcal{T}|\}, \omega^C \in \Omega(\mathcal{I}_\tau) \tag{3.24}$$

$$L_{t,h} - ls_{t,\omega^C} - PV_{t,\omega^S} + bc_{t,\omega^C} - bd_{t,\omega^C} = \sum_{i \in \mathcal{I}} nd_{i,t,\omega^C},$$
$$t \in \{\tau, \dots, |\mathcal{T}|\}, (\omega^I, \omega^S) \in \Omega(\mathcal{I}_\tau) \tag{3.25}$$

$$nd_{i,t,\omega^C} \leq \sum_{j \in \mathcal{J}} S_{h,i,j} \cdot 1_{[i,t,\omega^I]}, i \in \mathcal{I}, t \in \{\tau, \dots, |\mathcal{T}|\},$$
$$(\omega^I, \omega^S) \in \Omega(\mathcal{I}_\tau) \tag{3.26}$$

$$\sum_{i \in \mathcal{I}} nd_{i,t,\omega^C} \geq -\Gamma \cdot \sum_{i \in \mathcal{I}, j \in \mathcal{J}} S_{h,i,j}, t \in \{\tau, \dots, |\mathcal{T}|\},$$
$$(\omega^I, \omega^S) \in \Omega(\mathcal{I}_\tau) \tag{3.27}$$

$$\sum_{t=\tau}^{|\mathcal{T}|} \Pi_{\mathbb{R}_+}(nd_{i,t,\omega^C}) \leq \sum_{j \in \mathcal{J}} T_j \cdot S_{h,i,j} - UE_i, i \in \mathcal{I},$$
$$t \in \{\tau, \dots, |\mathcal{T}|\}, \omega^C \in \Omega(\mathcal{I}_\tau) \tag{3.28}$$

$$x_{t,b} - x_{t,\omega^C} = 0, t \in \{\tau, \dots, |\mathcal{T}|\}, b \in \mathcal{B}_t, \omega^C \in \Omega(\mathcal{I}_\tau) \tag{3.29}$$

$$bd_{t,\omega^C} \geq 0, bc_{t,\omega^C} \geq 0, e_{t,\omega^C} \geq 0,$$
$$ls_{t,\omega^C} \geq 0, i \in \mathcal{I}, t \in \{\tau, \dots, |\mathcal{T}|\}, \omega^C \in \Omega(\mathcal{I}_\tau) \tag{3.30}$$

Load shedding in the household is denoted as ls_{t,ω^C}. Home battery charge and discharge are denoted as bc_{t,ω^C} and bd_{t,ω^C} respectively. The energy level of the home battery is denoted as e_{t,ω^C}. The net demand of the household from the grid is denoted as nd_{i,t,ω^C}, and it is differentiated by reliability class $i \in \mathcal{I}$. The household is allowed to inject excess rooftop solar supply back to

the grid without compensation, which we represent in the following model by the fact that we allow the net demand nd to assume negative values.

The objective function (3.19) describes the goal of the household, which is to minimize its expected cost of interruption. The parameter $VOLL$ indicates the value of lost load. The conditional expectation $P_{\omega^C|\mathcal{I}_\tau}$ in the objective function is defined as

$$P_{\omega^C|\mathcal{I}_\tau} = \frac{P_{\omega^C}}{\sum_{\omega^C \in \Omega(\mathcal{I}_t)} P_{\omega^C}}. \tag{3.31}$$

Constraints (3.20) and (3.21) represent the battery discharge and charge constraints respectively, with BD_h and BC_h corresponding to the battery discharge and charge limits of household $h \in \mathcal{H}$ respectively. Constraint (3.22) corresponds to the energy limit constraint of the battery, with E_h the energy storage limit of household h. Constraint (3.23) represents the charging dynamics of the home energy battery for the first period of the horizon. Here, $e_{\tau-1}$ is a parameter that has been determined in the previous step of the rolling optimization. The charge and discharge efficiency of the battery are denoted as η_h^c and η_h^d for household h, respectively. Constraint (3.24) describes the dynamics of the battery beyond the first stage of the horizon. Constraint (3.25) expresses the power balance constraint in the household. The parameter $L_{t,h}$ is the inflexible demand of household h in stage t, while PV_{t,ω^S} corresponds to the rooftop solar supply sample that is obtained in step 1 of the performance evaluation described above. Constraint (3.26) expresses the upper limit on net demand that a household is entitled to. The indicator variable $1_{[i,t,\omega^I]}$ indicates whether a certain reliability level i is being served at a given stage of a sample path or not. Constraint (3.27) limits the power injected back to the grid, where Γ is a parameter chosen between 0 and 1. Constraint (3.28) expresses the energy limit of option $i \in \mathcal{I}$. We assume that the excess power is injected back to the grid for free, so the credit meter is not allowed to move backwards. $\Pi_{\mathbb{R}_+}$ projects the net demand to a non-negative value. The parameter $S_{h,i,j}$ in the right hand side is obtained from the menu choice model of the household, which is presented in section 3.3.2. The parameter UE_i in problem $(H_{h,\tau})$ corresponds to the amount of energy that has been used up for option i by household h up to stage τ in the performance evaluation simulation. Non-anticipativity is expressed in constraint (3.29).

The solution of $(H_{h,t})$ yields a net demand decision for each reliability option i for the current period, $nd^\star_{i,t}$, which we denote as $ND_{h,i,t}$ for every household $h \in \mathcal{H}$. The parameter $ND_{i,t}$ which is used in constraint (3.15) is then the sum of this net demand over all household types:

$$ND_{i,t} = \sum_{h \in \mathcal{H}} N_h \cdot ND_{h,i,t}, \tag{3.32}$$

where N_h is the number of households of type $h \in \mathcal{H}$ in the population. Note

that the implicit assumption in Eq. (3.32) is that the realization of uncertainty at every household of the same type is identical.

3.5 Case Study

This section presents a case study of the Belgian system in a forward-looking scenario of the year 2050. We work with representative days, each of which is split into six 4-hour blocks. In the case study, we first solve for the priority service pricing menu. Then we solve the multilevel demand subscription menu by fixing the three reliability levels and the price of full duration options as the solution from the priority service pricing menu design.

3.5.1 System Settings

The system configuration of conventional generator is the same as that in section 2.5.2. Wind and solar production profiles, and import profiles for the year 2015 with hourly resolution, are collected from [Eli19b]. These profiles are scaled up according to the projected value of the year 2050, according to the EU 2050 reference scenario [EC17]. Based on this data, we create the scenario set $\mathcal{S}$, and the sample path sets Ω^W and Ω^S. The procedure is detailed as follows.

We conduct the simulation using a set $\mathcal{S}$ of eight representative days (one weekday and one weekend in each season). We distinguish between weekdays and weekends because households generally consume more in the daytime of weekends than weekdays. Moreover, the industrial and commercial sectors tend to consumer more during weekdays. Each element of the set $\mathcal{S}$ corresponds to a typical time series of wind and solar production for the specific day type. The renewable production time series are the same for weekdays and weekends in the same season. The renewable production for each season is estimated as the average renewable production of the same season based on historical data.

We then create four scenario trees for Ω^W and Ω^S respectively, in order to represent the random evolution of renewable supply in each season. The renewable production scenarios of the weekday and weekend in the same season are described with the same scenario tree. Regarding Ω^W, the forecast production of wind supply is known and the actual production is characterized by 'H' or 'L', according to whether it is under-forecast or over-forecast. This concept is presented in figure 3.9. The probability of under/over-forecast and the average relative error at each time stage are estimated based on the historical data of year 2015. The scenario tree of a certain scenario is created using the data corresponding to the day type of the scenario. The renewable production in each scenario $s \in \mathcal{S}$ is scaled up or down based on the relative error at each stage, in order to represent the nodes of the scenario tree. A scenario tree of

the solar production is created in a similar way, in order to represent Ω^S. The solar production is assumed to be independent of the wind production. The validity of this assumption is checked by comparing the theoretical joint probability of wind under/over-forecast and solar under/over-forecast in each hour against the estimated joint probability based on the data of the year 2015. The seasonal variation of this data is shown in figures 3.7 and 3.8.

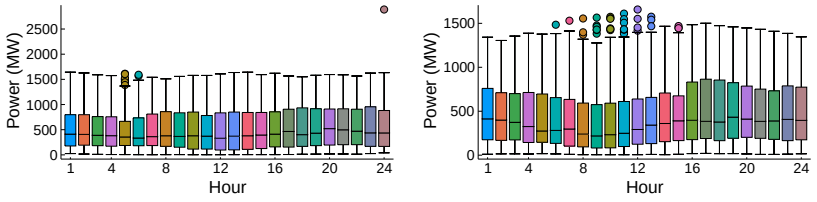

(a) Spring (b) Summer

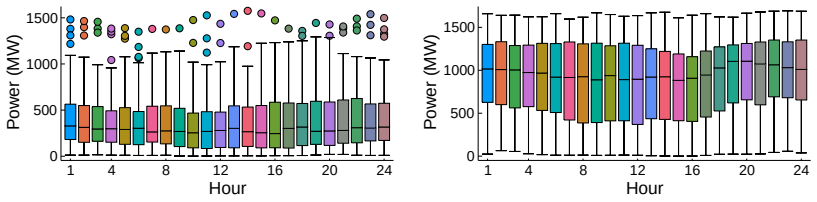

(c) Autumn (d) Winter

Figure 3.7: Comparison of the variation of wind production in different seasons of 2015 in Belgium.

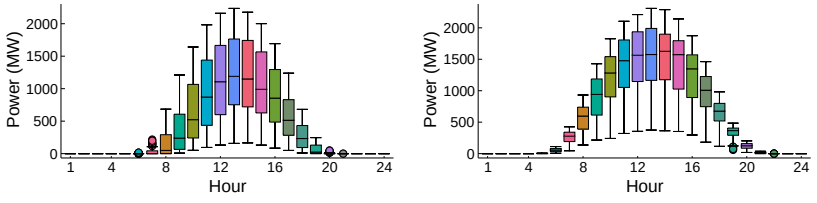

(a) Spring (b) Summer

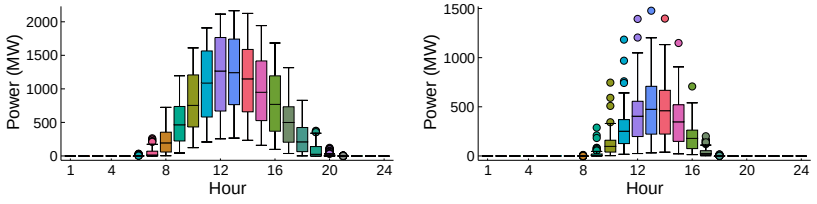

(c) Autumn (d) Winter

Figure 3.8: Comparison of the variation of solar production in different seasons of 2015 in Belgium.

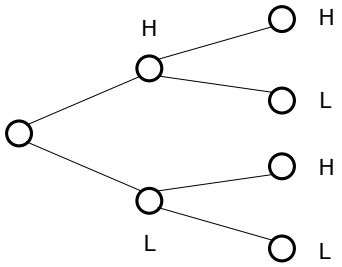

Figure 3.9: Scenario tree for wind production Ω^W. 'H' indicates higher actual production compared with the forecast production (under-forecast) while 'L' indicates lower actual production compared with the forecast production (over-forecast).

The pumped hydro storage in Belgium has a pumping capacity amounting to 1200 MW, while the energy storage capacity of pumped hydro amounts to 5700 MWh. Pumped hydro resources are assumed to have a roundtrip efficiency of 76.5% [PS17]. Pumped hydro storage is assumed to follow a fixed profile in the producer model of section 3.4. The profile is calculated by a deterministic model, by dispatching the system against the average production of renewable supply at both the system level and household level.

The total load profile of year 2015 is also available from [Eli19b]. The industrial and commercial load is extracted from the total load profile according to *Synthetic Load Profiles (SLPs)* [Syn17]. Synthetic load profiles are normalized electricity consumption time series with 15-minute resolution that are publicly available for the residential and non-residential sectors. The load profiles are scaled up to the year 2050 according to the EU 2050 reference scenario [EC17].

Based on the industrial and commercial SLPs, we represent the load of the non-residential sector by a fixed profile. Two categories of residential SLPs (S21 and S22) describe two categories of households. According to the data, 82% of the grid connections correspond to S21 households, and 18% correspond to S22 households [VI14]. The average profiles of S21 and S22 are presented in figure 3.10. Furthermore, we assume that (i) 25% of the households is equipped with a PV panel with a maximum power of 2.5 kW per household[3], (ii) one third of the households with a PV panel is equipped with a large battery, (iii) one third of the households with a PV panel is equipped with a smaller battery, and (iv) one third of the households with a PV panel is not equipped with a battery. The technical specifications[4] of household batteries are presented in

[3]Following this assumption, local solar production accounts for 38.6% of the total solar supply.

[4]The cost of the Moixa Smart Battery (the small battery in our case study) amounts to £4450, including an installation fee. Tesla prices the Powerwall (the large battery in our case study) at a cost of $6,500, whereas the supporting hardware costs $1,100. The installation fee of the Tesla Powerwall is estimated between $9,600 and $15,600 [Ene20d]. We use the

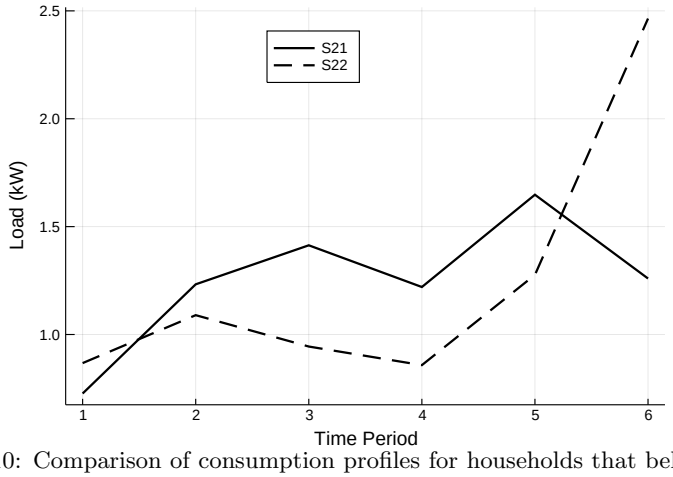

Figure 3.10: Comparison of consumption profiles for households that belong to SLP categories S21 and S22.

Table 3.1: Technical specifications of household batteries in the case study of section 3.5.

Battery Type	Large [Tes20]	Small [Moi20]
Energy Storage Limit (E, kWh)	13.5	3.84
Power Limit (BD/BC, kW)	5	0.85
Efficiency (η_c/η_d, %)	95	95
Warranty (Years)	10	10
Overnight Cost (€)	11,100	5,120

Table 3.2: Characteristics of different types of households in the case study of section 3.5.

Type	1	2	3	4	5	6	7	8
SLP Category	S21	S22	S21	S22	S21	S22	S21	S22
PV Panel	Yes	Yes	Yes	Yes	Yes	Yes	No	No
Battery Size	Large	Large	Small	Small	No	No	No	No
Proportion (%)	6.83	1.5	6.83	1.5	6.83	1.5	61.5	13.5

table 3.1. In total, we model eight types of households. Their characteristics are presented in table 3.2.

3.5.2 Optimal Menus

Table 3.3 presents the priority service menu. The first column presents the reliability of each option, whereas the second column presents the price for a

average as an approximation of the total cost of installation of the Tesla battery.

Table 3.3: Priority service menu in the case study of section 3.5.

Reliability (%)	Price (€/kW-month)
58.5	26.4
85.3	39.3
100.0	48.5

Table 3.4: Multilevel demand subscription menu in the case study of section 3.5.

Reliability (%)	Duration (%)	Price (€/kW-month)
58.5	33.3	14.9
	66.7	22.9
	100	26.4
85.3	33.3	22.1
	66.7	34.1
	100	39.3
100.0	33.3	27.3
	66.7	42.1
	100	48.5

kW of service over a month (i.e., this service corresponds to 720 kWh of energy if the reliability is 100%).

Table 3.4 presents the optimal multilevel demand subscription menu. Note that, when a given strip is topped up with credits for the full duration of the service, the multilevel demand subscription service becomes equivalent to priority service for the same level of reliability. We thus obtain comparable menus by imposing that the price of a given reliability level for 24 hours of daily service in multilevel demand subscription equal the price of the corresponding reliability option under priority service pricing.

3.5.3 Policy Analysis

In the following, we summarize a number of observations that can be derived from our modeling framework.

3.5.3.1 Operational Efficiency

Table 3.5 presents key economic indicators for the different pricing policies that have been considered in the simulations. The load shedding cost is calculated according to the household rolling horizon model in the performance evaluation process, while the supply quantity and the production cost are computed from the producer model. The producer revenue is derived from the household menu selection model.

Compared to priority service, multilevel demand subscription is able to

Table 3.5: Comparison of priority service (PSP) and multilevel demand subscription (MDSP) in the case study of section 3.5 [unit: M €/month].

	Production Cost	Load Shedding Cost	Producer Revenue	Supply Quantity (GWh)
PSP	42.1	22.7	139.3	1514.4
MDSP	41.1	4.4	140.5	1534.3

supply slightly more power to the households at a slightly lower cost and reduces the load shedding cost of households significantly. This is a consequence of the limited ability of priority service to discriminate among flexible consumer classes. Concretely, under priority service pricing the producer infers a certain valuation for each priority class. This valuation is a crude approximation of the heterogeneous set of consumers within a given class. Thus, priority service may lead to an under-supply within a certain class if the *inferred* valuation of that class is lower than the marginal cost of serving the class, whereas a significant portion of consumers within the class may have a higher valuation than the one inferred by the producer. In contrast, multilevel demand subscription allows the aggregator to exploit the duration component in order to infer different valuation levels for each priority class at different time periods, rather than a fixed valuation level throughout the entire duration. In addition, the revenue of the producer increases slightly as well. Thus, multilevel demand subscription proves to be beneficial for both the producer and households because of better differentiation.

3.5.3.2 Service Comparison under Different Policies

Table 3.6 presents the priority service subscription for each type of household. Rows "Green" to "Red" correspond to the different reliability options, while "Capacity" presents the total subscription quantity and "Energy" indicates the total energy that the household is entitled to, assuming that the reliability of each option is delivered. Table 3.7 presents the multilevel demand subscription for each type of household. For each color, the first three rows indicate different duration levels, while the last row presents the total subscribed capacity under each reliability level. The "Capacity" row of the table sums up the total subscribed capacity for all options. The last row presents the subscribed energy, which is computed by taking into consideration the reliability and duration of each option.

By comparing the last two rows of table 3.6 with the last two rows of table 3.7, we observe that the total subscribed capacity of each household under multilevel demand subscription is higher than that under priority service. On the other hand, the subscribed energy is less. This observation is driven by the offer of options with shorter duration in multilevel demand subscrip-

Table 3.6: Priority service subscription for each type of household [Energy in kWh; others in kW].

Types	1	2	3	4	5	6	7	8
SLP	Day Peak	Night Peak	Day Peak	Night Peak	Day Peak	Night Peak	Day Peak	Night Peak
PV	Yes	Yes	Yes	Yes	Yes	Yes	No	No
Battery	Large	Large	Small	Small	No	No	No	No
Green	0.043	0.04	0.017	0.021	0	0	0	0
Yellow	0.156	0.312	0.134	0.087	0.122	0.19	0.024	0.19
Red	1.114	1.311	1.117	1.555	1.435	1.787	1.577	1.787
Capacity	1.313	1.663	1.268	1.663	1.557	1.977	1.6	1.977
Energy	30.54	38.4	29.78	39.39	36.94	46.77	38.32	46.78

Table 3.7: Multilevel demand subscription for each type of household [Energy in kWh; others in kW].

Types	1	2	3	4	5	6	7	8
SLP	Day Peak	Night Peak	Day Peak	Night Peak	Day Peak	Night Peak	Day Peak	Night Peak
PV	Yes	Yes	Yes	Yes	Yes	Yes	No	No
Battery	Large	Large	Small	Small	No	No	No	No
Green-1	0.152	0.356	0.336	0.303	0.251	0.087	0.339	0.87
Green-2	0.315	0	0	0	0	0	0	0
Green-3	0	0	0	0	0	0	0	0
Subtotal	0.467	0.356	0.336	0.303	0.251	0.087	0.179	0.87
Yellow-1	0	0.046	0.063	0.11	0.229	0.396	0.155	0.34
Yellow-2	0	0	0	0	0	0	0	0
Yellow-3	0.104	0	0	0	0	0	0	0
Subtotal	0.104	0.046	0.063	0.11	0.229	0.396	0.155	0.34
Red-1	0	0.37	0	0.131	0.749	0.437	0.419	0.492
Red-2	0	0	0	0.347	0	0.768	0.39	0.141
Red-3	0.962	1.293	1.139	1.185	0.837	0.804	0.859	1.43
Subtotal	0.962	1.663	1.139	1.663	1.586	2.008	1.668	2.064
Capacity	1.533	2.064	1.538	2.076	2.066	2.492	2.161	2.492
Energy	28.88	35.96	29.35	37.21	28.82	38.18	32.84	43.26

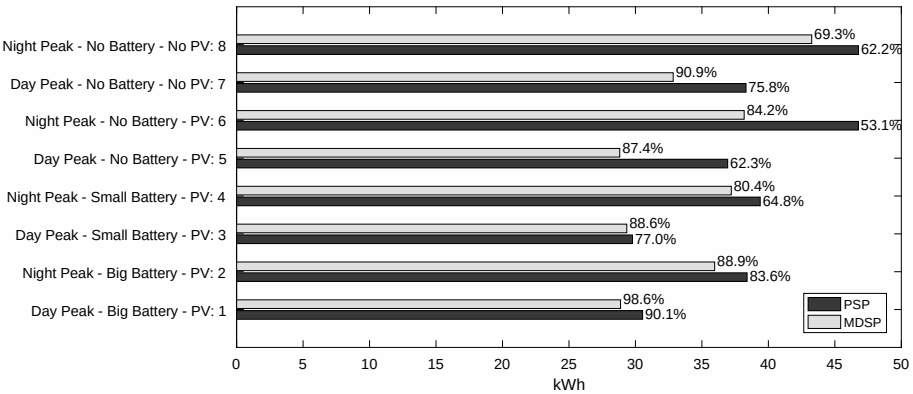

Figure 3.11: Comparison of subscribed energy for different types of households. The percentage on the right of the bars represents the amount of procured energy that is actually consumed by the household.

tion. Consequently, multilevel demand subscription is not only advantageous to households by allowing higher peak capacity when needed, but also favorable to the producer because the subscribed energy demand is closer to the real consumption of households.

The bars in figure 3.11 present the total amount of energy that each household type is entitled to after procuring the corresponding service. The percentage on the right of the bars presents the amount of procured energy that is actually consumed by the household. With a large battery, households can make better use of the purchased power. Furthermore, the service is provided for the entire horizon under priority service, thereby resulting in higher subscribed energy but lower utilization percentage for households without a large battery. Under multilevel demand subscription, the lowest utilization ratio amounts to 69.3%, which is a significant improvement relative to the lowest ratio under priority service, which amounts to 53.1%. This result is driven by the fact that households can choose options of a shorter duration under multilevel demand subscription. Multilevel demand subscription therefore allows households to better exploit the subscribed energy.

3.5.3.3 Impact of Storage on the Demand for Capacity

We observe in table 3.6 that, as the size of the household battery decreases, the household tends to subscribe to a greater quantity for the "Red" (reliable) option. We arrive to similar observations in the case of table 3.7. Specifically, as the size of the battery decreases, the household tends to subscribe to a larger total quantity, as well a higher quantity under the "Red" option. By comparing the total subscribed capacity of different households in the"Capacity" row, we

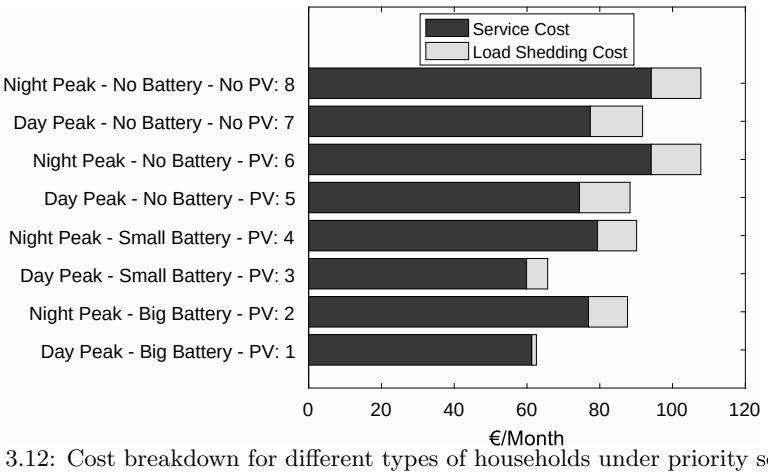

Figure 3.12: Cost breakdown for different types of households under priority service.

can conclude that the battery reduces the capacity demand of a household.

3.5.3.4 Benefits of PV Panels

Figure 3.12 decomposes the total cost of each household into the cost of procuring a priority service contract, and load shedding cost. The service cost is computed using the household menu selection model presented in section 3.D. Instead, the load shedding cost is quantified using the household rolling horizon model in the performance evaluation process that is presented in section 3.4.2.

By comparing household type 6 with type 8, we can see that if a household only installs PV panels without a battery, it is possible that he experiences a similar total cost as that of a household which installs neither. This is due to the evening consumption, which cannot be covered by PV panels. Note that the priority service menu is a purely capacity-based tariff, and it motivates households with PV panels to invest in storage. This is in contrast to the current energy-based "net-metering" tariff, where households with PV panels are significantly advantaged. Thus, we conclude that PV panels are not necessarily rewarding for households that are subscribed to priority service or multilevel demand subscription if these households do not possess batteries. This observation indicates that a capacity based tariff may fail to promote the installation of rooftop PV panels for households without local storage.

3.5.3.5 Benefits of Local Storage under Different Policies

It is observed from figure 3.12 that the battery enables households to reduce their total cost. This observation suggests that residential consumers face in-

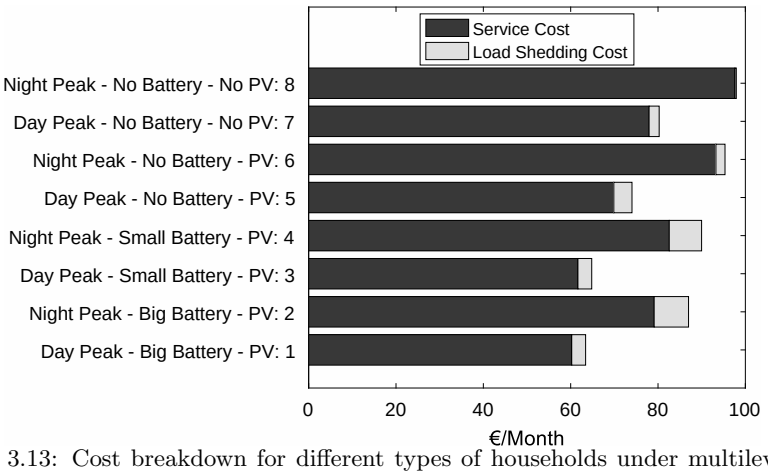

Figure 3.13: Cost breakdown for different types of households under multilevel demand subscription.

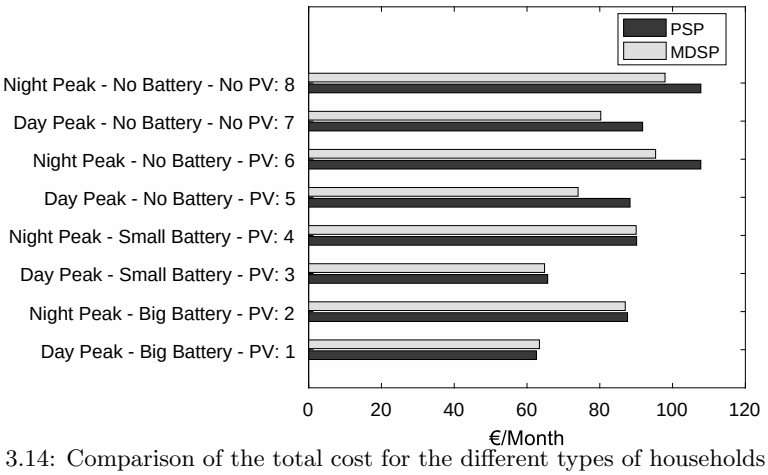

Figure 3.14: Comparison of the total cost for the different types of households under priority service and multilevel demand subscription in the case study of section 3.5.

centives for installing local storage in their house under a priority service contract.

We arrive to similar observations in figure 3.13, where we present the cost breakdown for households under multilevel demand subscription. Note, however, that the differences among households are less significant than those observed in priority service. We therefore observe that storage is more valuable to households under priority service than under multilevel demand subscription. This is due to the fact that multilevel demand subscription contains implicitly

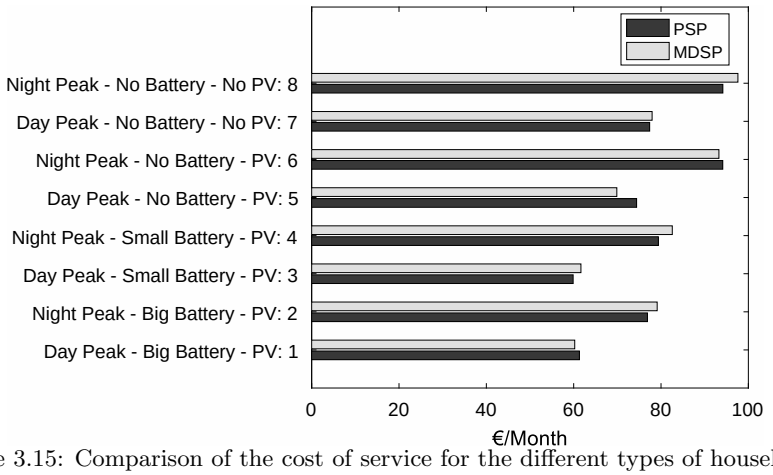

Figure 3.15: Comparison of the cost of service for the different types of households.

an energy cost in addition to the capacity cost, while the battery is mainly beneficial in terms of reducing the capacity cost.

3.5.3.6 Cost Comparison of Households under Different Policies

Figures 3.14 and 3.15 compare the total cost and bill of the household types under the priority service and multilevel demand subscription schemes, respectively. We can observe that households 5 - 8 under multilevel demand subscription tend to face a lower total cost, even if certain households face a higher service cost under multilevel demand subscription. By contrast, the total cost of households 1 - 4 are very close under priority service and multilevel demand subscription. This observation is due to the fact that the batteries contribute to reducing the peak net demand of the households, which implies that the benefits brought about by the shorter duration options in multilevel demand subscription decrease. In summary, the total cost of a household equipped with a battery under multilevel demand subscription is almost identical to that under priority service. On the other hand, if the household does not own a battery, the savings achieved by multilevel demand subscription are more significant.

3.5.3.7 Cost-Benefit Analysis of Local Storage

We are interested in conducting a cost-benefit analysis of investing in batteries. Tables 3.8 and 3.9 provide more information regarding the costs of different households under priority service and multilevel demand subscription. We also need to calculate the monthly cost of installing batteries, which is given as

$$\frac{OC \cdot r/12}{1 - 1/(1+r)^T},$$

Table 3.8: Detailed results for each type of household under priority service in the case study of section 3.5. "Load" corresponds to the daily inflexible energy demand in the household, while "PV Prod." presents the expected production from PV panels. The quantity of power injected back to the grid is indicated by "Injection". "Battery Energy" shows the energy left in the battery at the end of the day. The subscribed energy, assuming that the reliability of each option is delivered, is presented as "Subscription". The percentage of utilization for each subscribed option is depicted in the row indicated as "Utilization". The last three rows provide the cost breakdown for each household type, including the service cost and load shedding cost. The last five rows correspond to figures. 3.12 - 3.11.

(a) Household types 1-4

Types	1	2	3	4
SLP	Day Peak	Night Peak	Day Peak	Night Peak
PV	Yes	Yes	Yes	Yes
Battery	Large	Large	Small	Small
Load (kWh)	30	30	30	30
PV Prod. (kWh)	12.61	12.61	12.61	12.61
Injection (kWh)	0.73	4.17	3.73	6.93
Battery Energy (kWh)	1.98	2.63	0.44	0.38
Subscription (kWh)	30.54	38.4	29.78	39.39
Utilization (%)	90.09	83.59	77.03	64.78
Service Cost (€/M)	61.31	76.89	59.88	79.39
LoadShedding Cost (€/M)	1.27	10.73	5.8	10.73
Total Cost (€/M)	62.58	87.62	65.68	90.12

(b) Household types 5-8

Types	5	6	7	8
SLP	Day Peak	Night Peak	Day Peak	Night Peak
PV	Yes	Yes	No	No
Battery	No	No	No	No
Load (kWh)	30	30	30	30
PV Prod. (kWh)	12.61	12.61	0	0
Injection (kWh)	6.55	8.35	0	0
Battery Energy (kWh)	0	0	0	0
Subscription (kWh)	36.94	46.77	38.32	46.78
Utilization (%)	62.29	53.09	75.79	62.19
Service Cost (€/M)	74.41	94.14	77.4	94.16
LoadShedding Cost (€/M)	13.9	13.62	14.37	13.61
Total Cost (€/M)	88.31	107.76	91.77	107.77

where OC, r and T denote the overnight investment cost, annual discount rate and the lifespan of the battery, respectively. The assumptions on these parameters are as follows.

- Overnight cost of the battery. In table 3.1, we present the overnight cost of two types of batteries in April, 2020. However, Lithium-ion batteries have reached gigawatt-scale markets, driving approximately 14% annual declines in battery costs between 2007 and 2014 [PAK16], and it is expected to keep dropping dramatically in the future. IEA expects utility-scale battery pack costs to fall to around 100$/kWh by 2030 [Pav19]. BloombergNEF is more optimistic and estimates this target can be reached by 2024 due to economy of scale and improving efficiencies [Ste19]. A study conducted by International Renewable Energy Agency concludes the total installed cost for Lithium-ion batteries for stationary applications will drop to between 145$/kWh and 480$/kWh depending on battery chemistry in 2030. Since we are considering a forward-looking scenario in 2050, the overnight cost is assumed to be 10% to 30% of the current cost, or equivalently 82.2€/kWh to 246.67 €/kWh for the large battery and 133.33 €/kWh to 400 €/kWh for the small battery.

- We assume the annual discount rate to be 3% - 10%.

- Lifespan of the battery. A ten-year warranty is offered by battery manufacturers currently, but the lifespan of the battery can be longer [Sen20], so we use 15 to 20 years as a reasonable assumption.

Based on these assumptions, the monthly cost of the large battery is estimated to be between 6.22 €/month and 36.48 €/month and that of the small battery ranges from 2.86 €/month to 16.83 €/month.

By comparing the total cost of household type 1 with type 5 under priority service in table 3.8, the cost reduction of a household with a day peak from installing a large battery is quantified at 27.75 €/month. Similarly, by comparing type 2 with type 6, the cost reduction amounts to 20.14 €/month for a household with a night peak. Contrasting with the monthly cost of the large battery, it is possible the investment cost of the large battery can not be justified. However, the battery is oversized for the household[5], because the cost reduction by investing in a small battery is close. The cost reduction due to the installation of the small battery amounts to 22.63 €/month for the household

[5]The average daily electricity consumption is 30 kWh for all types of households in this case study. In practice, large households with an average daily electricity consumption between 13.7 and 41.1 kWh account for approximately 27% of the Belgian households, while very large households with an average daily electricity consumption above 41.1 kWh account for approximately 4 %. Other households exhibit an average daily electricity consumption below 13.7 kWh [JDA+12].

Table 3.9: Detailed results for each type of household under multilevel demand subscription in the case study of section 3.5.

(a) Household types 1-4

Types	1	2	3	4
SLP	Day Peak	Night Peak	Day Peak	Night Peak
PV	Yes	Yes	Yes	Yes
Battery	Large	Large	Small	Small
Injection (kWh)	0.32	2.31	5.78	9.85
Battery Energy (kWh)	1.7	1.93	0.52	0.48
Subscription (kWh)	28.88	35.96	29.35	37.21
Utilization (%)	98.58	88.88	88.64	80.4
Service Cost (€/M)	60.24	79.12	61.66	82.58
LoadShedding Cost (€/M)	3.18	7.87	3.16	7.4
Total Cost (€/M)	63.41	87	64.82	89.99

(b) Household types 5-8

Types	5	6	7	8
SLP	Day Peak	Night Peak	Day Peak	Night Peak
PV	Yes	Yes	No	No
Battery	No	No	No	No
Injection (kWh)	8.09	14.89	0	0
Battery Energy (kWh)	0	0	0	0
Subscription (kWh)	28.82	38.18	32.84	43.26
Utilization (%)	87.42	84.17	90.88	69.3
Service Cost (€/M)	69.88	93.26	77.96	97.61
LoadShedding Cost (€/M)	4.16	2.08	2.3	0.31
Total Cost (€/M)	74.04	95.34	80.27	97.93

with a day peak and 17.64 €/month for the household with a night peak. In comparison with the monthly cost of the small battery, the investment cost can be justified.

We proceed to analyze the cost savings under multilevel demand subscription. By comparing the total cost of different types of households in table 3.9, we conclude the benefit of installing the large battery ranges from 8.34 €/month to 10.63 €/month and the small battery is able to save the households 5.35 €/month to 9.22 €/month. Under these conditions, the investment cost of batteries can only be recovered in relatively optimistic scenarios.

3.A Nomenclature

The notation used in this chapter follows closely the notation that is presented in section 2.A. The notation which is required for representing prosumers who own rooftop solar and local storage is introduced as needed for section 3.4.

Sets

$\mathcal{G}$	Set of generators
$\mathcal{L}, L$	Set of consumer types and its cardinality
$\mathcal{H}, H$	Set of households and its cardinality
$\mathcal{T}, \lvert\mathcal{T}\rvert$	Set of time periods and its cardinality
$\mathcal{I}, I$	Set of reliability options and its cardinality
$\mathcal{J}, J$	Set of duration options and it cardinality
$\mathcal{S}$	Set of renewable production scenarios of the producer
Ω^W	Set of wind production sample paths
Ω^S	Set of solar production sample paths
Ω^I	Set of sample paths of interruption of colors
Ω^C	Set of sample paths, equivalent to $\Omega^I \times \Omega^S$

Parameters

Π^+	Upper bound of menu prices
T_j	Duration of option j
$V_l(T_j)$	Valuation of consumer type l when the duration is T_j [€/MWh]
D_l	Demand of consumer l [MW]
$\bar{V}_i$	Average valuation of group i [€/MWh]
P_s	Probability of scenario s
$P^s_{\omega^W}$	Probability of sample path ω^W of scenario tree Ω^W in scenario s, similarly for $P^s_{\omega^S}$, $P^s_{\omega^I}$, $P^s_{\omega^C}$
$W_{t,s}$	Wind production at hour t in scenario s [MW]
$S_{t,s}$	Solar production at hour t in scenario s [MW]
S_{t,ω^S}	Solar production at hour t in scenario ω^S [MW]
W_{t,ω^W}	Wind production at hour t in scenario ω^W [MW]
$VOLL$	Value of lost load, assumed to be 500 €/MWh
BD_h	Battery charge capacity in household h [MW]
BC_h	Battery discharge capacity in household h [MW]
E_h	Battery energy capacity in household h [MWh]
η^d_h	Battery discharge efficiency in household h
η^c_h	Battery charge efficiency in household h
$L_{t,s,h}$	Load of household h at stage t in scenario s [MW]
N_h	Number of households of type h
PV_{t,s,ω^S}	Production from rooftop PV panel at stage t in sample path ω^S, scenario s [MW]
FL	Fuse limit imposed on the household model [MW]
Γ	Ratio of PV injection to the capacity limit of the household

Variables

$\pi_{i,j}$	Price of option (i,j) [€]
r_i	Reliability of option i [%]
$\mu_{l,i,j}$	Binary decision of consumer l for option (i,j)
$y_{l,i,j}$	Auxiliary variable to represent $\pi_{i,j} \cdot \mu_{l,i,j}$
$w_{l,i,j}$	Auxiliary variable to represent $r_{i,j,t} \cdot \mu_{l,i,j}$
$s_{l,i,j}$	The subscription quantity of consumer l under option (i,j) [MW]
$s_{i,j}$	The total subscription quantity under option (i,j) [MW]
$d_{i,j,t,s}$	Supply to option (i,j) at hour t in scenario s [MW]
$p_{g,t,s}$	Production of generator g at hour t in scenario s [MW]
$m_{g,t,s}$	Start up decision of generator g at hour t in scenario s
$n_{g,t,s}$	Shut down decision of generator g at hour t in scenario s
$o_{g,t,s}$	Unit commitment decision of generator g at hour t in scenario s
ls_{t,s,ω^S}	Load shedding at stage t in sample path ω^S, scenario s
bd_{t,s,ω^S}	Discharge power of the battery at stage t in sample path ω^S, scenario s
bc_{t,s,ω^S}	Charge power of of the battery at stage t in sample path ω^S, scenario s
e_{t,s,ω^S}	Energy stored in the battery at stage t in sample path ω^S, scenario s
nd_{t,s,ω^S}	Net demand from the grid at stage t in sample path ω^S , scenario s
nd_{i,t,s,ω^C}	Net demand from option i at stage t in sample path ω^C , scenario s

Functions

h_g	Cost function of generator g, including production costs, startup and minimum load costs
f_g	Constraints of unit commitment problems, including minimum up and down times, ramp rates and production limits

3.B Modeling the Multilevel Demand Subscription Menu Design Problem as a Stackelberg Equilibrium (Cont.)

3.B.1 Optimality Conditions of the Consumer Model

Following the consumer model presented in section 3.3, we derive the dual (CD_l) of the optimal menu selection problem so as to arrive to a MILP formu-

lation of the Stackelberg equilibrium.

$$(CD_l): \min_{\gamma_l} \gamma_l \cdot D_l \tag{3.33}$$

$$\text{s.t. } \gamma_l \geq r_i \cdot V_l(T_j) - \pi_{i,j},\ i \in \mathcal{I}, j \in \mathcal{J} \tag{3.34}$$

$$\gamma_l \geq 0. \tag{3.35}$$

The optimality conditions of the lower-level problem can be expressed equivalently as the set of primal feasibility conditions, dual feasibility conditions, and the condition of strong duality:

$$s_{l,i,j} \geq 0,\ i \in \mathcal{I}, j \in \mathcal{J}, l \in \mathcal{L} \tag{3.36}$$

$$\sum_{i \in \mathcal{I}, j \in \mathcal{J}} s_{l,i,j} \leq D_l, l \in \mathcal{L} \tag{3.37}$$

$$\gamma_l \geq r_i \cdot V_l(T_j) - \pi_{i,j}, i \in \mathcal{I}, j \in \mathcal{J}, l \in \mathcal{L} \tag{3.38}$$

$$\gamma_l \geq 0, l \in \mathcal{L} \tag{3.39}$$

$$\gamma_l \cdot D_l = \sum_{i \in \mathcal{I}, j \in \mathcal{J}} s_{l,i,j} \cdot \Big(r_i \cdot V_l(T_j) - \pi_{i,j}\Big), l \in \mathcal{L} \tag{3.40}$$

When the optimality conditions of the lower-level problem are introduced as constraints to the upper-level problem, we face non-convex constraints resulting from the products $r_i \cdot \mu_{l,i,j}$ and $\pi_{i,j} \cdot \mu_{l,i,j}$. We represent these products using McCormick envelopes. We do so by noting that the reliability variable is naturally bounded in the interval $0 \leq r_i \leq 1$, and by imposing a price limit on the menu offering, $0 \leq \pi_{i,j} \leq \Pi^+$. This allows us to express $\pi_{i,j} \cdot \mu_{l,i,j}$ by a new variable $y_{l,i,j}$, and $r_i \cdot \mu_{l,i,j}$ by a new variable $w_{l,i,j}$. The strong duality constraint (3.40) for the full population of load types $l \in \mathcal{L}$ can then be rewritten as follows:

$$\gamma_l = \sum_{i \in \mathcal{I}, j \in \mathcal{J}} w_{l,i,j} \cdot V_l(T_j) - \sum_{i \in \mathcal{I}, j \in \mathcal{J}} y_{l,i,j}, l \in \mathcal{L} \tag{3.41}$$

$$y_{l,i,j} \leq \Pi^+ \cdot \mu_{l,i,j}, i \in \mathcal{I}, j \in \mathcal{J}, l \in \mathcal{L} \tag{3.42}$$

$$y_{l,i,j} \geq 0, i \in \mathcal{I}, j \in \mathcal{J}, l \in \mathcal{L} \tag{3.43}$$

$$y_{l,i,j} \leq \pi_{i,j}, i \in \mathcal{I}, j \in \mathcal{J}, l \in \mathcal{L} \tag{3.44}$$

$$y_{l,i,j} \geq \Pi^+ \cdot \mu_{l,i,j} + \pi_{i,j} - \Pi^+, i \in \mathcal{I}, j \in \mathcal{J}, l \in \mathcal{L} \tag{3.45}$$

$$w_{l,i,j} \leq \mu_{l,i,j}, i \in \mathcal{I}, j \in \mathcal{J}, l \in \mathcal{L} \tag{3.46}$$

$$w_{l,i,j} \geq 0, i \in \mathcal{I}, j \in \mathcal{J}, l \in \mathcal{L} \tag{3.47}$$

$$w_{l,i,j} \leq r_i, i \in \mathcal{I}, j \in \mathcal{J}, l \in \mathcal{L} \tag{3.48}$$

$$w_{l,i,j} \geq \mu_{l,i,j} + r_i - 1, i \in \mathcal{I}, j \in \mathcal{J}, l \in \mathcal{L} \tag{3.49}$$

$$r_i \leq 1, i \in \mathcal{I} \tag{3.50}$$
$$\pi_{i,j} \leq \Pi^+, i \in \mathcal{I}, j \in \mathcal{J} \tag{3.51}$$
$$r_i \geq 0, \pi_{i,j} \geq 0, \mu_{l,i,j} \in \{0,1\}, i \in \mathcal{I}, j \in \mathcal{J}, l \in \mathcal{L} \tag{3.52}$$

3.B.2 The Producer Model

Binary vectors $\mathbf{m}, \mathbf{n}, \mathbf{o}$ indicate startup, shutdown and commitment decisions respectively. The non-negative vector $\mathbf{p}$ corresponds to the dispatch of conventional units. The non-negative vector $\mathbf{d}$ corresponds to the amount of power that is offered in different options under different scenarios and time periods. In addition, the producer owns a set of renewable assets. Their production is characterized by a set of scenarios, $\mathcal{S}$. The menu design problem of the producer can be expressed as follows.

$$\max_{\mathbf{m},\mathbf{n},\mathbf{o},\mathbf{d},\mathbf{p},\boldsymbol{\pi}} \sum_{l \in \mathcal{L}} \sum_{\substack{i \in \mathcal{I} \\ j \in \mathcal{J}}} s^{\star}_{l,i,j}(\pi) \cdot V_l(T_j) \cdot r_i - \sum_{s \in \mathcal{S}} P_s \cdot \sum_{g \in \mathcal{G}} h_g(\mathbf{m}_{g,s}, \mathbf{n}_{g,s}, \mathbf{o}_{g,s}, \mathbf{p}_{g,s}) \tag{3.53}$$

$$\text{s.t.} \quad f_g(\mathbf{m}_{g,s}, \mathbf{n}_{g,s}, \mathbf{o}_{g,s}, \mathbf{p}_{g,s}) \leq 0, g \in \mathcal{G}, s \in \mathcal{S} \tag{3.54}$$
$$\sum_{\substack{i \in \mathcal{I} \\ j \in \mathcal{J}}} d_{i,j,t,s} = \sum_{g \in \mathcal{G}} p_{g,t,s} + W_{t,s} + S_{t,s}, t \in \mathcal{T}, s \in \mathcal{S} \tag{3.55}$$
$$d_{i,j,t,s} \leq \sum_{l \in \mathcal{L}} s^{\star}_{i,j,l}(\pi) \cdot N_{j,t}, i \in \mathcal{I}, j \in \mathcal{J}, t \in \mathcal{T}, s \in \mathcal{S} \tag{3.56}$$
$$r_i \cdot \sum_{l \in \mathcal{L}} s^{\star}_{i,j,l}(\pi) \cdot T_j = \sum_{s \in \mathcal{S}} P_s \cdot \sum_{t \in \mathcal{T}} d_{i,j,t,s}, i \in \mathcal{I}, j \in \mathcal{J} \tag{3.57}$$
$$d_{i,j,t,s} \geq 0, p_{g,t,s} \geq 0, i \in \mathcal{I}, j \in \mathcal{J}, g \in \mathcal{G}, t \in \mathcal{T}, s \in \mathcal{S} \tag{3.58}$$
$$m_{g,t,s} \in \{0,1\}, n_{g,t,s} \in \{0,1\}, o_{g,t,s} \in \{0,1\}, g \in \mathcal{G}, t \in \mathcal{T}, s \in \mathcal{S} \tag{3.59}$$

The goal of the producer, which is expressed in the objective function of Eq. (3.53), is to maximize social welfare. The first term in the objective function represents the consumer benefit, as estimated from the producer based on load duration curve data, with $\mathcal{L}$ representing the set of consumer types in the load duration curve. This consumer benefit depends on the reaction of consumers to the price menu. The second term in the objective function corresponds to the expected production cost of the producer. The parameter P_s is the probability of scenario $s \in \mathcal{S}$. The function $h_g(\mathbf{m}_{g,s}, \mathbf{n}_{g,s}, \mathbf{o}_{g,s}, \mathbf{p}_{g,s})$ expresses the production cost of a generator, while the vector of constraints in Eq. (3.54) encodes linear production constraints that relate to unit commitment and dispatch of conventional units. Power balance is expressed in constraint (3.55), where $W_{t,s}$ and $S_{t,s}$ indicate the amount of wind and solar production in period t and

scenario s, respectively. Constraint (3.56) expresses the fact that a consumer type can only be served if that type is requesting power in a given interval, and if that interval is served under option $j \in \mathcal{J}$ (i.e. if $N_{j,t} = 1$). Constraint (3.57) ensures that an option $i \in \mathcal{I}$ receives reliability r_i.

3.B.3 The Bilevel Model

Given a choice $s^{\star}_{l,i,j}$ of menu options by consumer types, the producer model is a welfare maximizing commitment and dispatch of the system. The task of the producer is to offer a price menu $\{r_i, T_j, \pi_{i,j}\}, i \in \mathcal{I}, j \in \mathcal{J}$ so that consumers' reaction $s^{\star}_{l,i,j}$ is compatible with the optimal social welfare. Then the bilevel model can be written as

$$\max_{\mathbf{m,n,o,d,p,r,\pi}} \sum_{l\in\mathcal{L}} \sum_{\substack{i\in\mathcal{I}\\ j\in\mathcal{J}}} s^{\star}_{l,i,j} \cdot V_l(T_j) \cdot r_i - \sum_{s\in\mathcal{S}} P_s \cdot \sum_{g\in\mathcal{G}} h_g(\mathbf{m}_{g,s}, \mathbf{n}_{g,s}, \mathbf{o}_{g,s}, \mathbf{p}_{g,s}) \tag{3.60}$$

$$\text{s.t.} \quad (3.54) - (3.59) \tag{3.61}$$

$$s^{\star}_{l,i,j} \in \arg\max_{s_{l,i,j}\geq 0} \{ \sum_{i\in\mathcal{I}, j\in\mathcal{J}} s_{l,i,j} \cdot \Big(r_i \cdot V_l(T_j) - \pi_{i,j} \Big) : \sum_{i\in\mathcal{I}, j\in\mathcal{J}} s_{l,i,j} \leq D_l, i \in \mathcal{I}, j \in \mathcal{J} \}. \tag{3.62}$$

To arrive at an MILP reformulation, we replace the product $s^{\star}_{l,i,j} \cdot V_l(T_j) \cdot r_i$ with its McCormick envelope in the objective function, yielding

$$\max_{\mathbf{m,n,o,d,p,\pi,r,w,y,\mu}} \sum_{\substack{i\in\mathcal{I}\\ j\in\mathcal{J}}} \sum_{l\in\mathcal{L}} D_l \cdot V_l(T_j) \cdot w_{l,i,j} - \sum_{s\in\mathcal{S}} P_s \cdot \sum_{g\in\mathcal{G}} h_g(\mathbf{m}_{g,s}, \mathbf{n}_{g,s}, \mathbf{o}_{g,s}, \mathbf{p}_{g,s}) \tag{3.63}$$

The constraints of the producer can be expressed as follows:

$$f_g(\mathbf{m}_{g,s}, \mathbf{n}_{g,s}, \mathbf{o}_{g,s}, \mathbf{p}_{g,s}) \leq 0, g \in \mathcal{G}, s \in \mathcal{S} \tag{3.64}$$

$$\sum_{\substack{i\in\mathcal{I}\\ j\in\mathcal{J}}} d_{i,j,t,s} = \sum_{g\in\mathcal{G}} p_{g,t,s} + W_{t,s} + S_{t,s}, t \in \mathcal{T}, s \in \mathcal{S} \tag{3.65}$$

$$d_{i,j,t,s} \leq \sum_{l\in\mathcal{L}} D_l \cdot N_{j,t} \cdot \mu_{i,j,l}, i \in \mathcal{I}, j \in \mathcal{J}, t \in \mathcal{T}, s \in \mathcal{S} \tag{3.66}$$

$$\sum_{l\in\mathcal{L}} D_l \cdot T_j \cdot w_{i,j,l} = \sum_{s\in\mathcal{S}} P_s \cdot \sum_{t\in\mathcal{T}} d_{i,j,t,s}, i \in \mathcal{I}, j \in \mathcal{J} \tag{3.67}$$

$$d_{i,j,t,s} \geq 0, p_{g,t,s} \geq 0, i \in \mathcal{I}, j \in \mathcal{J}, g \in \mathcal{G}, t \in \mathcal{T}, s \in \mathcal{S} \tag{3.68}$$

$$m_{g,t,s} \in \{0,1\}, n_{g,t,s} \in \{0,1\}, o_{g,t,s} \in \{0,1\}, g \in \mathcal{G}, t \in \mathcal{T}, s \in \mathcal{S} \tag{3.69}$$

Note that in Eq. (3.66), which corresponds to Eq. (3.56), we have replaced

the optimal choice $s^{\star}_{l,i,j}(\pi)$ with its binary alternative, $D_l \cdot \mu_{l,i,j}$, by relying on proposition 3. Note, also, that in Eq. (3.67), which corresponds to Eq. (3.57), we have replaced the product $s^{\star}_{l,i,j}(\pi) \cdot r_i$ with its McCormick envelope.

The MILP formulation of the bilevel problem can then be summarized as follows.

- Maximize system welfare, as expressed in Eq. (3.63)
- subject to the upper-level constraints of the producer (3.64) - (3.69)
- subject to lower level primal feasibility constraints (3.36) - (3.37)
- subject to lower level dual feasibility constraints (3.38) - (3.39)
- subject to the McCormick envelope of the lower level strong duality condition, (3.41) - (3.52)

3.C Estimation of Demand Functions

Recall that, as input to the problem CP_l in section 3.3.1, the producer requires the valuation of an increment D_l of power. The idea of our approach is to estimate the marginal value of an increment in the fuse limit of a household. Due to the coexistence of storage and solar in a household, there is no guarantee that this incremental value is a concave function of the duration of consumption, therefore in a second step we compute the closest concave approximation. This function, $V_l(t)$ serves as input to the menu design problem.

In order to clarify the procedure that we adopt, we present the following model (HV_h), which is used for quantifying the marginal value of a fuse limit increase to a household h which has a certain known installation of solar supply, storage, and non-flexible demand. The model is described as follows. The notation used in this model is identical to that of section 3.4.2. The only new parameter that is added to the model is FL in constraint (3.78), which corresponds to the fuse limit of the household. Constraint (3.78) effectively imposes a fuse limit, and the dual multiplier λ_{t,s,ω^H} of this constraint is used for quantifying the incremental value of the fuse limit. Concretely, the valuation for an additional unit of power in period t of actual operations, given fuse limit FL, is computed as

$$\sum_{s \in \mathcal{S}, \omega^S \in \Omega^S} \lambda_{t,s,\omega^S}, t \in \mathcal{T}.$$

We derive this valuation for different levels of FL, in order to derive a demand function for increments of power for the household at a given operating interval.

The model can be described as follows:

$$(HV_h):$$

$$\min_{\mathbf{x}=(\mathbf{ls},\mathbf{nd},\mathbf{bd},\mathbf{bc},\mathbf{e})} \sum_{s\in\mathcal{S}}\sum_{t\in\mathcal{T}}\sum_{\omega^S\in\Omega^S} VOLL\cdot P_s\cdot P^s_{\omega^S}\cdot ls_{t,s,\omega^S} \tag{3.70}$$

$$\text{s.t. } bd_{t,s,\omega^S}\le BD_h, t\in\mathcal{T}, s\in\mathcal{S}, \omega^S\in\Omega^S \tag{3.71}$$

$$bc_{t,s,\omega^S}\le BC_h, t\in\mathcal{T}, s\in\mathcal{S}, \omega^S\in\Omega^S \tag{3.72}$$

$$e_{t,s,\omega^S}\le E_h, t\in\mathcal{T}, s\in\mathcal{S}, \omega^S\in\Omega^S \tag{3.73}$$

$$e_{1,s,\omega^S}+bd_{1,s,\omega^S}/\eta^d_h - bc_{1,s,\omega^S}\cdot\eta^c_h = 0, s\in\mathcal{S}, \omega^S\in\Omega^S \tag{3.74}$$

$$e_{t,s,\omega^S}-e_{t-1,s,\omega^S}+bd_{t,s,\omega^S}/\eta^d_h - bc_{t,s,\omega^S}\cdot\eta^c_h = 0,$$
$$t\in\{2,\dots,|\mathcal{T}|\}, s\in\mathcal{S}, \omega^S\in\Omega^S \tag{3.75}$$

$$e_{T,s,\omega^S}=0, s\in\mathcal{S}, \omega^S\in\Omega^S \tag{3.76}$$

$$L_{t,s,h}-ls_{t,s,\omega^S}+bc_{t,s,\omega^S}-PV_{t,s,\omega^S}-bd_{t,s,\omega^S}-nd_{t,s,\omega^S}=0,$$
$$t\in\mathcal{T}, s\in\mathcal{S}, \omega^S\in\Omega^S \tag{3.77}$$

$$(\lambda_{t,s,\omega^S}): nd_{t,s,\omega^S}\le FL, t\in\mathcal{T}, s\in\mathcal{S}, \omega^S\in\Omega^S \tag{3.78}$$

$$x_{t,s,b}-x_{t,s,\omega^S}=0, t\in\mathcal{T}, b\in\mathcal{B}_t, s\in\mathcal{S}, \omega^S\in\Omega^S \tag{3.79}$$

$$bd_{t,s,\omega^S}\ge 0, bc_{t,s,\omega^S}\ge 0, e_{t,s,\omega^S}\ge 0, ls_{t,s,\omega^S}\ge 0,$$
$$t\in\mathcal{T}, s\in\mathcal{S}, \omega^S\in\Omega^S \tag{3.80}$$

The demand functions for the eight types of households that are simulated in section 3.5 are presented in figure 3.16 (note the difference in numbering in the horizontal axis for different households, since household consumption is not necessarily synchronized). We then aggregate the demand increments of the system level , according to the number of households in each type. We obtain, in this way, a system-level demand function, which is presented in figure 3.17a. Note that these valuation functions are not concave. In order to obtain the concave functions $V_l(t)$ in Eq. (1) of problem (CP_l) of section 3.3.1 which approximate the value functions of figure 3.17a as closely as possible, we solve a least-square fit of the function of figure 3.17a which yields a function that differs from that of figure 3.17a as little as possible, while respecting the concavity of $V_l(t)$. The system-level demand function after the least-square fit is presented in figure 3.17b. The mapping $\tau(t)$ is obtained by ordering the total benefits under the demand function at each time stage in descending order. For example, in figure 3.17b, the marginal value is highest for the aggregate demand function during the second stage, we thus obtain $\tau(2)=1$.

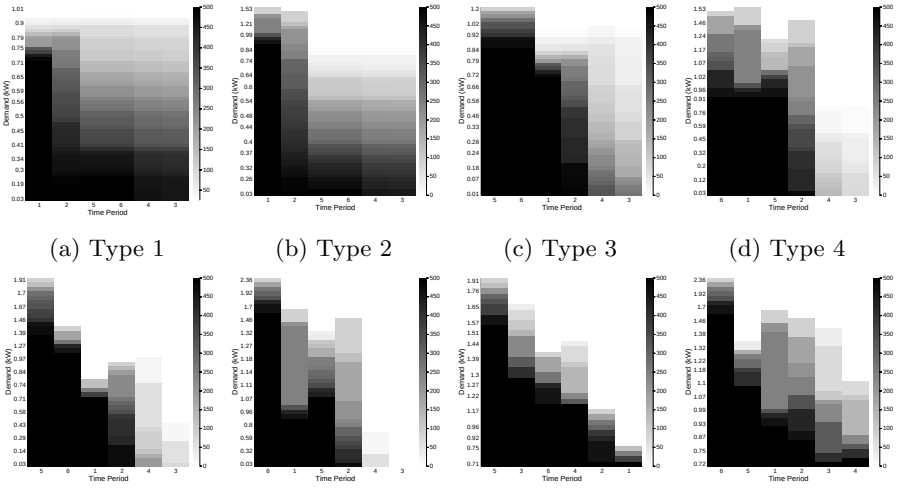

(a) Type 1 (b) Type 2 (c) Type 3 (d) Type 4

(e) Type 5 (f) Type 6 (g) Type 7 (h) Type 8

Figure 3.16: Comparison of demand functions for the eight types of households that are simulated in section 3.5. The x-axis corresponds to the time period of the load duration curve, while the y-axis presents the fuse limit. The darkness indicates the valuation for an increment of fuse capacity, which ranges from 0 to 500 €/MWh.

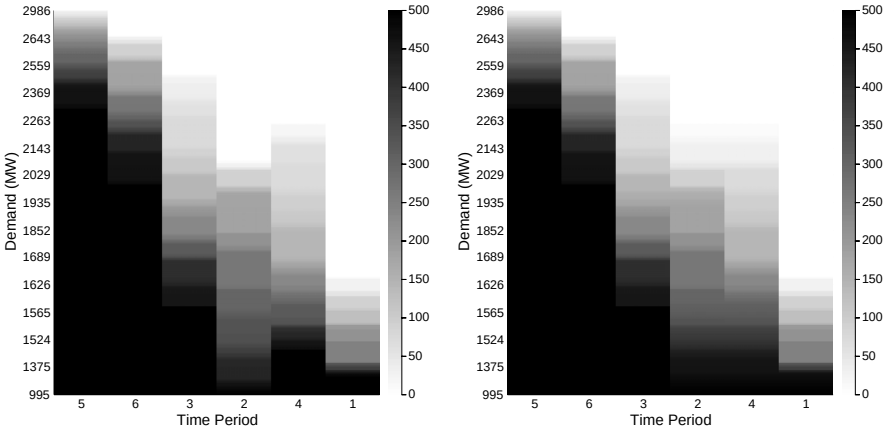

(a) (b)

Figure 3.17: The system-level demand function (left), and its concave approximation (right).

3.D Household Menu Selection Problem

Once the household is presented with a multilevel demand subscription menu, it can decide on which options to procure. The menu selection problem of the household can be described as follows, which is solved by each household. The notation used in this section follows the notation of section 3.4.2.

$$(HC_h):$$

$$\min_{\substack{\mathbf{s},\mathbf{x}=\\(\mathbf{ls},\mathbf{nd},\mathbf{bd},\mathbf{bc},\mathbf{e})}} \quad P_s \cdot \Big(\sum_{t\in\mathcal{T}} \sum_{\omega^C\in\Omega^C} VOLL \cdot P^s_{\omega^C} \cdot ls_{t,s,\omega^C} + \sum_{i\in\mathcal{I},j\in\mathcal{J}} \pi_{i,j} \cdot s_{i,j} \Big) \tag{3.81}$$

$$\text{s.t.} \quad bd_{t,s,\omega^C} \leq BD_h, t \in \mathcal{T}, s \in \mathcal{S}, \omega^C \in \Omega^C \tag{3.82}$$

$$bc_{t,s,\omega^C} \leq BC_h, t \in \mathcal{T}, s \in \mathcal{S}, \omega^C \in \Omega^C \tag{3.83}$$

$$e_{t,s,\omega^C} \leq E_h, t \in \mathcal{T}, s \in \mathcal{S}, \omega^C \in \Omega^C \tag{3.84}$$

$$e_{1,s,\omega^C} + bd_{1,s,\omega^C}/\eta^d_h - bc_{1,s,\omega^C} \cdot \eta^c_h = 0, s \in \mathcal{S}, \omega^C \in \Omega^C \tag{3.85}$$

$$e_{t,s,\omega^C} - e_{t-1,s,\omega^C} + bd_{t,s,\omega^C}/\eta^d_h - bc_{t,s,\omega^C} \cdot \eta^c_h = 0,$$
$$t \in \{2,\ldots,|\mathcal{T}|\}, s \in \mathcal{S}, \omega^C \in \Omega^C \tag{3.86}$$

$$L_{t,s,h} - ls_{t,s,\omega^C} + bc_{t,s,\omega^C} - PV_{t,s,\omega^S} - bd_{t,s,\omega^C} = \sum_{i\in\mathcal{I}} nd_{i,t,s,\omega^C},$$
$$t \in \mathcal{T}, s \in \mathcal{S}, (\omega^I \times \omega^S) \in \Omega^C \tag{3.87}$$

$$nd_{i,t,s,\omega^C} \leq \sum_{j\in\mathcal{J}} s_{i,j} \cdot 1_{[i,t,\omega^I]}, i \in \mathcal{I}, s \in \mathcal{S}, (\omega^I,\omega^S) \in \Omega^C \tag{3.88}$$

$$\sum_{i\in\mathcal{I}} nd_{i,t,s,\omega^C} \geq -\Gamma \cdot \sum_{i\in\mathcal{I},j\in\mathcal{J}} s_{i,j}, s \in \mathcal{S}, (\omega^I,\omega^S) \in \Omega^C \tag{3.89}$$

$$\sum_{t\in\mathcal{T}} \Pi_{\mathbb{R}_+}(nd_{i,t,s,\omega^C}) \leq \sum_{j\in\mathcal{J}} T_j \cdot s_{i,j}, i \in \mathcal{I}, t \in \mathcal{T}, s \in \mathcal{S}, \omega^C \in \Omega^C \tag{3.90}$$

$$x_{t,s,b} - x_{t,s,\omega^C} = 0, t \in \mathcal{T}, b \in \mathcal{B}_t, s \in \mathcal{S}, \omega^C \in \Omega^C \tag{3.91}$$

$$bd_{t,s,\omega^C} \geq 0, bc_{t,s,\omega^C} \geq 0, e_{t,s,\omega^C} \geq 0, ls_{t,s,\omega^C} \geq 0,$$
$$i \in \mathcal{I}, t \in \mathcal{T}, s \in \mathcal{S}, \omega^C \in \Omega^C \tag{3.92}$$

The first stage of this menu selection problem is the subscription level $s_{i,j}$. This decision is not indexed by day type $s \in \mathcal{S}$, because the subscription remains the same over all seasons and weekdays / weekends. By contrast, the daily operational decisions of the household, $\mathbf{x} = (\mathbf{ls}, \mathbf{nd}, \mathbf{bd}, \mathbf{bc}, \mathbf{e})$, are indexed by $s \in \mathcal{S}$ and $\omega^C \in \Omega^C$. Note that we estimate a different scenario tree for each day type, with $P^s_{\omega^C}$ corresponding to the probabilities of the scenario tree for

Table 3.10: Priority service menus under different VOLL assumptions.

VOLL (€/MWh)	Reliability (%)	Price (€/kW-month)
200	56.6	19.4
	78.4	27.8
	100.0	38.0
500	58.5	26.4
	85.3	39.3
	100.0	48.5
3000	71.2	39.9
	90.4	69.7
	100.0	105.9

day type $s \in \mathcal{S}$. The notation and constraints of this model are the same as those in section 3.4.2. We point out the following main differences between the household choice model (HC_h), and the model $H_{h,\tau}$ of section 3.4.2:

- The optimization of the household choice (HC_h) is conducted over the full horizon $t \in \mathcal{T}$, whereas the rolling optimization of the household dispatch is performed from a given stage τ until the end of the horizon.
- The objective function in the menu choice model (HC_h) is the expected load shedding cost of the household, *plus* the cost of subscribing to a given menu. By contrast, in the rolling optimization problem ($H_{h,\tau}$), the household has already chosen a specific option, and is only interested in minimizing its expected cost from stage τ until the end of the day.
- The right hand side of constraint (3.88) in the household choice model (HC_h) is a decision, whereas in the corresponding constraint (3.26) of model ($H_{h,\tau}$) in section 3.4.2 it is a parameter. More specifically, the optimal subscription $s^{\star}_{i,j}$ of (HC_h) is stored as a parameter $S_{h,i,j}$, and is used as input to the performance evaluation model ($H_{h,\tau}$) of section 3.4.2.

3.E Impact of VOLL on Menu Design

The value of lost load (VOLL) in the case study of this chapter is assumed to be 500 €/MWh, which is consistent with the maximum valuation estimated in Chapter 2. In table 3.10, we compare the priority service menus for different values of VOLL. There are two major observations:

- The reliability levels tend to increase in the case of a higher VOLL. With a high VOLL, the value of serving a certain option increases, so the reliability level is largely driven by the available capacity of the system. In

contrast, the value of serving a certain option decreases when VOLL decreases. Consequently, the option could be interrupted when the marginal cost of the system is higher than the valuation, even if the capacity is not exhausted. This results a lower reliability level.

- The prices are higher when the VOLL is higher. This price increase is driven by the increased value of serving a certain, option and by the reliability increment from the lowest-reliability option (see equation 2.10).

Chapter 4

Conclusions and Perspectives

This thesis focuses on the design of new pricing policies for residential consumers based on nonlinear pricing theory, in order to mobilize demand response in the residential sector. We mainly investigate two quality-differentiated products, namely priority service and multilevel demand subscription. The latter is considered as an extension of the former.

We first reformulate priority service pricing as a bilevel model of a Stackelberg game, which couples the problem of menu design with unit commitment. We are thus able to extend the classical theory of priority service [CW87] by including non-convex costs and constraints in the model. We further develop a decomposition algorithm for solving the problem heuristically, and compare the performance of priority service with flat tariffs and real-time pricing on a realistic case study of the Belgian electricity market.

This framework for modeling a market equilibrium under priority service is then generalized to multilevel demand subscription. The extra component of energy charges in multilevel demand subscription increases implementation complexity from the perspective of both the utility and households. On the upside, multilevel demand subscription improves operational efficiency by allowing the utility to better discriminate flexible consumers. We examine the trade-off between simplicity and operational efficiency using a stochastic programming framework. The impacts of both pricing schemes on the utility and households are analyzed. In the following, we first present a summary of our conclusions, and then discuss a list of areas for future work that have been inspired by the present research.

4.1 A Summary of Conclusions

4.1.1 Case Study Comparing Flat Tariff, Priority Service and Real-Time Pricing

(a) **The benefits of priority service:** Priority service is able to achieve higher efficiency compared to a flat tariff, due to the self-selection of consumers which enables the utility to differentiate consumers. The efficiency gain increases with the increase of the number of options offered in the price menu and our study of the Belgian power system demonstrates that priority service can reap 61.4% to 77.1% of the gains of real-time pricing by using a menu that consists of 3 to 5 options.

(b) **Interruption patterns:** A powerful feature of our proposed model is that it reveals the interruption patterns associated with a given level of reliability. A continuous interruption of 20 hours is possible for an option that nominally interrupts customers for 4.4 minutes per hour (when distributed evenly). The severity of such continuous interruptions needs to be carefully accounted for in the development of aggregator services.

4.1.2 Case Study Comparing Priority Service and Multilevel Demand Subscription

(a) **Operational efficiency:** Under multilevel demand subscription, the utility is able to supply more energy to households at a lower cost, while the service inconvenience of households is also reduced.

(b) **Service comparison:** Due to the offer of options with shorter duration, the total subscribed capacity of each household under multilevel demand subscription is higher than that under priority service. On the other hand, the subscribed energy is less. In addition, under multilevel demand subscription, the lowest utilization ratio of the subscribed energy amounts to 69.3%, which is a significant improvement relative to the lowest ratio under priority service, which amounts to 53.1%

(c) **Cost comparison of households under different policies:** The total cost of a household equipped with a battery under multilevel demand subscription is almost identical to that under priority service. On the other hand, if the household does not own a battery, the savings achieved by multilevel demand subscription are more significant.

(d) **Cost-benefit analysis of local storage:** The batteries are more rewarding for households under priority service, and the investment cost can be justified. In contrast, the investment cost of batteries can only

be recovered in relatively optimistic scenarios under multilevel demand subscription.

4.2 Future Areas of Research

(a) **Modeling of risk preferences:** In our models for menu design, we focus on consumers who are risk-neutral. Thus we are able to represent the utility function of the consumer as an affine function of reliability and then reformulate the bilevel menu design problem into an MILP. We would like to extend the model to consider risk aversion [Rab00]. The modeling approach of risk aversion and the methodology to solve the Stackelberg game with risk-averse consumers are to be investigated.

(b) **Aggregator competition:** When the price menu is designed, we focus on the setting where the producer is a benevolent planner that maximizes social welfare. This follows the standard literature on nonlinear pricing [Rob93, CW87, COSW86]. We are interested in extending the model to consider aggregator competition. This model may be cast as an equilibrium problem with equilibrium constraints, where aggregators maximize profit by offering different price menus and consumers aim at extracting the highest possible surplus [JT06, BH05, CO16].

(c) **Evenly distributed interruption patterns:** In our model, the reliability is defined over the entire horizon, so the interruption patterns are not captured explicitly. The definition of reliability can be revised to guarantee that the promised reliability is delivered on a daily or weekly basis, in order to ensure more evenly distributed interruption patterns.

(d) **Integrating capacity expansion into menu design:** Another direction of interest is to apply the bilevel approach in order to incorporate capacity expansion planning considerations in the design of the menu [JT07].

(e) **Accounting for the grid tariff:** In our menu design model, we have exclusively focused on the tariff component related to the production of electricity. However, the grid (transmission and distribution network) tariff accounts for approximately 60% of the electricity bill of residential consumers in Belgium [Ele20a]. In the backdrop of increasing numbers of prosumers, the design of novel grid tariffs has attracted the attention of researchers and grid operators [GBD18, ABG19, GBLC$^+$19]. It would be an interesting extension to incorporate the grid tariff into the price menus, which is to be investigated.

(f) **Improved representation of the household model:** We are interested in further improving Chapter 3 by considering more diverse household types, flexible appliances, a longer horizon, a more detailed model of uncertainty and sizing of batteries.

(g) **Development of home energy management systems:** In Chapter 3, households select options from the price menu and consume electricity optimally according to our models. Admittedly, if the behavior of the household is not optimal, the operational efficiently of the proposed pricing schemes would be undermined. For example, if a household overprocures the red option, the producer may end up serving low-valuation demand with high-cost generators. One solution to this problem is the development of home energy management systems, which assist households with managing electricity consumption based on machine learning techniques or optimization models [AS17, GP19]. Belgium is one of the pioneers in the establishment of an adequate regulatory framework for demand response [Eco19]. In particular, the roll-out of smart meters shall reach all customers in Flanders no later than 2034 and 80% customers in Wallonia by 2029. In addition, the Belgian government has started to subsidize households with energy management systems [Lam20].

Bibliography

[ABG19] Magnus Askeland, Thorsten Burandt, and Steven A Gabriel. A stochastic mpec approach for grid tariff design with demand side flexibility. *IEEE Transactions on Power Systems*, 2019. under review.

[AP17] Ignacio Aravena and Anthony Papavasiliou. Renewable energy integration in zonal markets. *IEEE Transactions on Power Systems*, 32(2):1334–1349, 2017.

[AS17] SL Arun and MP Selvan. Intelligent residential energy management system for dynamic demand response in smart buildings. *IEEE Systems Journal*, 12(2):1329–1340, 2017.

[BEKS17] Jeff Bezanson, Alan Edelman, Stefan Karpinski, and Viral B Shah. Julia: A fresh approach to numerical computing. *SIAM review*, 59(1):65–98, 2017. URL: `https://doi.org/10.1137/141000671`.

[BH05] Severin Borenstein and Stephen Holland. On the efficiency of competitive electricity markets with time-invariant retail prices. *RAND Journal of Economics*, 36(3):469–493, Autumn 2005.

[BHBW19] Lionel Bloch, Jordan Holweger, Christophe Ballif, and Nicolas Wyrsch. Impact of advanced electricity tariff structures on the optimal design, operation and profitability of a grid-connected pv system with energy storage. *Energy Informatics*, 2(1):16, 2019.

[BJR02] Severin Borenstein, Michael Jaske, and Arthur Rosenfeld. Dynamic pricing, advanced metering and demand response in electricity markets. Technical Report 105, University of California Energy Institute, October 2002.

[BL12] Eilyan Bitar and Steven Low. Deadline differentiated pricing of deferrable electric power service. In *IEEE 51st Annual Conference on Conference on Decision and Control (CDC)*, 2012.

[BPC+11] Stephen Boyd, Neal Parikh, Eric Chu, Borja Peleato, and Jonathan Eckstein. Distributed optimization and statistical learning via the alternating direction method of multipliers. *Foundations and Trends in Machine Learning*, 3(1):1–122, 2011.

[BX17] Eilyan Bitar and Yunjian Xu. Deadline differentiated pricing of deferrable electric loads. *IEEE Transactions on Smart Grid*, 8(1):13–25, 2017.

[Cal09] Duncan S. Callaway. Tapping the energy storage potential in electric loads to deliver load following and regulation, with application to wind energy. *Energy Conversion and Management*, 50:1389–1400, 2009.

[CB14] Wim Cardinaels and Isabelle Borremans. Linear: Demand response for families. Technical report, Linear consortium, 2014. URL: `http://www.linear-smartgrid.be/sites/default/files/Linear%20Final%20Report%20-%20lr2.pdf`.

[CCMGB06] Antonio J Conejo, Enrique Castillo, Roberto Minguez, and Raquel Garcia-Bertrand. *Decomposition techniques in mathematical programming: engineering and science applications*. Springer Science & Business Media, 2006.

[CEC19] CECI. Clusters at CECI, March 2019. URL: `http://www.ceci-hpc.be/clusters.html`.

[Cha12] Hung-po Chao. Competitive electricity markets with consumer subscription service in a smart grid. *Journal of Regulatory Economics*, 41(1):155–180, 2012.

[CHLW16] Tsung-Hui Chang, Mingyi Hong, Wei-Cheng Liao, and Xiangfeng Wang. Asynchronous distributed admm for large-scale optimization—part i: Algorithm and convergence analysis. *IEEE Transactions on Signal Processing*, 64(12):3118–3130, 2016.

[CO16] Clay Campaign and Shmuel Oren. Firming renewable power with demand response: An end to end aggregator business model. *Journal of Regulatory Economics*, 50(1):1–37, 2016.

[COSW86] Hung-Po Chao, Shmuel S. Oren, Stephen A. Smith, and Robert B. Wilson. Multilevel demand subscription pricing for electric power. *Energy Economics*, pages 199–217, October 1986.

[CQV15] Wei Chen, Li Qiu, and Pravin Varaiya. Duration-deadline jointly differentiated energy services. In *IEEE 54th Annual Conference on Decision and Control (CDC)*, 2015.

[CRS+17] Berk Celik, Robin Roche, Siddharth Suryanarayanan, David Bouquain, and Abdellatif Miraoui. Electric energy management in residential areas through coordination of multiple smart homes. *Renewable and Sustainable Energy Reviews*, 80:260–275, 2017.

[CVC15] Carles Cervilla, José Villar, and Fco Alberto Campos. Bi-level optimization of electricity tariffs and pv distributed generation investments. In *2015 12th International Conference on the European Energy Market (EEM)*, pages 1–5. IEEE, 2015.

[CW87] Hung-Po Chao and Robert Wilson. Priority service: Pricing, investment and market organization. *The American Economic Review*, 77(5):899–916, December 1987.

[CWK14] Chen Chen, Jianhui Wang, and Shalinee Kishore. A distributed direct load control approach for large-scale residential demand response. *IEEE Transactions on Power Systems*, 29(5):2219–2228, 2014.

[DLB+15] Reinhilde D'hulst, Wouter Labeeuw, Bart Beusen, Sven Claessens, Geert Deconinck, and Koen Vanthournout. Demand response flexibility and flexibility potential of residential smart appliances: Experiences from large pilot test in Belgium. *Applied Energy*, 155:79–90, 2015.

[DWBM16] Naïm R Darghouth, Ryan H Wiser, Galen Barbose, and Andrew D Mills. Net metering and market feedback loops: Exploring the impact of retail rate design on distributed pv deployment. *Applied Energy*, 162:713–722, 2016.

[EC17] European Commission. EU reference scenario 2016, October 2017. URL: `https://ec.europa.eu/energy/en/data-analysis/energy-modelling`.

[EC20] European Commission. Clean energy for all europeans package, February 2020. URL: `https://ec.europa.eu/energy/en/topics/energy-strategy/clean-energy-all-europeans`.

[Eco19] FPS Economy. Regulation 2019/943 - article 20: Belgian implementation plan, Nov 2019. URL: `https://economie.fgov.be/sites/default/files/Files/Energy/Belgian-electricity-market-Implementation-plan.pdf`.

[EDF20] EDF. Nos offres d'électricité à prix de marché, February 2020. URL: `https://particulier.edf.fr/fr/accueil/offres/electricite-bis/offres-marche.html`.

[Ele20a] Electrabel. Conditions et fiches de prix, February 2020. URL: https://www.engie.be/fr/energie/electricite-gaz/prix-conditions.

[ELE20b] SU ELECTRICITY. Tarifa social, February 2020. URL: https://sueletricidade.pt/pt-pt/page/626/tarifa-social.

[Ele20c] Slovenské Elektrárne. CENÍK ELEKTRICKÉ ENERGIE, February 2020. URL: https://cz.seas.sk/data/contentlink/cenik-domacnosti-special-2020-web.pdf.

[Eli19a] Elia. Ancillary services: Volumes & prices, March 2019. URL: http://www.elia.be/en/suppliers/purchasing-categories/energy-purchases/Ancillary-services/Ancillary-Services-Volumes-Prices.

[Eli19b] Elia. Grid data, November 2019. URL: https://www.elia.be/en/grid-data.

[ELM20] ELMUEMASZ. Villamos energia tarifák, February 2020. URL: https://www.dei.gr/en/oikiakoi-pelates/timologia.

[End20] Endesa. Our products, February 2020. URL: https://www.endesa.com/en/catalog/light.

[Ene20a] Energia. The power behind your savings, February 2020. URL: https://www.energia.ie/price-plans.

[Ene20b] Kotimaan Energia. Suosituimmat sähkösopimukset, February 2020. URL: https://www.kotimaanenergia.fi/sahkoa-kotiin.

[Ene20c] Elektro Energija. CENIK OSKRBE IN STORITEV, February 2020. URL: https://www.elektro-energija.si/za-dom/dokumenti-in-ceniki.

[Ene20d] EnergySage. The Tesla Powerwall home battery complete review, February 2020. URL: https://news.energysage.com/tesla-powerwall-battery-complete-review/.

[Eno20] Enovos. Green electricity for your home, February 2020. URL: https://www.enovos.lu/en/individuals/electricity.

[FG02] Ahmad Faruqui and Stephen George. The value of dynamic pricing in mass markets. *The Electricity Journal*, 15(6):45–55, 2002.

[FHH10] Ahmad Faruqui, Dan Harris, and Ryan Hledik. Unlocking the 53 billion savings from smart meters in the EU: How increasing the adoption of dynamic tariffs could make or break the EU's smart grid investment. *Energy Policy*, 38(10):6222–6231, 2010.

[FS10a] Ahmad Faruqui and Sanem Sergici. Household response to dynamic pricing of electricity: a survey of 15 experiments. *Journal of regulatory Economics*, 38(2):193–225, 2010.

[FS10b] Ahmad Faruqui and Sanem Sergici. Household response to dynamic pricing of electricity: a survey of 15 experiments. *Journal of regulatory Economics*, 38(2):193–225, 2010.

[FSW17] Ahmad Faruqui, Sanem Sergici, and Cody Warner. Arcturus 2.0: A meta-analysis of time-varying rates for electricity. *The Electricity Journal*, 30(10):64–72, 2017.

[GBD18] Niels Govaerts, Kenneth Bruninx, and Erik Delarue. Impact of distribution tariff design on the profitability of aggregators of distributed energy storage systems. In *2018 15th International Conference on the European Energy Market (EEM)*, pages 1–5. IEEE, 2018.

[GBLC+19] Niels Govaerts, Kenneth Bruninx, Hélène Le Cadre, Leonardo Meeus, and Erik Delarue. Spillover effects of distribution grid tariffs in the internal electricity market: an argument for harmonization? *Energy Economics*, 84:104459, 2019.

[GCGBR09] Lina P Garcés, Antonio J Conejo, Raquel García-Bertrand, and Rubén Romero. A bilevel approach to transmission expansion planning within a market environment. *IEEE Transactions on Power Systems*, 24(3):1513–1522, 2009.

[GHP07] Paul R. Gribik, William W. Hogan, and Susan L. Pope. Market-clearing electricity prices and energy uplift. Technical report, John F. Kennedy School of Government, Harvard University, 2007.

[Gil14] Hans Christian Gils. Assessment of the theoretical demand response potential in europe. *Energy*, 67:1–18, 2014.

[GJP18] Axel Gautier, Julien Jacqmin, and Jean-Christophe Poudou. The prosumers and the grid. *Journal of Regulatory Economics*, 53(1):100–126, 2018.

[GOS+19] Veronika Grimm, Galina Orlinskaya, Lars Schewe, Martin Schmidt, and Gregor Zöttl. Optimal design of retailer-prosumer electricity tariffs using bilevel optimization, 2019. URL: `https://opus4.kobv.de/opus4-trr154/frontdoor/index/index/docId/274`.

[GP19] Céline Gérard and Anthony Papavasiliou. A comparison of priority service versus real-time pricing for enabling residential demand response. In *2019 IEEE Power & Energy Society General Meeting (PESGM)*, Aug 2019.

[Gud20] Gudbrandsdal. Power agreements, February 2020. URL: `https://www.ge.no/en/power-agreements/`.

[HAE+14] 50Hertz, Amprion, Elia, TennetT, and TransnetBW. Potential cross-border balancing cooperation between the belgian, dutch and german electricity transmission system operators. *Technical Report*, October 2014. URL: `http://www.elia.be/~/media/files/Elia/users-group/141008_Final_report.pdf`.

[HBPV18] Elaine T Hale, Lori A Bird, Rajaraman Padmanabhan, and Christina M Volpi. Potential roles for demand response in high-growth electric systems with increasing shares of renewable generation. Technical report, National Renewable Energy Lab.(NREL), Golden, CO (United States), 2018.

[Hel20] Helen. Electricity products and prices, February 2020. URL: `https://www.helen.fi/en/electricity/homes/electricity-products-and-prices/`.

[HHS10] Sekyung Han, Soohee Han, and Kaoru Sezaki. Development of an optimal vehicle-to-grid aggregator for frequency regulation. *IEEE Transactions on smart grid*, 1(1):65–72, 2010.

[HYW00] Bingsheng He, Hai Yang, and Shengli Wang. Alternating direction method with self-adaptive penalty parameters for monotone variational inequalities. *Journal of Optimization Theory and applications*, 106(2):337–356, 2000.

[JDA+12] Kaat Jespers, Yoko Dams, Kristien Aernouts, Pascal Simus, Frederic Jacquemin, and Laurent Delaite. Energy consumption survey for belgian households. Technical report, FPS Economy, SMEs, Self-employed and Energy- STATISTICS BELGIUM, 2012. URL: `https://emis.vito.be/sites/emis.vito.be/files/articles/3331/2015/Eurostatenquete_onderzoeksrapport.pdf`.

[JT06] Paul Joskow and Jean Tirole. Retail electricity competition. *RAND Journal of Economics*, 37(4):799–815, Winter 2006.

[JT07] Paul Joskow and Jean Tirole. Reliability and competitive electricity markets. *The Rand Journal of Economics*, 38(1):60–84, 2007.

[KDPV+15] Vyacheslav V Kalashnikov, Stephan Dempe, Gerardo A Pérez-Valdés, Nataliya I Kalashnykova, and José-Fernando Camacho-Vallejo. Bilevel programming and applications. *Mathematical Problems in Engineering*, 2015, 2015.

[KHW+19] Peter Kohlhepp, Hassan Harb, Henryk Wolisz, Simon Waczowicz, Dirk Müller, and Veit Hagenmeyer. Large-scale grid integration of residential thermal energy storages as demand-side flexibility resource: A review of international field studies. *Renewable and Sustainable Energy Reviews*, 101:527–547, 2019.

[Kub18] Merla Kubli. Squaring the sunny circle? on balancing distributive justice of power grid costs and incentives for solar prosumers. *Energy policy*, 114:173–188, 2018.

[KZ18] Kibaek Kim and Victor M Zavala. Algorithmic innovations and software for the dual decomposition method applied to stochastic mixed-integer programs. *Mathematical Programming Computation*, pages 1–42, 2018.

[Lam20] Laurent Lambrecht. Philippe henry sur le photovoltaïque: "le tarif prosumer sera supprimé au-dessus d'un certain niveau d'autoconsommation", May 2020. URL: `https://www.lalibre.be/economie/mes-finances/philippe-henry-le-tarif-prosumer-sera-supprime-au-dessus-d-un-certain-niveau-d-autoconsommation-5eaefddc7b50a67d2e0804cc`.

[LH15] Nan Li and Kory W. Hedman. Economic assessment of energy storage in systems with high levels of renewable resources. *IEEE Transactions on Sustainable Energy*, 6(3):1103–1111, July 2015.

[MAG05] Alexis L Motto, José M Arroyo, and Francisco D Galiana. A mixed-integer lp procedure for the analysis of electric grid security under disruptive threat. *IEEE Transactions on Power Systems*, 20(3):1357–1365, 2005.

[Mal20] Malarenergi. Teckna elavtal, February 2020. URL: `https://www.malarenergi.se/el/elavtal/teckna/`.

[MO16] Kostas Margellos and Shmuel Oren. Capacity controlled demand side management: A stochastic pricing analysis. *IEEE Transactions on Power Systems*, 31(1):706–717, 2016.

[Moi20] Moixa. Moixa smart battery user manual, February 2020. URL: `https://www.moixa.com/wp-content/uploads/2019/02/V4_Moixa_User_Manual_online_UM004.pdf`.

[MVV20] MVV. Unsere stromtarife, February 2020. URL: https://www.mvv.de/energie/strom/stromprodukte/.

[MWSR15] Ilan Momber, Sonja Wogrin, and Tomás Gómez San Román. Retail pricing: A bilevel program for pev aggregator decisions using indirect load control. *IEEE Transactions on Power Systems*, 31(1):464–473, 2015.

[MXLF15] Yuting Mou, Hao Xing, Zhiyun Lin, and Minyue Fu. Decentralized optimal demand-side management for PHEV charging in a smart grid. *IEEE Transactions on Smart Grid*, 6(2):726–736, 2015.

[Naz20] Servizio Elettrico Nazionale. Usi domestici, February 2020. URL: https://www.servizioelettriconazionale.it/it-IT/tariffe/uso-domestico.

[NLBK18] Anders Nilsson, David Lazarevic, Nils Brandt, and Olga Kordas. Household responsiveness to residential demand response strategies: Results and policy implications from a swedish field study. *Energy policy*, 122:273–286, 2018.

[NNPPV16] Ashutosh Nayyar, Matias Negrete-Pincetic, Kameshwar Poolla, and Pravin Varaiya. Duration differentiated energy services with a continuum of loads. *IEEE Transactions on Control of Network Systems*, 3(2):182–191, 2016.

[NPNP+16] Matias Negrete-Pincetic, Ashutosh Nayyar, Kameshwar Poolla, Florian Salah, and Pravin Varaiya. Rate-constrained energy services in electricity. *IEEE Transactions on Smart Grid*, 2016.

[Ore13] Shmuel S Oren. A historical perspective and business model for load response aggregation based on priority service. In *2013 46th Hawaii International Conference on System Sciences*, pages 2206–2214. IEEE, 2013.

[Ore17] Shmuel S. Oren. Distributed resource integration in the US: A markets perspective. In *CITIES 4th General Consortium Meeting*, 2017. URL: http://smart-cities-centre.org/wp-content/uploads/Oren-Distributed_Resource_Integration_in_the_US_from_a_markets_perspective.pdf.

[Ors20] Orsted. Få den strøm der passer til dig, February 2020. URL: https://privat.orsted.dk/el/.

[PAK16] Ignacio Pérez-Arriaga and Christopher Knittel. Utility of the future. Technical report, MIT Energy Initiative, December 2016.

[Pav19] Claudia Pavarini. Battery storage is (almost) ready to play the flexibility game, February 2019. URL: https://www.iea.org/commentaries/battery-storage-is-almost-ready-to-play-the-flexibility-game.

[PBF13] Alex Papalexopoulos, Jacob Beal, and Steven Florek. Precise mass-market energy demand management through stochastic distributed computing. *IEEE Transactions on Smart Grid*, 4(4):2017 – 2027, August 2013.

[PM14] Pierre Pinson and Henrik Madsen. Benefits and challenges of electrical demand response: A critical review. *Renewable and Sustainable Energy Reviews*, 39:686–699, 2014.

[PO13] Anthony Papavasiliou and Shmuel S. Oren. Multi-area stochastic unit commitment for high wind penetration in a transmission constrained network. *Operations Research*, 61(3):578–592, May / June 2013.

[PO14] Anthony Papavasiliou and Shmuel S. Oren. Large-scale integration of deferrable demand and renewable energy sources in power systems. *IEEE Transactions on Power Systems*, 29(1):489–499, January 2014.

[POO11] Anthony Papavasiliou, Shmuel S. Oren, and Richard P. O'Neill. Reserve requirements for wind power integration: A scenario-based stochastic programming framework. *IEEE Transactions on Power Systems*, 26(4):2197–2206, November 2011.

[PRE20] PRE. Elektřina - přehled produktů, February 2020. URL: https://www.pre.cz/cs/domacnosti/elektrina/.

[PS15] Anthony Papavasiliou and Yves Smeers. Energy-only markets with deferrable demand. In *12th International Conference on the European Energy Market*, Lisbon, May 2015.

[PS17] Anthony Papavasiliou and Yves Smeers. Remuneration of flexibility using operating reserve demand curves: A case study of Belgium. *The Energy Journal*, pages 105–135, 2017.

[PSdMd19] Anthony Papavasiliou, Yves Smeers, and Gauthier de Maere d'Aertrycke. Study on the general design of a mechanism for the remuneration of reserves in scarcity situations. Technical report, 2019. URL: https://www.creg.be/sites/default/files/assets/Publications/Notes/Z1986Annex.pdf.

[Rab00] Matthew Rabin. Risk aversion and expected-utility theory: A calibration theorem. *Econometrica*, 68(5):1281–1292, 2000.

[Rob93] Robert. *Nonlinear pricing*. Oxford University Press, 1993.

[RP98] Sesh Rao and EDWARD R Petersen. Optimal pricing of priority services. *Operations Research*, 46(1):46–56, 1998.

[SA13] Rainer Stamminger and Verena Anstett. The effect of variable electricity tariffs in the household on usage of household appliances. *Smart Grid and Renewable Energy*, 4(4), 2013.

[Sag12] Claudia Sagastizábal. Divide to conquer: decomposition methods for energy optimization. *Mathematical programming*, 134(1):187–222, 2012.

[SAP+15] Goran Strbac, Marko Aunedi, Danny Pudjianto, Fei Teng, Predrag Djapic, Richard Druce, Alon Carmel, and Konrad Borkowski. Value of flexibility in a decarbonised grid and system externalities of low-carbon generation technologies. Technical report, Imperial College London and NERA Economic Consulting, 2015.

[SEE20] SEE. Our prices, February 2020. URL: `http://www.southern-electric.co.uk/OurPrices/`.

[Sen20] Andrew Sendy. Is the tesla powerwall the best solar energy storage solution in 2020?, February 2020. URL: `https://www.solarreviews.com/blog/is-the-tesla-powerwall-the-best-solar-battery-available`.

[SFOO19] Trevor Sweetnam, Michael Fell, Eleni Oikonomou, and Tadj Oreszczyn. Domestic demand-side response with heat pumps: controls and tariffs. *Building Research & Information*, 47(4):344–361, 2019.

[SH20] Public Power Corporation SA.-Hellas. Residential tariffs, February 2020. URL: `https://www.dei.gr/en/oikiakoi-pelates/timologia`.

[Sio12] Ramteen Sioshansi. Modeling the impacts of electricity tariffs on plug-in hybrid electric vehicle charging, costs and emissions. *Operations Research*, 60(3):506–516, May-June 2012.

[SMM18] Tim Schittekatte, Ilan Momber, and Leonardo Meeus. Future-proof tariff design: Recovering sunk grid costs in a world where consumers are pushing back. *Energy economics*, 70:484–498, 2018.

[SS09] Ramteen Sioshansi and Walter Short. Evaluating the impacts of real time pricing on the usage of wind power generation. *IEEE Transactions on Power Systems*, 24(2):516–524, May 2009.

[Ste19] Pippa Stevens. The battery decade: How energy storage could revolutionize industries in the next 10 years, December 2019. URL: `https://www.cnbc.com/2019/12/30/battery-developments-in-the-last-decade-created-a-seismic-shift-that-will-play-out-in-the-next-10-years.html`.

[Sto02] Steven Stoft. *Power System Economics*. IEEE Press and Wiley Interscience, 2002.

[Syn17] Synergrid. Synthetic load profiles (SLP), October 2017. URL: `http://www.synergrid.be/index.cfm?PageID=16896`.

[TAU20] TAURON. Prad z serwisantem 24h, February 2020. URL: `https://www.tauron.pl/dla-domu/prad/prad-z-usluga/prad-z-serwisantem-24h`.

[Tes20] Tesla. Technical specs, February 2020. URL: `https://www.tesla.com/powerwall`.

[Vat20] Vattenfall. Check je energie deal, February 2020. URL: `https://www.vattenfall.nl/producten/energie/`.

[VDF+15] Koen Vanthournout, Benjamin Dupont, Wim Foubert, Catherine Stuckens, and Sven Claessens. An automated residential demand response pilot experiment, based on day-ahead dynamic pricing. *Applied Energy*, 155:195–203, 2015.

[Ver20] Verbund. Bei verbund finden sie das perfekte strom-angebot, February 2020. URL: `https://www.verbund.com/de-at/privatkunden/strom`.

[VI14] Louise Van Isterdael. *The potential of demand-side management in Belgium*. PhD thesis, GHENT UNIVERSITY, 2014.

[Vit20] Viteos. Tarifs électriques, February 2020. URL: `https://viteos.ch/infos-pratiques/tarifs-electriques/`.

[WC14] Isabelle Borremans Wim Cardinaels. Linear: Demand response for families. *Technical Report*, 2014. URL: `http://www.linear-smartgrid.be/sites/default/files/boekje_linear_okt_2014_boekje_web.pdf`.